CEREBROVSCULAR DYSFUNCTION IN PRIMARY BLAST TRAUMATIC BRAIN INJURY

by

Alan Stewart Yeoh

A dissertation submitted to the faculty of
The University of Utah
in partial fulfillment of the requirements for the degree of

Doctor of Philosophy

Department of Bioengineering

The University of Utah

December 2016

The University of Utah Graduate School

STATEMENT OF DISSERTATION APPROVAL

The dissertation of Alan Stewart Yeoh

has been approved by the following supervisory committee members:

Kenneth L. Monson	, Chair	05/10/16 Date Approved
Patrick A. Tresco	, Member	10/27/16 Date Approved
Vladimir Hlady	, Member	05/10/16 Date Approved
Jeffrey A. Weiss	, Member	10/27/16 Date Approved
Mark A. Mahan	, Member	05/10/16 Date Approved

and by Patrick A. Tresco , Chair/Dean of the Department/College/School of Bioengineering

and by David B. Kieda, Dean of The Graduate School.

ABSTRACT

Injury from explosive blast is a growing public health threat worldwide with complex mechanisms and limited treatment and prevention pathways. Blast-related traumatic brain injury (bTBI) is a multimodal injury event in which cerebral blood vessels play a central role in both the mechanical and physiological response to blast loading. This dissertation seeks to define the nature of vessel injury from primary blast loading by measuring injury thresholds for vasculature in bTBI by assessing blood-brain barrier (BBB) integrity and disruption, examining which types of vessels are affected, and mapping the distribution of injury in the brain. To assess the consequences of vascular injury, we measured inflammatory changes in glial cell activity with immunohistological techniques, and evaluated changes in behavior in a rodent model of bTBI. The importance of overpressure duration and impulse are examined by performing matched assays with two distinct blast tube devices capable of producing a wide range of blast wave characteristics. Exploration in measuring changes in cerebral blood flow, blood oxygen levels, and cerebral hemorrhage is described. Our primary findings include the presence of focal deposits of IgG in the parenchymal brain tissue indicating an elevated permeability of the blood-brain barrier, a heterogeneous distribution of these lesions among various brain structures, changes in astrocyte glial fibrillary acidic protein (GFAP) expression at lesion locations, and decrease

in nociception and pedal withdrawal reflex following primary blast exposure. Changes in macrophage and neural cell populations were observed using markers for IBA1, CD68, and NeuN. Injury levels between devices were broadly similar; however, some differences in both histology and behavior were seen following high-impulse blast testing. Blast injury research remains an important topic with many unanswered questions, and further effort will provide help to those afflicted and preventative protection for those at risk.

TABLE OF CONTENTS

ACKNOWLEDGEMENTS

Funding for this research was provided by the Department of Defense (W81XWH-08-1-0295). The author would like to acknowledge Jordan Walker and Louise Butler for assistance with tissue processing, imaging, and data analysis for work done in Chapter 2, Dr. David Bell for development and characterization of the low-impulse blast tube used in Chapters 2 and 3, Dr. Dan Kauffman and Dr. Raymond Kesner for assistance with development and training in behavioral testing in Chapters 3 and 4, Dr. Brittany Coats and Dan Shedd for operation and description of the high-impulse shock tube in Chapter 4, and Dr. Ed Hsu and Dr. Osama Abdullah for access and use of the Small Animal Imaging Facility for MRI imaging in Chapter 5. Thanks are also given to Dr. Elena Budko, Dr. Ben Christensen, and Dr. Patrick Tresco for training and assistance with histological techniques and animal handling and surgery training used throughout this dissertation, to Dr. Ken Monson as the advisor for this thesis and for his patience and support of work done, and to my parents Alan and Alayne and my fiancée Stephani for their years of love, support, and patience for me during this work.

CHAPTER 1

INTRODUCTION

1.1 Significance of Blast Injury

Human trauma from explosive devices is sadly a frequent occurrence in both unstable and unexpected regions of our modern world. Since Nobel's invention of nitroglycerin in 1847, explosives have shaped the nature of warfare, and thus battlefield casualties, like no other factor. More than 50% of combat injuries during the 20th century were the result of explosive devices.[1] More recently, this problem has grown in magnitude, as increased occurrence of asymmetrical warfare scenarios and the rise of improvised explosive devices (IEDs) have placed soldiers at greater risk than ever from blast injury. In the United States' 21st century conflicts in Iraq and Afghanistan, 73% of all combat injuries were reported as explosives related.[2] This danger is also a growing threat to civilian populations worldwide, with an estimated 82% of the 32,727 deaths from terrorist attacks in 2014 caused by bomb blasts.[3] Blast injury is not just limited to distant battlefields and restless foreign insurgencies – 36,110 bombing incidents were reported in the United States between 1983 and 2002, leading to nearly six thousand injuries.[4] These numbers represent only bombings committed for the purpose of terrorism or criminal intent, and do not include blast injuries resulting from industrial accidents, fireworks, land mines and unexploded

ordinance, or for injuries sustained during actual military combat worldwide. Blast injury is a complex multimodal trauma, and understanding of basic mechanisms will drive innovation in protective gear and treatment options.

1.2 Physical Nature of Blast

An explosion results from a rapid release of energy resulting in a sharp increase in localized pressure. Typically this involves the release or production of high temperature gases through chemical means, rupture of a physical container, nuclear reaction, or some combination. These gasses rapidly expand in volume, accelerating themselves and any fragments or debris to high-velocity. The energy release rate is limited by the detonation velocity, or the rate through the explosive media that the chemical reaction of runaway bond breaking propagates. Typical high performance explosive has a detonation velocity of 8 km/s.[5] This rapidly expanding volume of hot gas creates a pressure pulse that expands spherically outward from its origin. For the case of a high explosive detonation in air, a fireball of detonation exhaust products, surrounded by a thin layer of compressed superheated air, expands outward at supersonic velocity relative to the atmospheric speed of sound.[6] As the volume of the system increases, the pressure drops and velocity of the product cloud decreases. At a point determined by the type of explosive and charge size, the driving pressure of the explosion is reduced enough that the outward velocity of the growing gas cloud falls below the ambient speed of sound, and the shocked air layer detaches from the product cloud as a pressure pulse and continues to propagate outward.[5]

As the speed of sound in a medium is dependent on the local pressure

and temperature, a pressure pulse of arbitrary shape will undergo a dramatic transformation. Since the speed of sound is greater in the higher pressure regions of the arbitrary pressure pulse, higher pressure waveform components travel faster than lower pressure components.[5] These high pressure components pile up at the leading edge of the spherically expanding waveform, increasing the steepness of the pressure pulse wave profile. This reaches a limit where a sharp discontinuity is formed, known in generalized form as a shock wave,[5] which travels at supersonic velocity relative to the ambient medium. The shock wave front has been measured at around 200 nm thick,[6] on the same scale as the mean free gas molecular path. The shock wave is followed by the lower pressure components of the original overpressure pulse, and as they travel at velocity proportional to their pressure, they form a decaying pressure – time profile. This profile dips below external ambient pressure as gas compressed by the passage of the wave front inertially rebounds and over-expands.[7] This idealized pressure - time profile is known as the Friedlander Waveform (Figure 1.1), and is modeled by the equation:

$$P(t) = P_s e^{-\frac{t}{t^*}} \left(1 - \frac{t}{t^*}\right)$$

The maximum pressure value of the shock wave is known as the *peak overpressure*, P_s. The time period where the pressure remains above ambient is known as the *positive phase duration*, t^*, and lasts in the milliseconds range for typical explosions encountered.

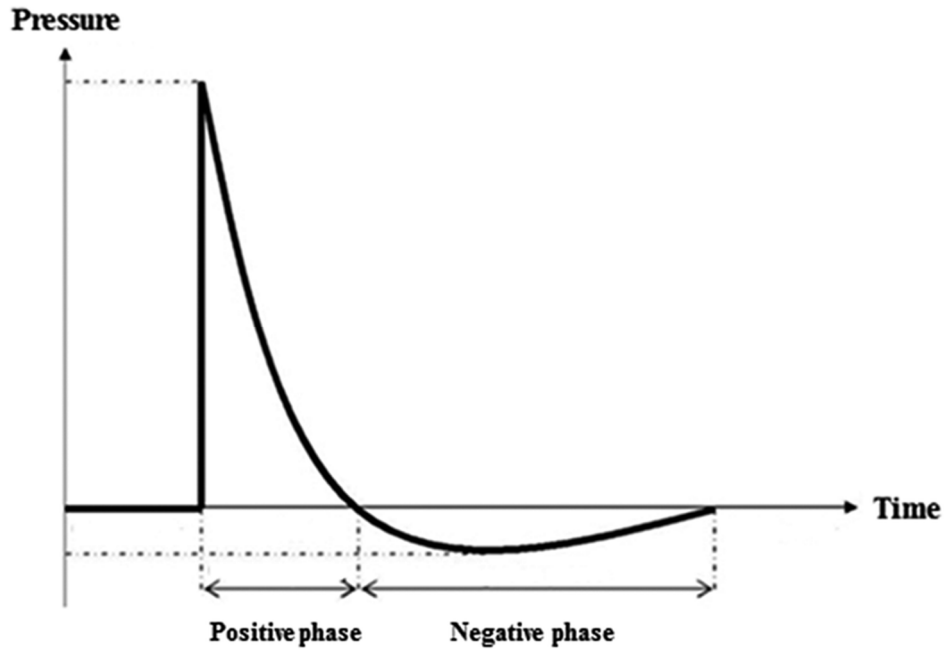

Figure 1.1: Idealized Friedlander waveform showing various characteristics of a blast overpressure wave.

The area under the curve is known as the *positive impulse*, and is proportional to the total energy contained by the waveform, making both the peak overpressure and the positive phase important factors in determining injury severity.

The time period that pressure drops below ambient is known as the *negative phase duration*. This negative pressure phase is influenced by the high speed gale of explosive products and displaced air that follows the blast wave, known as the *blast wind*,[5] and also by the negative pressure effect of the rising fireball of gas in an explosion.[7] The negative phase plays an important role in structural interactions and injury mechanics, as it is often seen in the aftermath of an outdoor bombing that nearby windows have blown outwards into the street.[7] However, the negative phase is difficult to replicate in the laboratory setting due

to the physics of shock tube devices that are used to simulate a blast wave, and are often misrepresented, underestimated, or ignored in the literature. The area under the curve during the negative phase is known as the *negative impulse*, and along with the positive impulse makes up the *total impulse* of the blast wave.

The Friedlander waveform is an approximation of a blast wave under idealized conditions of a spherical free air burst explosion, but real-life blast wave profiles are often much more complicated. Blast waves interact with surfaces and structures and can reflect or refract from them. In the simplest case of blast wave reflection from a head on impact with a unyielding surface, the strength of the reflected wave is dependent on a nonlinear function of the ratio of the speed of the wave compared to the ambient speed of sound, called the *Mach number (M)*. For a weak shock travelling near the speed of sound (M ~ 1), the reflection coefficient is 2, up to a theoretical maximum of 8 for very strong shock waves in air.[5] For oblique angle reflections, the shock wave is reflected back into the direction of flow. However, unlike light or sound, in blast wave constructive and destructive interference, the incident angle does not equal the angle of reflection. This is exemplified when the angle of incidence exceeds 40°, where the reflected shock detaches from the surface and the flow travels parallel to and the shock front perpendicular to the surface.[5] This phenomenon is known as the *Mach Stem,* and is important as it directs the blast wind along the surface at high-velocity. Finally, blast wave reflections from more complicated enclosed geometries such as the interior of buildings or vehicles can increase significantly through constructive interference and reverberation, substantially increasing the risk and severity of injury.

1.3 Injury from Blast Exposure

Injuries from explosive blast are divided into four categories based on mechanism. *Primary Blast Injury* is caused by the blast overpressure wave and its interaction with tissue. *Secondary Blast Injury* results from fragments and debris accelerated by the explosion. *Tertiary Blast Injury* occurs when the body or part of the body is accelerated by the blast wind, often into a rigid object. Finally, *Quaternary Blast Injury* results from thermal, chemical, or electromagnetic damage caused by the explosion.

Primary blast injuries result from the interaction of energy from the overpressure wave and tissue. Exact injury mechanisms responsible for tissue disruption are unclear; however, spallation, or internal surface fragmentation resulting when the blast wave transmits through media of differing densities in the body, is considered important.[8, 9] As the transmitted blast wave encounters tissue, the speed of sound abruptly changes reflection and change in wave frequency occurs, depositing energy.[10, 11] Air filled organs such as the lungs, inner ear, and gastrointestinal tract are particularly vulnerable. Blast lung, characterized by pulmonary edema and embolism without external signs of injury, is one of the primary causes of mortality following a blast event involving unarmored persons.[12, 13] Cavitation is thought to be another mechanism by which blast does damage to tissue.[14] Cavitation occurs when voids or bubbles are created in liquid due to high forces acting on it, often adjacent to the surface imparting force on the liquid. These cavities then rapidly collapse, creating high temperatures and pressures within them, and are a major cause of mechanical damage and wear in engineering fields such as impeller design.[14] Finally, inertial

effects are suspected to cause injury during blast.[9-11] Again, at boundaries where densities vary, the rapid cycle of compression and decompression from the blast wave causes the lighter media to accelerate faster than the denser ones, leading to high shear stresses at the interface.[8, 15]

Secondary blast injuries are categorized as those resulting from penetrating injury from bomb fragments and debris accelerated by the explosion. As the blast wave and product gasses are initially travelling at supersonic speeds, splinters of bomb casing, vehicle parts, and rocks and dust can be hurtled at velocities exceeding that of a rifle bullet for hundreds of meters.[16] Bombs, whether manufactured or improvised, are often designed to shatter a hardened steel casing into many small fragments, or have nails or bits of scrap metal added to increase the damage caused by flying projectiles. In addition, the rapidly moving product cloud and displaced air in the blast wind can exceed hurricane velocities, and cause traumatic dismemberment and amputation.[17] Secondary blast injuries from flying fragments are the most common type of bomb-related injury, and present the largest radius of threat from the epicenter of a blast.[18, 19] However, penetrating injuries are well understood by medicine, and conventional body armor and vehicles can provide protection from shrapnel.

Tertiary blast injuries result from sudden displacement of the body or body parts by momentum transfer from the blast wave and blast wind. Injuries are often incurred when the body is thrown against the ground, the inside of a vehicle, or a structure.[8] Coup-contrecoup injuries, where the brain impacts the interior surface of the skull, can also occur due to the acceleration of the skull. Finally, quaternary blast injuries occur when flames, intense heat, and toxic smoke cause burns,

inhalation injury, and asphyxiation. Additionally, the explosive detonation can create a strong electromagnetic pulse,[8] whose effect on biology is not well understood. Chemical, biological, or radiological factors are also potential injury mechanisms; however, thankfully, these types of incidents have been rare.

The effects of blast on the central nervous system have been recorded since World War 1 as shell shock, but were diagnosed as psychological distress from witnessing the horrors of war. Historically, blast injury research has focused on injury to air-filled organs such as blast lung barotrauma.[20, 21] More recently, the incidence of neurological issues reported clinically following blast exposure has driven focus to blast-related traumatic brain injury (bTBI) during the last two decades. Complaints of headache, light and noise sensitivity, memory problems, depression, insomnia, anxiety, behavioral changes, and other cognitive impairment are common among personnel post blast exposure, even with no external signs of injury.[22-26] Indeed, mild traumatic brain injury (mTBI) has been called the “signature injury” of US conflicts in Iraq and Afghanistan in the 21st century.[27] Several hypotheses exist to explain mechanisms behind bTBI. Skull flexure from blast overpressure loading[28-30] is suspected to cause intracranial tissue deformation and pressure oscillations, resulting in injury. Since the coupled mechanical system of skull and brain varies widely between species, this factor should be considered in designing animal studies. Transmission of a pressure wave from the thoracic region through large blood vessels and into the brain has long been thought to produce damage from this “vascular surge” in both cases of blast and ballistic injury.[11, 31, 32] Animal studies using body armor have shown lower intracranial pressure than unprotected subjects,[8, 33] supporting this

conclusion. Finally, direct transmission of the overpressure wave through the skull and into brain tissue has been proposed as responsible for bTBI. Intracranial pressure sensors have verified that the blast overpressure waveform can be measured in-vivo with minimal attenuation of the peak overpressure.[34] The aforementioned spalling, cavitation, and inertial impedance mismatches causing shear forces are likely direct damage mechanisms behind brain injury.

It is important to recognize that blast injury is a complex polytrauma event, and that bTBI may include effects from primary, secondary, tertiary, and quaternary blast. Hypoxia from pulmonary barotrauma can cause vagally mediated bradycardia through pulmonary vagal reflex, which can lead to ischemia and vasospasm in the brain, as well as systemic hypotension.[35] Blast-related stretching and shearing of tissue can cause hemorrhage, releasing hemoglobin and causing platelet degranulation, which initiates proinflammatory and coagulation cascades.[36] Much effort has been applied to finding a reliable biomarker for blast injury to use as a diagnostic tool for soldiers following blast injury,[37-39] but despite promising animals studies, a useful clinical assay remains elusive. Imaging techniques such as fMRI have shown some promise for injury diagnosis,[38, 40, 41] but face challenges in field application due to bulk and expense of imaging scanners.

Primary blast injury displays features unique from conventional head trauma,[42-44] commonly exhibiting edema, vasospasm, and intracranial hemorrhage, even in the absence of external injury. Recent blast-induced traumatic brain injury (bTBI) research has described numerous other traits of bTBI. Studies report neuronal swelling, oxidative stress, reactive gliosis, and

cognitive impairment following bTBI.[33, 43, 45] EEG recordings have found temporary depression of cortical activity following blast.[43, 46]

Some focus has been applied to the role of blood vessels in the brain during bTBI; however, the role cerebrovasculature plays in blast injury is not fully clear. Cerebral edema[35] and increases in intracranial pressure[47] indicate that dysfunction of cerebral vasculature plays a significant role in bTBI, while vasospasm,[33, 44] cerebral hypotension, and hypoxia[48] are commonly reported in hospitalizations involving moderate to severe bTBI. Increased blood-brain barrier (BBB) permeability is commonly reported.[49-51] The blood-brain barrier is maintained by the combined function of cerebrovascular endothelial cells, tight junction (TJ) molecules such as occludins, claudins, and cadherins between cells, the capillary ECM basement membrane, pericytes, and astrocytic projecting end feet.[52] Disruption of any of these constituents, whether through mechanical stretching and shearing or through secondary inflammatory insult, can lead to neuroinflammation and neurodegeneration.[26, 53] Immune cell mediated BBB disruption has been reported following bTBI,[26, 54] as well as extravasation of IgG and other large molecular markers such as albumin bound Evans Blue dye following blast injury.[50, 54] These findings highlight the need to further characterize vascular injury in bTBI.

1.4 Experimental Models of Blast TBI

Research into primary bTBI has been complicated by the variety of methods used to produce overpressure, as well as testing conditions that have compounded the effects of tertiary blast type effects that have more in common

mechanistically with traditional models of TBI. Blast overpressure in the laboratory is produced by either detonation of a small free-field explosive charge, or by use of a blast simulation shock tube. Free-field blast from explosives has long been used to study overpressure effects on biology[20, 21, 46, 55-57] and produces an accurate Friedlander type overpressure wave, but is less commonly in modern literature. Regulatory and practical concerns over purchase and detonation of high explosives has limited their use to a handful of labs with the correct licensing and appropriate armored facilities, and has created the need for an alternative method of producing blast overpressure. Safety reasons, as well as cost and facility limits, often require scaling constraints so that often only grams of explosive are used, which alters the overpressure duration of the blast wave from what would be experienced in a real-life bomb scenario. Finally, explosive detonation makes separating the effects of primary blast from secondary and tertiary difficult.

Due to hurdles encountered in the use of actual explosives, the most common research tool for bTBI is the blast tube. Blast tubes consist of a method to generate local high pressure at a closed end of the tube, called the driver section. Pressure is then suddenly released to expand freely down the tube to its open end along what is known as the driven section. The driver section can be a physical chamber charged to high static pressure separated by a membrane or valve, or it can be a much smaller charge of high explosive,[43, 58, 59] which has its expansion wave concentrated by the tube toward a target. Of these, the high pressure chamber / membrane rupture model has gained dominance in the field for its repeatability, tunable peak overpressure and positive phase duration, and

ease of use. Clinically relevant overpressures exceeding 550 kPa[26] and ten milliseconds[60] are possible using these systems.

Care must be taken to provide a long enough driver section, as the high pressure components of the shock wave propagate both forward and backward from membrane rupture and reflect off the internal back plate of the shock tube.[49] This reflected wave travels faster through the higher density media in the driver section and eventually catches up with the shock wave front propagating towards the open end of the tube. It is crucial for the length of the driven section to allow the reflected wave to catch up to the blast wave front for the shock tube to accurately simulate a free-field blast wave form.[61, 62] Driver sections are often charged with a light gas such as hydrogen or helium, as the speed of sound in these gasses is higher, and full blast wave development can occur in a shorter driven span.[49] Light gasses also have the advantage of less momentum transfer down the length of the tube and confounding secondary / tertiary blast injury type effects.

A limitation of blast tube research is the large amount of driver gas that follows the overpressure wave down the tube which is analogous to blast wind, although typically greater in magnitude as it propagates linearly and does not expand spherically until it exits the tube, which can make isolating primary blast difficult. A variant tube design uses combustion, typically either oxygen-hydrogen or oxyacetylene,[61, 63] which reduces the molar gas fraction needed and thus the amount of high speed gas ejected down the tube. The tradeoffs for these systems are possible confounding quaternary-type injury from high temperature combustion products, and the danger of oxygen deprivation injury in the tube

following blast.

One major limitation of blast tube design is that overpressure waveforms are often significantly different than what would be seen in an equivalent overpressure and impulse free-field explosion. Positive phase duration is often lengthened, peak overpressure is distorted, and negative phase is often absent from blast tube pressure traces.[49, 61, 64, 65] The physics of a planar expansion wave in a blast tube and a spherical overpressure expansion from a free-field explosion are considerably different, and there is some controversy on the appropriateness of shock tubes for blast wave simulation.[64, 66, 67] Other models have used creative methods to simulate blast wave overpressure such as laser accelerated cavitation,[68, 69] or high intensity focused ultrasound,[70, 71] but it is unclear if these are accurate surrogates for blast overpressure waves. Regardless of what model is selected to produce blast overpressure, careful consideration needs to be made for the particular advantages and drawbacks of each model, and extraneous effects need to be accounted for when drawing conclusions.

1.5 Objective Statement

Blast traumatic brain injury is a serious public health issue with limited options for prevention and treatment, particularly with respect to the mechanisms of primary blast. Additionally, cerebral blood vessels play a crucial role biomechanically and functionally in bTBI which merits further study. Our objective is to characterize vascular dysfunction in traumatic brain injury resulting from blast overpressure exposure at the lower thresholds of injury detection using

rodent animal models. Lack of complete insight about blast TBI has resulted in limited clinical options for injured persons, and revealing details about vascular injury in blast will both help advance medical therapies and also allow for the creation of more complete constitutive models for injury simulation and protective gear design. Injury from blast overpressure (BOP) remains a major challenge; however, greater understanding of injury mechanisms will lead to new treatment paths and improved quality of life for those afflicted.

1.6 Chapter Summary

This dissertation contains an introductory chapter followed by four chapters detailing work done to characterize vessel response in bTBI, and finished with conclusion and summary chapter. Chapter 2 contains a published study on the distribution of focal IgG deposit that is evidence of disruption to the blood-brain barrier as a result of primary blast injury from a tabletop low-impulse device. The blast overpressure wave is characterized, primary blast is verified, and injury severity and lesion distribution in the brain are measured for several overpressures and survival times.

Chapter 3 contains a study that expands on the work done in Chapter 2 by assessing inflammatory and behavior consequences of BBB disruption from primary blast. Astrocytic, microglial, and neuronal response are assayed immunohistochemically, and behavioral changes for motor function, anxiety, memory, and tactile response are interrogated using behavioral testing techniques.

Chapter 4 contains a subsequent study that explores the role of positive

phase duration and impulse on animal function, based on a need for comparison between results from the short-duration, low-impulse device used in Chapters 2 and 3, and results from the literature reporting greater injury severity. Identical assays were performed for direct comparison of inflammatory and behavioral changes.

Chapter 5 contains refined immunohistological examination of blast animals for inflammatory response. Thin section analysis, an expanded marker panel, and a discussion on IgG quantification are included.

Chapter 6 contains additional methods attempted to characterize primary blast injury and vascular response. Fluorescent dextran perfusion and susceptibility-weighted imaging MRI were used to examine BBB disruption, hemorrhage, and edema, while fluorescent microsphere injection was performed to measure changes in cerebral blood flow following blast exposure.

Chapter 7 contains a summary of research done and concluding discussion and statements.

CHAPTER 2

DISTRIBUTION OF BLOOD-BRAIN BARRIER DISRUPTION IN PRIMARY BLAST INJURY

Reused with permission from Annals of Biomedical Engineering
October 2013, Volume 41, Issue 10, pp 2206-2214 with additional detail on immunohistological and imaging methods included for this dissertation.

2.1 Abstract – Chapter 2

Traumatic brain injury (TBI) resulting from explosive-related blast overpressure is a topic at the forefront of neurotrauma research. Compromise of the blood-brain barrier (BBB) and other cerebral blood vessel dysfunction is commonly reported in both experimental and clinical studies on blast injury. This study used a rifle primer-driven shock tube to investigate cerebrovascular injury in rats exposed to low-impulse, pure primary blast at three levels of overpressure (145, 232, and 323 kPa) and with three survival times (acute, 24, and 48 hour). BBB disruption was quantified immunohistochemically by measuring immunoglobulin G (IgG) extravasation with image analysis techniques. Pure primary blast generated small lesions scattered throughout the brain. The number and size of lesions increased with peak overpressure level, but no significant difference was seen between survival times. Despite laterally directed blast exposure equal numbers of lesions were found in each hemisphere of the brain.

These observations suggest that cerebrovascular injury due to primary blast is distinct from that associated with conventional TBI.

2.2 Introduction

Trauma resulting from exposure to explosive blast is an omnipresent and increasing component of modern warfare, accounting for more than half of combat injuries during the last hundred years, a percentage which has grown in the 21st century to 73% of all US military casualties in Iraq and Afghanistan.[45] Injuries from explosives are commonly categorized by mechanism, including primary, secondary, tertiary, and quaternary injury modes.[36] Because of primary blast's apparent role in both mortality and morbidity, understanding injury from blast overpressure (BOP) is a major challenge facing modern military and civilian medicine.

Blast overpressure is caused by a sudden release of energy that results in rapid expansion of high pressure gas into the ambient environment. As a pressure pulse of arbitrary shape travels through a medium, higher pressure components of the pulse travel faster than lower pressure parts, since the speed of sound in the higher pressure regions of the wave is greater.[5] This causes the wave components to add constructively and create a sharp rise in pressure, or a shock. The shock begins to degrade into a blast wave as rarefaction waves catch up to the shock front, and the resulting pressure-time wave shape is idealized by a Friedlander curve. In this ideal curve, pressure decreases rapidly following the peak; this region of greater-than-atmospheric pressure is called the positive phase. The pressure then temporarily drops below the atmospheric level, forming

the negative phase. Real-life blast waves often interact with structures or the ground and thus are reflected and amplified or distorted from the idealized curve.

Early studies discovered that primary blast exposure causes damage to the lungs, including alveolar hemorrhage, interstitial edema, and rupture of the alveolar septa, which results in interference with gas exchange function or vascular air embolism, often fatally.[20] However, as recent advances in body armor have apparently protected the lungs and increased survival rates from blast exposure,[33] neurological deficits resulting from blast have come into focus.

Recent blast-induced traumatic brain injury (bTBI) research has investigated numerous biomarkers and other indicators of injury. Some of these studies have reported reactive gliosis, neuronal swelling, cognitive impairment, and oxidative stress following bTBI.[33, 43, 45] EEG recording has also found momentary depression of cortical activity following blast.[43, 46] In addition, vascular dysfunction, manifest as cerebral edema[35] and increases in intracranial pressure,[47] has been observed, and vasospasm has been shown to be common in soldiers hospitalized with moderate to severe bTBI.[33, 44] Cerebral hypotension and hypoxia following bTBI[48] are additional indicators of vascular dysfunction. Finally, increases in blood-brain barrier (BBB) permeability have also been reported.[49-51]

Although numerous recent experiments have characterized brain injury from blast, a limited amount of this research has addressed cerebrovascular injury. In addition, reported findings have been produced using a variety of experimental approaches that include diverse loading modes, making it difficult to draw direct comparisons. Because vascular dysfunction is at the heart of much of

the observed blast pathology, our aim was to characterize disruption of the cerebral vasculature in pure primary blast loading.

2.3 Materials and Methods

Male Sprague-Dawley rats (average weight 328 g) were used according to protocols approved by both the University of Utah IACUC and USAMRMC ACURO. Animals were allowed access to food and water ad libitum during testing. Eighty animals were tested in total, with either seven or eight animals in each of the nine overpressure-survival time groups, plus one control group of eleven animals.

Primary blast was generated by detonating the primer in an otherwise empty casing in a modified 0.308 bolt-action rifle (Savage Arms; Axis) with a 55.8 cm barrel, based on an approach described previously.[58] The stock of the rifle was removed to allow connection to a bench top fixture. To increase explosive yield and overpressure levels, a custom, hardened steel casing was machined to hold a .50 caliber rifle primer (CCI, #35); hardened steel was necessary to avoid plastic deformation of the primer pocket during detonation, thus allowing repeatable blasts using the same casing.

Blast overpressure was measured using a high frequency pressure sensor (PCB Piezotronics; ICP 102B15) connected to a signal conditioner (PCB Piezotronics; 482C05), the output of which was sampled at 2.5 MHz (National Instruments; NI PXI-6133). The sensor was positioned at various off-axis testing locations (parameterized by distance from the center of the muzzle and by angle of the position vector relative to the barrel axis) to characterize the pressure field.

All measurements were made with the sensor mounted perpendicular to the direction of wave propagation (side-on) to capture static pressure. The cartridge was cleaned following each shot, and multiple measurements were made at each location to evaluate repeatability. Analysis of sensor measurements taken at various locations near the muzzle showed a sharp increase in overpressure where gas jet effects existed; test locations were chosen to minimize this effect. The sensor was removed during rat exposures, as pressure reflections off the sensor head would have influenced blast wave shape and intensity. Rat head motion during testing was monitored using high-speed video (8800 fps; Vision Research, Phantom MiroEX4-M).

Prior to blast exposure, the animal was anesthetized with 5% inhalation isoflurane and immobilized in a Kevlar sling to minimize injury to the lungs. The animal was positioned with its head was outside the Kevlar sling and offset from the muzzle to avoid loading by the exiting gas jet and burning propellant[72]. Distance and angle were adjusted, as described for the pressure sensor, to produce one of three levels of blast overpressure (145, 232, or 323 kPa); distance was defined from the center of the muzzle to the furthest projecting lateral point of the ipsilateral supraorbital process. Following blast exposure, animals were sacrificed at 5 minutes, 24 hours, or 48 hours, and extent of vascular injury was evaluated. Euthanasia was performed by isoflurane overdose followed by transcardial perfusion with 150 ml of phosphate buffered saline (PBS) and 150 ml of 4% paraformaldehyde (PFA) at 42 $mL*min^{-1}$. Brains were removed by decapitation and removal of the parietal skull plates and post-fixed in PFA for 24 hours. Control animals received isoflurane induction but no blast injury.

Brain tissue between the pineal gland and the olfactory lobes was serially sectioned into 100 μm coronal sections by vibratome. Sections were processed using indirect immunohistochemistry for rat IgG (0.5 mg/ml, Biotinylated GtxRt IgG1, Southern Biotech, Birmingham, AL). Briefly, antibodies were diluted in blocking solution consisting of 4% (v/v) goat serum, 0.1% (v/v) Triton-X, 0.5% (w/v) sodium azide in PBS. Free floating tissue sections were batch incubated in block for 1 hour at room temperature and then for 24 hours in primary antibody solution at room temperature. After three rinses in PBS (1 hour/rinse) to remove unadsorbed antibody, sections were incubated with fluorescently labeled secondary (0.5 mg/ml, Streptavidin-conjugated AlexaFluor-594 1:500, 2 Invitrogen, Carlsbad, CA) for 24 hours at room temperature and again rinsed three times with PBS (1 hour/rinse). Sections were counterstained with DAPI (10 mM) to image cell nuclei. Brain sections were mounted on glass microscope slides with Fluoromount-G (Southern Biotech) and then protected with glass cover slips.

Immunoglobulin G (IgG) extravasation was used to detect displaced plasma in brain tissue. Sections were imaged using a Coolsnap digital camera (1040x1392 image resolution) mounted to an upright epifluorescent microscope (Nikon; Eclipse E600) using a 4x (NA = 0.13) objective at 2.5 seconds exposure time and controlled mercury lamp and aperture settings. Images were light field corrected using no-primary controls. Complete images were then constructed by montaging individual snapshots (Adobe Photoshop CS). The high resolution images were then analyzed using a semi-automated script written in Vision Assistant (National Instruments; LabView) to measure lesion size and location

within the section. The script used color thresholding to identify regions of high fluorescence and then several particle filtering steps were applied to determine what constituted a lesion. Threshold levels were determined by three independent evaluators blinded to animal treatment. Size filters removed very small particles to reduce noise and flagged large particles for subsequent manual verification. Likely lesions typically had a bright focal area surrounded by a gradient that faded into the surrounding tissue over a distance of a few hundred microns. This diffusive boundary was judged to be a critical feature of a likely rupture in the BBB and was used to remove particulate matter that could register as a false positive. Particles were judged as one lesion as long as they contained continuous pixels. IgG fluorescence was consistently associated with the ventricles, choroid plexus, and leptomeninges, due to exposure of these structures to cerebrospinal fluid (CSF), as has been observed in similar studies.[51, 73, 74] Manual preprocessing was performed to ensure that these structures were not counted as injuries.

One section every 500 μm was evaluated for immunohistology; twelve sections were examined from each brain. In addition, one full brain block for each overpressure level was examined in its entirety to determine an appropriate sampling rate. These serial cases also made it possible to investigate lesion persistence through neighboring sections. The total number of lesions, by section, was determined in each of the serial cases. Staggered sampling of these cases was then performed by selecting every fifth section (5^{th}, 10^{th}, 15^{th}… or 6^{th}, 11^{th}, 16^{th}…; etc.) and comparing the number of lesions in each of the five sample groups to ensure consistency. The number of lesions in the different collections

varied within about 5% of each other, suggesting that evaluating one section every 500 μm was sufficient.

To determine if any particular structures in the brain were more susceptible to injury, generalized anatomical regions were identified using a digitized rat brain atlas,[75] and region image masks were created. Lesion locations were then associated with major brain structures using a Vision Assistant script. Histological images were matched with atlas plates by identifying landmark structures for each brain.

Statistical significance of peak overpressure and survival time was determined using two-way ANOVA (Excel). Post-hoc t-tests with false discovery rate (FDR) correction using the Benjamini & Hochberg method with a family wise error rate of 0.05 were then used to examine significance between blast levels. Reported values list mean ± standard deviation unless otherwise noted. Differences were considered to be significant for p-values less than 0.05.

2.4 Results

The described blast device produced a primary blast overpressure wave consistent with a Friedlander curve, beginning with a rapid increase in pressure associated with a positive pressure impulse that was followed by a longer negative pressure phase (Fig. 2.1). Blast wave characteristics associated with the various exposures are summarized in Table 2.1. As shown, peak pressure decreased and positive phase duration increased with distance from the tube exit. While pressure rose and fell sharply at Locations 1 and 2, a secondary

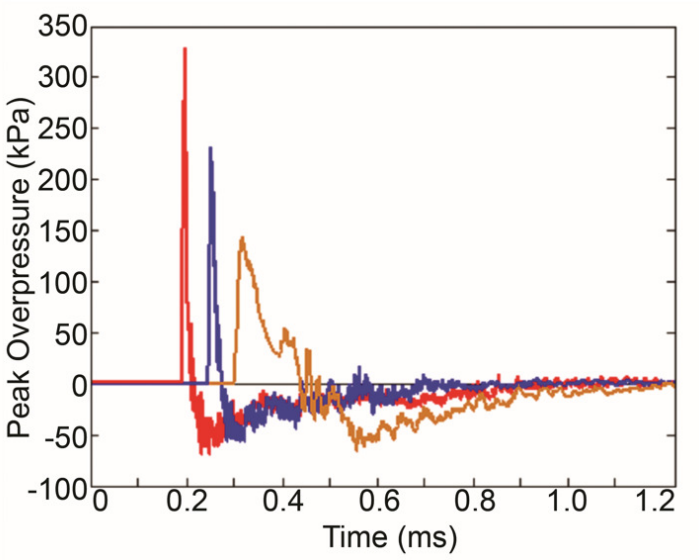

Figure 2.1: Representative pressure traces at the three test locations measured in air. Peak pressure values are 323, 232, and 145 kPa. The traces are offset to clearly display each waveform. Sampling at 2.5 MHz was confirmed to be sufficient by comparison to redundant sampling with a digital oscilloscope at 2 GHz.

Table 2.1: Summary of wave properties for positions used in animal blast exposures. Position is defined as the distance from the muzzle and its angle relative to the barrel axis.

Position	1.5 cm, 60°	2.5 cm, 60°	5.5 cm, 30°
Max Positive Pressure (kPa)	322.5 ± 5.7	231.2 ± 9.1	144.4 ± 3.4
Min Negative Pressure(kPa)	-71.2 ± 2.7	-62.1 ± 4.9	-64.4 ± 6.6
Positive Phase Duration (μs)	14.4 ± 2.3	20.3 ± 2.3	55.8 ± 4.2
Negative Phase Duration (μs)	876 ± 80	837 ± 115	845 ± 30
Positive Impulse (Pa*s)	1.86 ± 0.02	1.87 ± 0.02	3.47 ± 0.15
Negative Impulse (Pa*s)	-8.09 ± 0.25	-5.72 ± 0.35	-8.80 ± 0.42

pressure spike is visible in the descending pressure for Location 3. The cause of this is unclear, but this location's proximity to the tube axis suggests some possible contribution from the exit jet. The negative phase pressure was noisy but measured around -60 kPa for all three locations. High-speed video revealed negligible displacement of the animal's head during the overpressure exposure (Fig. 2.2), confirming that any loading by the exiting gas jet was minimal. The video sequence shows distortion of the nose and ipsilateral skin but no gross head motion.

Following blast exposure at any level and recovery from anesthesia, animals showed no obvious sign of distress or motor impairment. Gross examination of brains from both blast-exposed animals and controls revealed no visible hemorrhage on the brain surface. Superficial examination of lung tissue in preliminary animals exposed to blast without the Kevlar sling showed extensive pulmonary hemorrhage (not included in this study), but the lungs of animals tested with the sling were superficially indistinguishable from controls. Pressure measurements taken inside the sling at positions approximating that of the lungs ranged from 6 to 26 kPa, which is below any published threshold for injury.

Immunohistology revealed generally small, focal regions of fluorescence associated with IgG outside of blood vessels (Fig. 2.3a). Light microscopy showed red blood cells associated with some lesions, indicating that these areas experienced hemorrhage or coagulation of blood within the vessel in addition to plasma leakage. In the three brains that were analyzed completely, lesions were scattered both within and across sections without any apparent distribution or dependence upon the site and direction of loading.

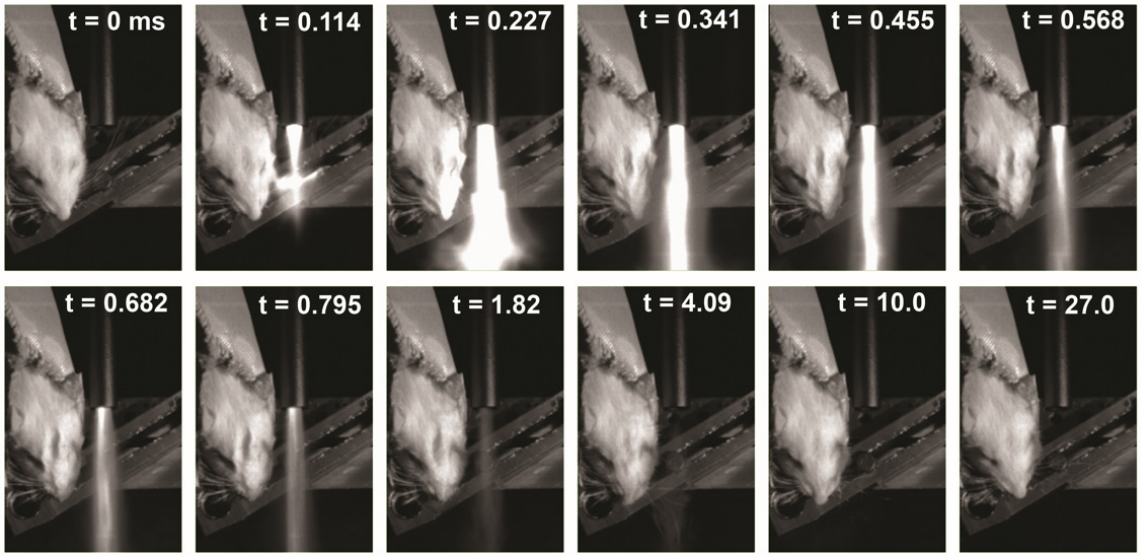

Figure 2.2: High-speed video (8800 fps, time in ms) of a 320 kPa blast exposure, viewed from above. The animal is offset downward relative to the barrel. The first eight frames are sequential and show the blast exposure and accompanying gas jet. The last four frames display progressively later time points. The images show displacement of the skin and fur but negligible overall motion of the head.

In contrast to lesions in conventional head trauma, there was no obvious preference for hemorrhage at, or near, the surface of the brain or at interfaces between structures, such as that of the white and gray matter. Many lesions (60.3%) persisted through more than one section. On average, each lesion spanned 2.9 sections, giving a lesion characteristic length of 290 μm along the axis perpendicular to the coronal plane.

Despite significant variability between animals, the number of lesions per brain increased significantly with peak overpressure ($p=0.012$; Fig. 2.4a). However, the 150 kPa group did not significantly differ from the control group ($p=0.119$), while the 230 kPa ($p=0.011$) and 320 kPa ($p=0.004$) levels were both different from controls. This suggests an injury threshold between 150 and 230

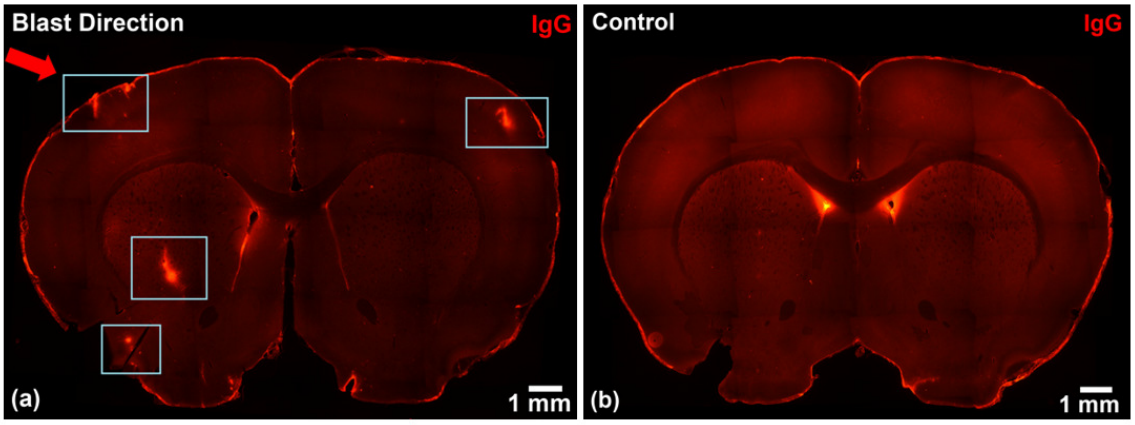

Figure 2.3: (a) Representative injuries (boxed) found in rats exposed to blast overpressure, compared to control brain (b). Images consist of 4x montages at a resolution of 2.27 µm. Bright areas associated with the pia-arachnoid and ventricles are believed to be due to low IgG concentrations inherent to CSF that was not flushed away during perfusion.

kPa under these loading conditions. Interestingly, the 230 and 320 kPa groups did not significantly differ from one another ($p=0.69$). It is not clear why some tests resulted in a particularly high number of lesions.

The total volume of brain affected by vascular disruption (product of lesion area and in-vivo section thickness) also increased with overpressure ($p<0.001$), up to a maximum of 1.34% of the 138.5±18.7 mm^3 of tissue sampled per brain (Fig. 2.4b). Again, lesioned volume in 150 kPa exposures was not significantly different from controls ($p=0.57$), but it was different for both 230 ($p=0.030$) and 320 kPa ($p<0.001$). However, the lesioned volume at the 320 kPa level was significantly larger than the 230 kPa exposure ($p=0.021$) in this case.

Average lesion area was relatively constant across the three levels of blast exposure, with an overall average value of 0.072 ± 0.15 mm^2, or an equivalent circular diameter of around 300 µm. This agrees well with the observed lesion persistence depth, suggesting that average injury shape was

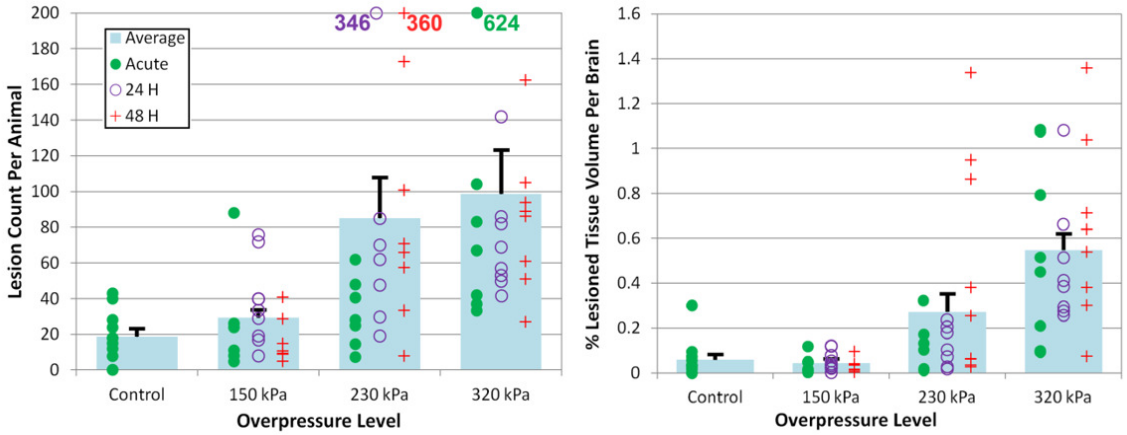

Figure 2.4: (a) Mean number of lesions per animal by overpressure and survival time. Points represent total number of lesions in the tissue volume sampled for individual animals. Three animals with a particularly high number of injuries are noted at the top of the graph within their respective columns. Significant differences were found between control animals and the 230 kPa level ($p = 0.011$) and the 320 kPa level ($p = 0.004$). (b) Percentage of lesioned tissue volume per animal. Significant differences were found between controls and the 230 kPa level ($p = 0.030$) and the 320 kPa level ($p < 0.001$) and also between the 230 and 320 levels ($p = 0.021$). The off-the-chart cases in 4a did not correspond with the largest volumes in 4b. Error bars represent standard error.

relatively isotropic. However, most lesions (79%) were smaller than the average value. A median lesion area of 0.026 mm² (~185 µm diameter) illustrates the skewed size distribution. While there was not a significant dependence of lesion area on overpressure, the largest lesion areas occurred with the highest pressures. Interestingly, there was no correlation between survival time and either number of lesions ($p = 0.89$) or total lesion area ($p = 0.88$).

As was observed in the serially sectioned cases, lesions were distributed across both hemispheres of the brain, despite lateral blast exposure. The average hemorrhage location for all blast-exposed animals was 0.512 ± 0.239, with both axes normalized from 0 to 1.0 (Fig. 2.5). No level of blast exposure

showed a significant injury preference towards either the contralateral or ipsilateral hemisphere; however, a small trend towards the contralateral hemisphere in all test groups was noted.

Analysis of lesion distribution based on anatomical region (Fig. 2.6) found that the highest injury frequency occurred in the “other structures” category, which is composed primarily of the basal ganglia and septal nuclei, along with various other small nuclei and white matter tracts that did not fit into one of the larger regions. Interestingly, the hippocampus and thalamus appear to have the least amount of injury resulting from blast exposure.

2.5 Discussion

Blast-induced TBI is an area of intense research. Breakdown of the BBB and associated pathologies are well known to occur from overpressure exposure, but little is known about the relationship between primary blast and hemorrhage. This research aimed to characterize disruption of cerebral blood vessels from primary blast loading. Results show that low-impulse, pure primary blast generates small, focal lesions with a scattered distribution distinct from that of hemorrhage in conventional TBI.[76]

Numerous blast-induced TBI investigations have been conducted over the last decade. An important feature of the present study is its isolation of pure primary blast as a loading mechanism. The blast generator used here produced a Friedlander-like pressure wave. However, the very short duration of the wave distinguishes it from loading reported for typical free-field explosions in air, (e.g.[43]) where the positive phase duration is on the order of milliseconds. While

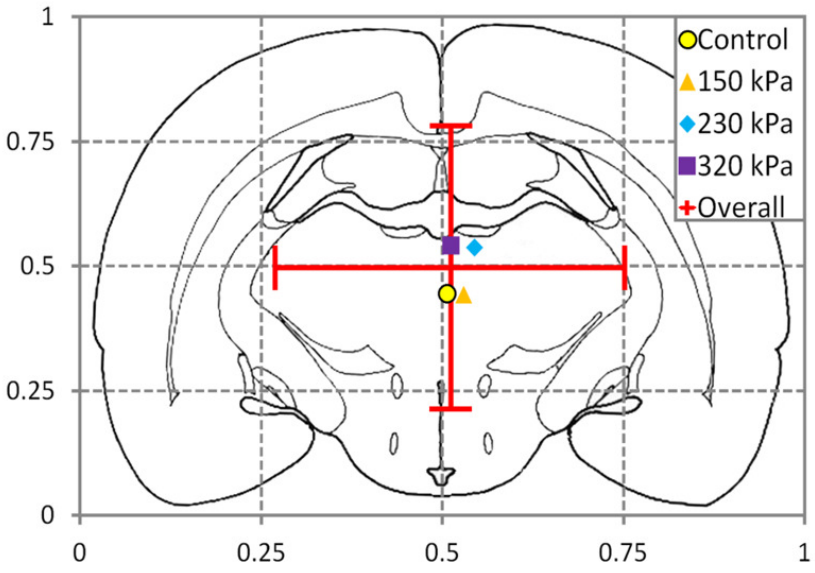

Figure 2.5: Mean (and standard deviation) coronal lesion distribution collapsed onto a representative brain atlas plate.

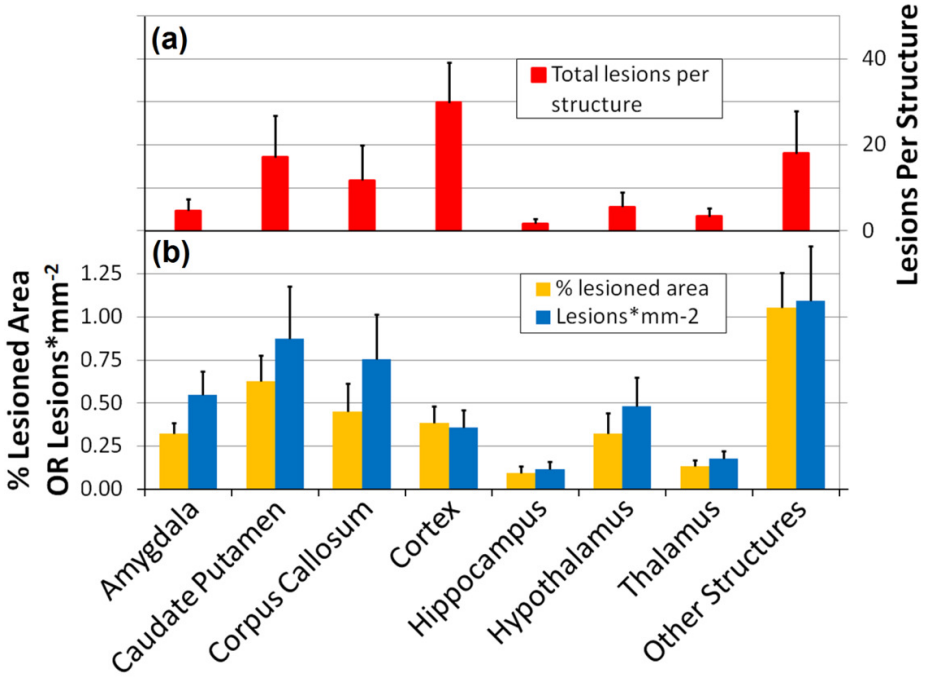

Figure 2.6: (a) Average number of lesions per brain sorted into generalized anatomical regions for all 230 and 320 kPa blast exposures (150 kPa animals were excluded due to lack of difference with controls). The *Other Structures* category includes septal nuclei, basal ganglia, and other small telencephalon and rhinencephalon structures. (b) Average percent lesioned area and number of lesions*mm^{-3}, serendipitously plotted on the same scale (1% being roughly equal to one lesion per mm^3).

positive durations associated with most shock tubes are generally more representative of actual explosions, animals tested inside these tubes experience both overpressure and high-velocity gas flow. As a result, the loading is not that of pure primary blast alone (although some have taken steps to minimize flow effects[77]) and it is not clear whether injuries are due to overpressure or flow impingement. Some blast injury investigations specifically focus on complex loading scenarios involving multiple modes of loading, including those also present in conventional TBI such as impact, penetration, and acceleration. These studies are important since many blast exposures involve such complexities, but it is usually not possible in such cases to identify which injuries were associated with which type of loading. While the duration of the blast wave in the present study is not claimed to be ideally representative of a typical explosion, it does allow isolation of the primary blast component of loading. In a similar recent study,[72] investigators reported a unique injury signature for primary blast relative to composite loading, though they did not consider vascular injury.

A notable finding of the present work is the symmetric pattern of small, isolated lesions scattered throughout the parenchyma. Only lateral loading was explored, but lesion distribution was symmetric relative to the midline regardless of peak overpressure level. This pattern is distinctly different from that seen in conventional head trauma where bleeding most commonly occurs at or near the brain surface.[76] A likely reason for this difference is the observed lack of head acceleration in the current model. Other potential tissue loading mechanisms include skull flexure[29, 30] and pressure wave propagation. It is unknown whether the impulse here was large enough to cause significant skull flexure. No cortical

lesions suggestive of skull bending, either under sutures or elsewhere, were consistently observed. However, some flexure, along with associated changes in pressure propagation patterns, would be expected. A question arises if the rat, with its much thinner skull, would experience more flexure than a human skull; however, the elastic modulus of rat skull is similar to that of human skull (5.9 vs. 7.5 GPa elastic modulus), and increases in stiffness at higher deformation speeds.[78] There may be some scaling factor at work where flexure is dependent on skull surface area exposed to blast vs. skull thickness in different species. We did not measure intracranial pressure (ICP), but others have reported that blast-induced ICP histories are similar to those in the surrounding air.[34, 77] It thus appears that the propagating pressure wave was responsible for the disruptions. The symmetric lesion distribution also suggests that the blast wave propagated through the brain without significant attenuation, even though the peak overpressure dissipated quickly in surrounding air over the same distance.

The symmetric, scattered nature of the lesions and their presence in multiple different brain structures prompts questions about why they appear in one location and not another. The answer is not clear. In our analysis of distribution through brain structures, there was no apparent preference for boundaries, though the high prevalence for lesions in smaller structures may indicate that mechanical impedance mismatches at the many interfaces in this region are important. A puzzling observation is the low occurrence of injury in the hippocampus and thalamus. The tissue in these areas may be naturally less susceptible to blast, or perhaps the ventricular boundary is somehow protective. Studies characterizing rat cerebrovascular geometry[79, 80] have shown that blood

vessel density is greater in gray matter than white matter and that various structures exhibit markedly different vessel patterns. It is not yet clear whether vascular geometry influenced the lesion distributions observed here. It may be that the scattered pattern is a result of wave interference causing non-uniform pressure distributions.

Because lesions were found in controls, we questioned whether all similar lesions should be dismissed as artifact, but results clearly show an increase in both lesion count and size with overpressure, so we conclude that they were largely blast-induced. The reason for their presence in controls is unknown, but other studies have similarly shown IgG in uninjured brains consistent with the understanding that some small amount of BBB permeability occurs in healthy animals.[51, 73, 74] As a result, some of the IgG collections identified here as lesions are likely unrelated to blast, but these would be present across all variables studied.

In contrast to our findings, other groups have reported blast-induced BBB breakdown with patterns similar to those of conventional TBI, including blood on the brain surface and diffuse distributions of IgG.[49-51] The parenchymal bleeding was primarily limited to the cortex in each of the studies, though ipsilateral,[51] contralateral,[49] and symmetric[50] distributions were separately reported. The marked differences between these studies and the present one are tempered somewhat with the observation of increased IgG intensity around small blood vessels within the less intense, larger IgG distributions.[49] Further, inspection of some of the immunostained brain slices presented in these reports shows a number of small, isolated regions of IgG with appearance and distribution similar

to the lesions described here. Each of the previous investigations was conducted at peak overpressure levels comparable to that of the present study, but with significantly longer durations (4-5 ms). The tests were also conducted inside, or at the end, of shock tubes where animals were exposed to high-velocity gas flow. It may be that the larger overpressure durations were directly responsible for the more extensive hemorrhage, but bleeding at the brain surface is also consistent with head acceleration,[81] likely present in some of these cases. Skull flexure likely played a role in fixed head tests.[50]

Results from the present study show that injury severity (lesion count and size) was dependent upon peak overpressure and that the threshold for the small lesions was between 150 and 230 kPa. Peak overpressure is the blast wave characteristic that is most often correlated with injury severity in blast research.[8, 20, 65] Although direct comparison between different blast wave generation methods and testing setups is difficult, studies testing several blast levels have invariably found increased evidence of injury at higher overpressures.[33, 65] While investigations addressing vascular injury are limited, Reneer[51] reported a positive trend of increasing IgG expression with increasing peak pressure. His data also showed an apparent threshold at about 150 kPa, similar to that seen here, even though their durations were much longer (5 ms).

Peak overpressure clearly plays a significant role in TBI severity, but other blast wave parameters, including pressure rate, and both positive and negative phase durations and impulses, may also be important factors. Our study did not directly address these other parameters, but changes in injury severity over the large range of overpressure investigated here were not dramatic, and all injuries

appeared to be relatively mild. A larger duration would be expected to result in more severe outcomes. Despite the relatively short positive phase duration and low-impulse in the present work, injuries were observed at overpressure levels similar to those in experiments with much longer durations and larger impulses.[49-51] This suggests that duration and impulse may play a relatively minor role, but this comparison is not reliable since, as discussed above, the nature of the injuries observed was different, and multiple modes of loading may have been involved in the earlier studies. In fact, Reneer[51] reported significantly more severe vascular injury at 175 kPa and 5 ms than at 250 kPa and 4 ms, indicating that even a relatively small change in duration was influential. Again, however, this may be more closely related to blast- or flow-induced acceleration than to wave propagation.

It is interesting that the other independent variable in our study, survival time, did not appear to be influential. This suggests that all lesions were acute and not a result of any delayed BBB opening associated with inflammation, as has been reported in conventional TBI.[82] The previous blast-induced BBB disruption studies had shown peak IgG at three[50] and 24 hours,[49] with resolution by three days, but again, these injuries were different from those we've reported. It is unknown why the time required to clear displaced IgG would be any different in the present case, but longer survival times should be studied to determine the time required for clearance.

As mentioned, the duration of the blast wave in this study was considerably shorter than that of a typical explosion. However, considering the different sizes of human and rat heads, it may be important to scale wave

duration with mass[55, 83] or head size. A study of lung overpressure injury estimated that testing small animals in air-driven shock tubes with several millisecond overpressure durations was equivalent to testing humans at nuclear-level durations and impulses.[65] As a matter of reference, underwater explosions have been shown to involve durations similar to those presented here but with much higher peak pressures.[84]

In addition to its short duration, the blast wave used in this study has a number of characteristics that are not representative of ideal free-field blast. As the wave expands into space from the end of the tube, it does so in an axisymmetric rather than a spherical fashion. The peak pressure is greatest along the axis of the barrel and decreases along the wave front toward the periphery. As a result, any target in the field is exposed to a pressure gradient along the wave front, perpendicular to the direction of propagation; in contrast, a spherical expansion results in the same pressure along the front. Additionally, because the peak pressure drops rapidly with distance from the end of the tube, it is necessary to place the target very near that exit. Consequently, there is considerable curvature to the wave front, again leading to a different pattern of loading than the nearly planar front of a free-field blast after traveling some distance. Despite these shortcomings, there was no sign of uneven loading reflected in the injuries we observed. Both of these effects would be reduced for a small target, so their lack of apparent influence here may be attributable to the small size of the rat head.

In conclusion, we report a pattern of primary blast-induced vascular injury that appears to be distinct from vessel damage associated with conventional TBI.

Together with a similar study where non-vascular brain injuries following primary and composite blast exposures were found to be different,[72] this research suggests that primary blast TBI is a unique entity. In both of these investigations, the injuries appeared to be mild, but more work is recommended to further define their characteristics and significance.

CHAPTER 3

BEHAVIORAL AND INFLAMMATORY CONSEQUENCES OF CEREBROVASCULAR DYSFUNCTION IN PRIMARY BLAST INJURY

3.1 Introduction

Traumatic brain injury resulting from exposure to explosive blast is an ever-present risk for military populations. Defense department records indicate that over 300,000 soldiers have suffered a TBI in the last decade, many of these blast-related. Victims of blast exposure often suffer long-term neurological dysfunction; limited options for either diagnosis or treatment, and the resulting years of rehabilitation and reduced quality of life makes blast TBI a significant medical issue for the foreseeable future.[44] A better understanding of injury mechanisms and progression will provide the knowledge foundation for improved therapies.

Blast overpressure is caused by a sudden expansion of high pressure gas into the ambient environment, and is described by an idealized Friedlander curve[5]. This curve contains features such as the maximum overpressure, positive phase, negative phase, and impulse that have been described previously[59]. In practice, blast waves will reverberate or interact with solid objects; distorting them from the idealized curve. Blast injuries are categorized by mechanism, generally

defined as primary, secondary, tertiary, and quaternary injury modes.[36] Early focus on primary blast exposure highlighted respiratory damage, including alveolar hemorrhage, interstitial edema, rupture of the alveolar septa, and vascular air embolism.[20, 21] Advances in body armor have improved thoracic protection and increased blast survival rates,[33] resulting in modern interest in blast-related neurological injury. Injury mechanics are currently unclear; however shearing, spalling, and cavitation have been suggested as brain tissue absorbs energy from the overpressure wave.[22] Other hypotheses include vascular surge from blast exposure to the body, and skull flexure.[29, 30] It is also unclear what relationship the physical characteristics of the blast wave, such as positive pressure phase duration, negative phase, total impulse, and peak pressure, have to injury severity.

Blast TBI has been extensively explored by recent research; however, limited attention has been paid to the response of the cerebral vasculature. Additionally, a variety of experimental approaches and diverse loading modes ranging from free-field explosions, compressed gas and combustion shock tubes, and even ultrasound[70] make direct comparisons difficult. Vascular dysfunction appears at the heart of most blast pathology, and conventional TBI research has highlighted the major role of blood vessels in both initial injury and subsequent inflammation and wound healing.

Our initial study[59] determined that our short overpressure duration primary blast injury device created focal BBB disruption and left depositions of IgG in the parenchymal brain tissue. The objective of this study was to further characterize our short overpressure duration blast injury model by performing an increased

panel of histological markers focused on areas of IgG extravasation, and to explore any resulting functional changes in behavior, and following development of injury out to 30 days. Our hypothesis was that reactive gliosis and neuronal cell death would occur at lesion locations, resulting in cognitive and motor dysfunction. A range of stains and immunohistochemical markers: GFAP, CD68, NeuN, NF-160, and Fluoro-Jade B, were used to identify the brain's inflammatory response and subsequent neuronal loss. Neuronal injury causing observable deficits in animal performance for our selected behavioral assays supports the idea that these lesions have a deleterious effect on animal health and are relevant clinically.

3.2 Materials and Methods

Primary blast overpressure was generated by detonating an oversize explosive primer in an otherwise empty casing in a modified 0.308 bolt-action rifle (Savage Arms; Axis) with a 55.8 cm barrel, based on an approach described previously[58, 59]. Open field and novel object recognition tests were performed in a circular arena 112 cm in diameter and enclosed in a confined space using black nylon curtains in a light- and temperature-controlled behavior room. A standard set of Von Frey fibers was used to elicit a pedal withdrawal response. Rat behavior was recorded using a video camera and analyzed using Ethovision v. 9.0 software.

Male Sprague-Dawley rats (average weight 337 ± 14 g) were used according to protocols approved by University of Utah IACUC. Animals were allowed access to food and water ad libitum during testing. Animals were first

anesthetized with 5% inhalation isoflurane and suspended in a Kevlar sling to protect the lungs. The animal's head was positioned offset from the muzzle to avoid gas jet loading or contact with burning propellant.[72] Distance and angle were adjusted to produce a 323 kPa blast exposure, with distance measured from the center of the muzzle to the furthest projecting lateral point of the ipsilateral supraorbital process. Following blast exposure, animals were sacrificed at 2 days, 7 days, and 30 days for histology in order to ascertain long-term inflammatory consequences of blast injury. Animals performed behavioral testing before blast exposure, and then following at each time point for as long as they were scheduled to survive. Euthanasia was performed by isoflurane overdose followed by transcardial perfusion with 150 ml of phosphate buffered saline (PBS) and 150 ml of 4% paraformaldehyde (PFA) at 42 $mL*min^{-1}$. Brains were removed and post-fixed in PFA for 24 hours. Control animals received isoflurane induction and suspension in the testing harness but no blast injury.

The open field paradigm has been widely used for evaluation of motor impairment and anxiety in rodents. Animals were acclimated to the behavior room for 1 hour before commencement of testing. At the beginning of testing, each rat was placed in a compartment (20x40 cm) in the open field arena for 1 minute acclimation, after which the compartment was lifted for the rat to freely explore the arena for 15 minutes. The arena was divided into four concentric zones and time spent in each zone was measured. Movement was recorded using a video capture system and metrics were analyzed with video tracking software to assess stressed or injured behavior. Each animal was then transported back to their cage after the session, and the apparatus was cleaned with 70% ethanol to

minimize scent cues between each tested animal.

Novel object recognition has been widely used for evaluation of spatial memory in rodents. It has been shown that animals with memory deficits tend to spend less time examining new objects in their environment than naive rats.[85] The circular arena and camera setup from the open field testing was used to evaluate behavior. Animals were acclimatized to the arena for 15 minutes and then allowed to explore two identical objects for 5 minutes during the sample phase. The animal was then restrained in the 20x40 cm compartment and the objects were removed for a 5 minute inter-trial interval (ITI). Finally, one familiar sample object and a novel object were placed in the same positions as the original sample phase objects and the animal's exploration was recorded for another 5 minutes. Each animal was then transported back to their cage after the session and the apparatus was cleaned. Testing occurred prior to blast, and then at 2, 7, and 30 days, depending on the survival group. Entirely new sets of novel and sample objects were used at each time point so that rats never saw the same novel or sample object in more than one test.

Animals were also tested for pain and reflex behavior using the Von Frey hair test. Testing was completed in the same light- and temperature-controlled behavior room as the open field test. Animals were again acclimated to the behavior room and placed in an array of six 15x30 cm mesh bottomed cages for 1 hour before commencement of testing. Von Frey hairs of ascending stiffness were applied to the bottom of the animal's paw until a pedal withdrawal reflex was observed using the up-down method, and pain thresholds were then calculated using Bruceton analysis. Following testing, animals were transported back to

their cages after the session and the apparatus was cleaned.

Brain tissue between the pineal gland and the olfactory lobes was serially sectioned into 100 µm coronal sections by vibratome. Sections were processed using indirect immunohistochemistry for rat IgG (0.5 mg/ml, Biotinylated GtxRt IgG1, Southern Biotech, Birmingham, AL). Briefly, antibodies were diluted in blocking solution consisting of 4% (v/v) goat serum, 0.1% (v/v) Triton-X, 0.5% (w/v) sodium azide in PBS. Free floating tissue sections were batch incubated in block for 1 hour at room temperature and then for 24 hours in primary antibody solution at room temperature. After three rinses in PBS (1 hour/rinse) to remove unadsorbed antibody, sections were incubated with fluorescently labeled secondary (0.5 mg/ml, Streptavidin-conjugated AlexaFluor-594 1:500, 2 Invitrogen, Carlsbad, CA) for 24 hours at room temperature and again rinsed three times with PBS (1 hour/rinse). Sections were counterstained with DAPI (10 mM) to image cell nuclei.

Immunoglobulin G (IgG) extravasation was used to detect displaced plasma in brain tissue. Sections were imaged using a Coolsnap digital camera (1040x1392 image resolution) mounted to an upright epifluorescent microscope (Nikon; Eclipse E600) using a 4x (NA = 0.13) objective at 2.5 seconds exposure time and controlled mercury lamp and aperture settings. Images were light field corrected using no-primary controls. Lesion size and location were measured using a semi-automated script written in Vision Assistant (National Instruments; LabView) described in detail previously[59].

Sections were co-stained for neuronal damage around IgG lesion locations using Fluoro-Jade B (0.0004% solution, Millipore, Billerica, MA), an

anionic derivative of fluorescein that indicates neuronal degeneration. Fluoro-Jade staining was done according to standard protocol involving, briefly: mounting to gelatin coated slide, graded alcohol dehydration, potassium permanganate solution, Fluoro-Jade incubation, xylene, and mounting. Adjacent sections from the 48-hour survival group were analyzed for glial fibrillary acidic protein (GFAP, 2.4 mg/ml, RbxRt anti-GFAP IgG1, Southern Biotech), a marker for astrocytes and astrogliosis. GFAP horizontal line intensity profiles were measured across single 10x objective (NA = 0.45) fluorescent microscope screen captures. Horizontal line profile height was defined as the mean pixel value of a horizontal bar two standard deviations of thresholded IgG lesion size (68.27% of mean diameter of lesion) in height across the image of each lesion. Since both IgG and Fluoro-Jade are expected to be cleared from the brain within 7 days,[74, 86] additional markers were used to determine sites of inflammation and neuronal loss (Table 3.1). Neuronal nuclei (NeuN, 2.0 mg/ml, Millipore) and neurofilament (NF-160, 0.5 mg/ml, Invitrogen) were visualized to examine the density of both nerve bodies and processes. Regions of low fluorescence in these combined markers (collocated with high fluorescence in the inflammatory marker it will be paired with) were expected to give likely lesion location for time points beyond 48 hours. Seven-day animals will have sections stained with combined NeuN/NF-160 and GFAP, and adjacent sections with NeuN/NF-160 and CD-68 (ED-1, 0.5 mg/ml, AbD Serotec, Raleigh, NC), a marker for activated macrophages and microglia. Primary antibodies for co-markers were batch incubated with IgG primary antibody for 24 hours at room temperature, rinsed 3x with PBS (1 hour/rinse), incubated with appropriate secondaries for 24 hours at RT, rinsed 3x,

and then mounted on glass slides and coverslipped with Fluoromount-G (Southern Biotech). Changes in 30 day survivals were queried using NeuN, NF-160, IgG, and GFAP markers. Statistical significance of peak overpressure and survival time was determined using one-way ANOVA and post-hoc Tukey HSD tests. Differences are considered to be significant for p-values less than 0.05.

3.3 Results

As observed with this injury model previously, animals exposed to blast displayed an increased number ($p < 0.0001$) of high fluorescence focal areas indicating locations of IgG extravasation and thus BBB dysfunction at 48 hours post injury (Figure 3.1). The number or volume of suspected lesions at 7 and 30 days were not significantly different from controls ($p = 0.86$ for 7 day and $p = 0.13$ for 30 day), indicating the transient nature of BBB permeability and clearance from tissue by phagocytic cells. A similar lesion incidence for this level of blast overpressure was observed in our previous study.[59]

A reduction in GFAP immunofluorescence intensity, surrounded by a slight increase in fluorescence, was observed at lesion locations at 48 hours. Average GFAP fluorescence decreased at the center of a lesion compared to background levels (Figure 3.2). Control images did not display this decrease in GFAP fluorescence intensity at high IgG fluorescence locations (Figure 3.3). Similarly, GFAP intensity did not appear to vary from background in 7 day or 30 day survivals, though it was not possible to assess regions where traumatic IgG lesions had been since they were cleared out by these later survival times.

Table 3.1: Histological assays and time points showing panel of markers used to characterize inflammation and neuronal degeneration post blast injury.

	Control	48 hour survival	7 day survival	30 day survival
IgG	x	x	x	x
GFAP	x	x	x	x
Fluoro-Jade	x	x		
NeuN/NF-160	x	x	x	x
CD68	x		x	

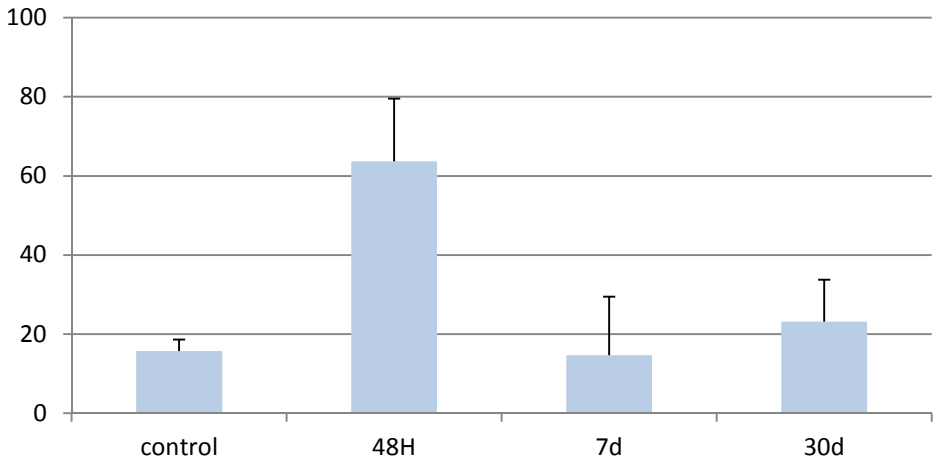

Figure 3.1: Focal IgG deposits in parenchymal tissue where blood-brain barrier breakdown suspected. Number of lesions increase 48 hours post blast, and revert to background control levels at 7 and 30 days.

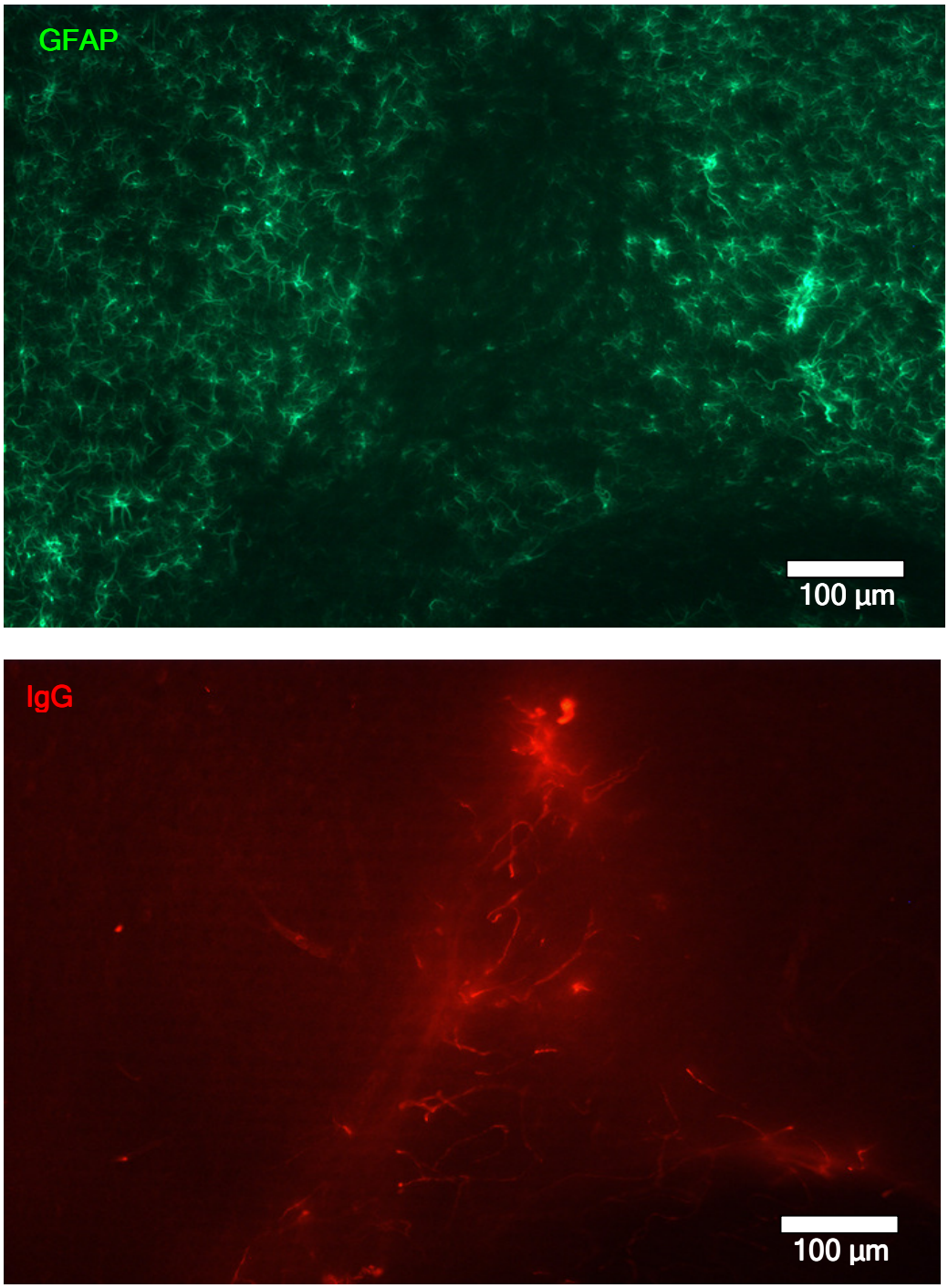

Figure 3.2: GFAP depletion co-localized with multiple IgG lesion cluster 48 hours post blast shown in this 10x image.

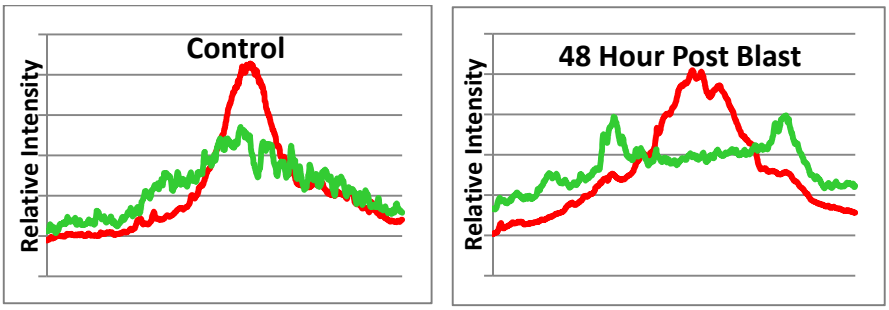

Figure 3.3: GFAP relative intensity line profile comparison to IgG at same location. GFAP decrease in lesion center, with increase on lesion periphery seen at 48 hours post blast, which was not seen at high IgG fluorescence / suspected lesion locations in control animals, or in 7 day or 30 day survival blast animals. Relative intensity was compared using base peak normalization, where local pixel intensity is divided by maximum pixel intensity in the image.

Some Fluoro-Jade B staining was observed associated with neuronal cell bodies in both controls and blast survivals; however, degradation of immunofluorescence by the Fluoro-Jade protocol disallowed co-localization analysis with lesion locations. No CD68 immunoreactivity was observed at the 7-day time point, and no characteristic differences in neuronal nuclei (NeuN) or neurofilament (NF-160) were seen between blast exposure survival times or controls.

Open field exploration showed a slight, nonsignificant difference ($p = 0.12$) in total distance travelled in blast animals compared to controls (Figure 3.4). Anxiety, measured as the ratio of center time against time spent at the perimeter of the arena, did not differ between bTBI animals and controls (Figure 3.5). Novel object recognition showed some changes to exploration time in blast animals compared to naive testing (Figure 3.6). A nonsignificant increase in exploratory behavior ($p = 0.11$) was seen 48 hours after blast exposure compared to baseline controls; however, this was also seen in our time matched controls. A similar

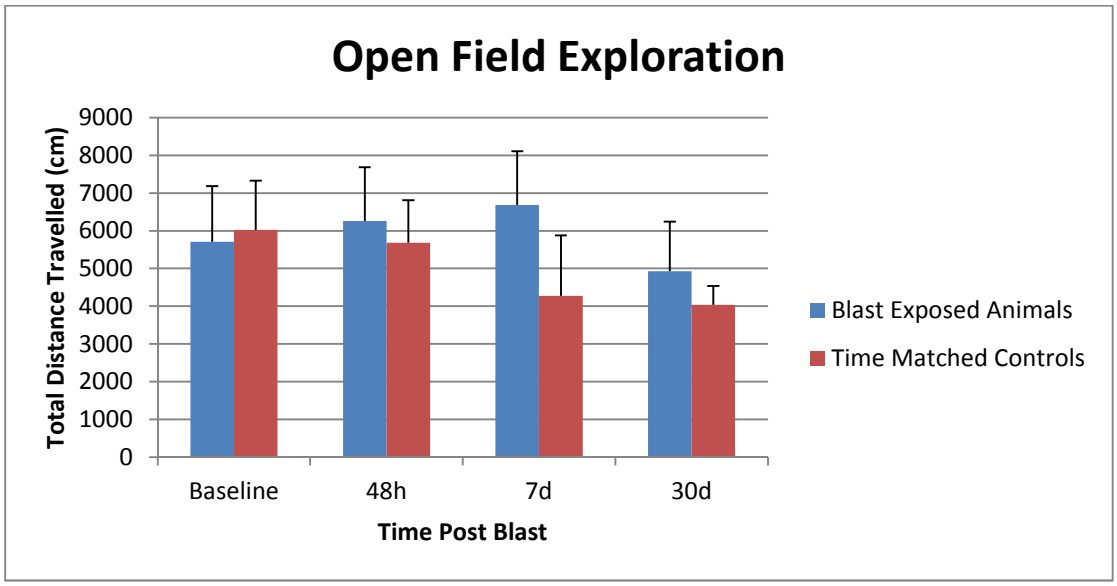

Figure 3.4: Open field test showing total distance travelled by rats exposed to blast as a measurement of motor function. No significant differences between time points for blast-exposed animals or controls.

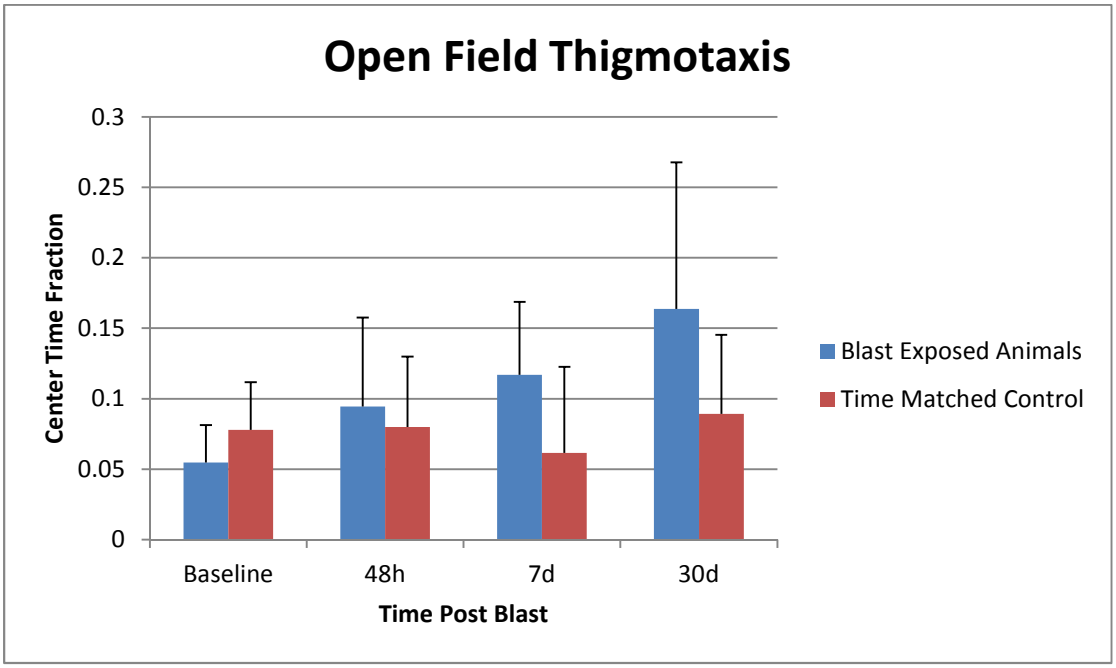

Figure 3.5: Open field test showing time spent by animal exploring center of arena, a measure of anxiety. No significant differences between time points for blast-exposed animals or controls.

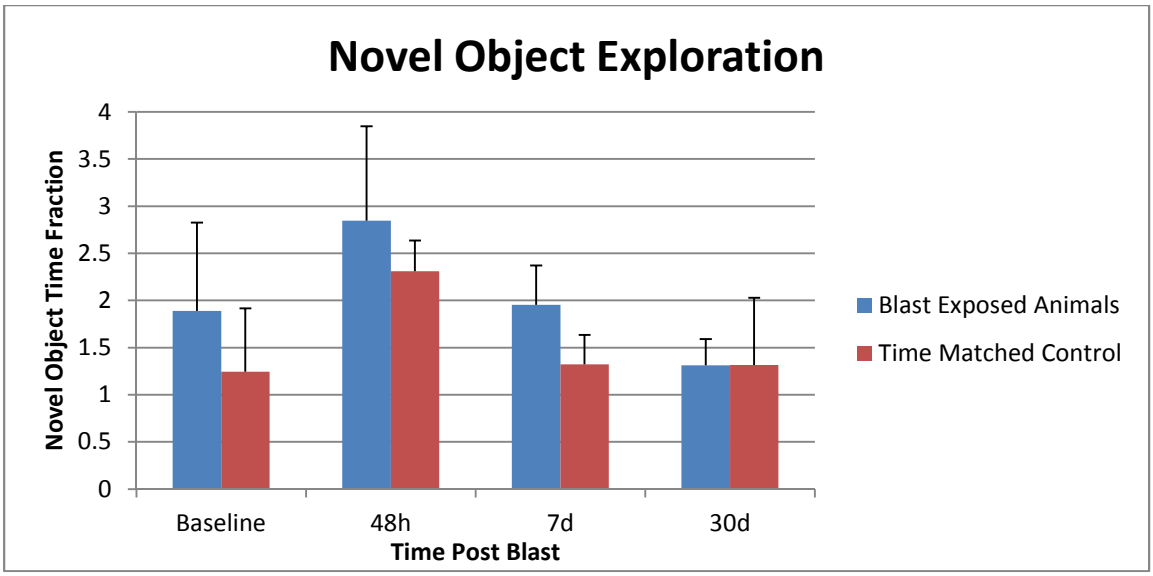

Figure 3.6: Novel object exploration showing time spent exploring novel object in arena vs. time spent re-examining familiar object from familiarization phase of test, a measurement of stimulus recognition and memory. A nonsignificant increase (p = 0.11 and p = 0.14) was seen at 48 hours from baseline tests for both groups.

decrease in novel object exploration was seen with both blast and naive groups.

Nociception testing using the Von Frey fiber assay displayed the most dramatic difference in behavior following blast injury. One hour post blast displayed a significant increase in stimulation thresholds (P = 0.012), which returned to baseline levels within 24 hours (Figure 3.7).

3.4 Discussion

The objective of this study was to determine mechanisms driving vascular injury and consequences of blood-brain barrier failure using a low-impulse blast tube. Our injury model appears to create a mild injury characterized by transient disruption of the blood-brain barrier; however, few clear outcomes were

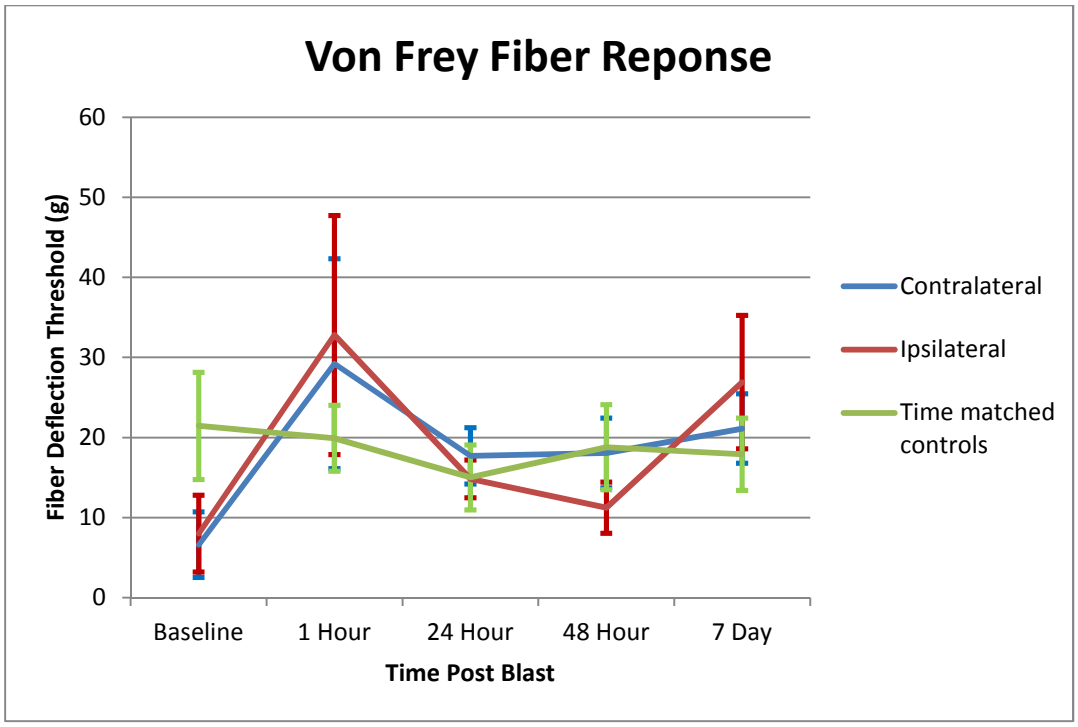

Figure 3.7: Von Frey nociception and pedal withdrawal reflex showing decrease in sensitivity 1 hour post blast. Fiber deflection threshold is the stiffness rating, equaling the mass required to bend the fiber when applied at 1 g.

measured for other markers of inflammation, or for behavioral effects. A mild inflammatory astrocytic response was observed as a result of low-impulse blast exposure and subsequent focal BBB disruption. Similarly to our previous study, a significantly higher number of IgG depositions occurred in blast-exposed brains at 48 hours compared to controls, which seems to resolve by 7 days back to background levels.

The presence of a low level of focal deposits of IgG in control animals is suspected to be from either capillary rupture during terminal perfusion, natural transient opening of the blood-brain barrier for cellular migration or angiogenesis, or false positive readings from our automated image analysis system. If vessel rupture during perfusion occurs, then caution is warranted in any analysis of

blood-brain barrier disruption using this common histological preparatory technique. However, the significantly higher incidence of lesions in blast-exposed animals indicates some effect from low-impulse primary blast. It may be the case that our blast exposure model caused weakening of some blood vessels, but not outright rupture, which then occurred during the perfusion process. This may explain the lack of other downstream inflammatory and behavioral effects in this model of mild bTBI. It has been recognized that the BBB is not entirely impermeable,[87-89] and that this presents a limitation for macromolecular extravasation assays such as Evans Blue dye, fluorescently labeled dextran, or IgG as markers for vascular disruption.[74, 90-93] This likely warrants accepting some standing "lesion" count and comparing blast levels to control cases. Finally, false positives are possible with our automated analysis script, despite our best efforts to minimize them and provide a conservative estimate for lesion number and size. However, it is unlikely any bias exists between test cases for this background level artifact, and highlights the importance of statistical comparison between controls and blast-exposed animals.

IgG lesions increase at our 48-hour time point, and then decrease to control background levels at later time points. This was expected due to clearance of IgG by both microglial phagocytosis and Fc-receptor-mediated efflux.[94] This limits the utility of using IgG as a vascular injury marker for bTBI at chronic time points. Possible alternatives are fluorescently labeled dextran or radiolabeled markers,[91] or microsphere perfusion.[95] Nevertheless, IgG has the advantage of being an endogenous agent, and is appropriate for short survival times.

Short-term survivals displayed an increase in GFAP immunofluorescence around the periphery of the IgG zone coupled with a decrease in fluorescent intensity in the center of the lesion, a finding that has not been reported in other studies of blast injury. GFAP levels are commonly assayed in bTBI and TBI; however, results have varied from a general increase,[16, 62, 96, 97] a decrease (6 hours) followed by an increase (24 hours),[98] or no change in levels.[49, 99-102] GFAP expression is highly heterogeneous throughout the brain, and it is difficult to try to ascertain where IgG depositions existed in animals that resulted from injury by measuring the GFAP fluorescent signal alone at time points after IgG has been cleared. However, as no evidence of GFAP reduction co-localized with IgG fluorescence was seen in either controls or later time points in this study, it appears that the high incidence of IgG lesions in our 48-hour animals represents a distinct astrocytic response following blast injury, and can help identify true lesions from perfusion or image analysis artifacts. A possible explanation for this may be some kind of immunohistological blocking effect against GFAP by IgG or some other plasma protein; however, if this were the case, we would expect to see it in all cases of IgG fluorescence, not just in 48-hour cases.

Our battery of additional markers did not show a discernible difference between blast-exposed brains and controls. The primary blast exposure model used may be insufficient to trigger cell death necessary to see a difference using the Fluoro-Jade-B, NeuN, or NF-160 markers. We also did not see a difference in microglial activation using CD68 between control animals and blast-exposed, although as macrophages do not become active until after 48 hours post injury, our time points were perhaps inappropriately selected for this particular marker

and examining at 3-5 days would have yielded more useful results.

Behavioral testing has been used to assess the consequences of bTBI. Some of the most common issues reported by bTBI patients are anxiety, impaired fine motor control, and memory dysfunction. Various studies have reported findings that share some typical features. Our study sought to characterize motor, anxiety, and memory behavioral deficits resulting from low-impulse blast exposure, especially in relation to focal BBB vascular rupture or dysfunction seen as a result from our device. In addition, nociception and mechanical sensibility in bTBI have not been explored, and thus the Von Frey fiber assay was used to investigate this unknown area.

A common test administered for motor function and general anxiety is the open field (OF) paradigm. OF testing showed a nonsignificant decrease in total distance travelled by bTBI rats, which was also seen in controls. This may be due to habituation of rats to the arena, or continuing growth and weight gain that rats showed over the 30-day time span, but appears to not be affected by low-impulse primary blast. Center time fraction, indicative of anxious and motor-impaired behavior,[16, 100, 101, 103-105] was highly variable during testing. Blast exposure did not demonstrate an effect, supporting our suspicion that our testing apparatus is at the threshold of detectable injury.

Previous work[103, 106] suggested that animals with significant TBI spend less time exploring a novel object placed into the arena than uninjured animals; however, our novel object results were inconclusive. During the novel object behavioral assay, animals in both the control and blast-exposed groups displayed an increase in exploratory behavior at the 48-hour time point. This is perhaps due

to increased habituation to the arena space. Others have reported distinct memory impairment from blast injury using larger scale blast tubes with longer overpressure durations,[85, 99, 107] highlighting the importance of impulse and overpressure duration in functional outcomes of blast injury. Literature[108] suggested that bTBI animals would be less sensitive to the Von Fray hair test, and require a stiffer fiber to elicit a pedal withdrawal reflex. We saw that this was indeed the case, requiring a fiber nearly twice as stiff to trigger response 1 hour after blast. Animals quickly return to baseline sensitivity, indicating that this effect is transient. Initial concerns over confounding effects from anesthesia were put to rest by fairly consistent behavior from our time matched control group.

Several other approaches were considered in assaying both cognitive performance and neuronal degeneration. Decreased motor function has been measured using Rotarod[16, 99, 109] skilled reaching task, and beam walk.[99] Increased anxiety in blast animals has been seen using elevated plus maze,[100, 104] acoustic startle,[101] and light/dark box.[105] Open field was selected for its low animal stress, repeatability, and resistance to animal learning bias.[110] Performance on the novel object recognition (NOR) test have reported a decrease in exploration of the unfamiliar object compared to baseline,[85, 99, 107] indicating a deficiency in memory. Likewise, Morris water maze testing has shown latency to find platform increase among blast-exposed animals,[100] and active avoidance associative memory learning has also shown a decline in performance for bTBI animals.[16] A Morris water maze apparatus was considered to test spatial learning and memory as an alternative to the novel object recognition test; however, it was rejected due to concern over the test's inherent

higher level of animal stress.[110]

Additionally, other neuronal degeneration and inflammation markers have been used to determine the effects of plasma in brain tissue. An amino cupric silver stain has been traditionally used to visualize degenerating axons, while a multitude of different inflammatory signal molecules have been used as tools for measuring traumatic brain injury, including: β-APP, amyloid precursor protein that is a major component of plaques in Alzheimer's disease and is evident following TBI[49, 111]; Tau, a CNS microtubule protein that has been linked to poor outcomes following TBI[98, 112]; myelin basic protein (MBP), a critical protein for axonal myelination and a TBI biomarker[113]; and S100B, a glial specific biomarker for blood-brain barrier permeability and CNS injury[35, 39, 113].

Although our short duration model of bTBI produced only mild injury, it highlights the importance of overpressure duration in injury severity. Even this type of mild bTBI may cause impairment in humans which was not measurable in rodent models using indirect behavioral testing. Since military personnel are exposed to blast overpressures of varying durations, it is important to understand the effects of impulse and any brain injury that might occur.

CHAPTER 4

THE EFFECT OF OVERPRESSURE DURATION ON INJURY SEVERITY

4.1 Introduction

Research on traumatic brain injury from explosive blast faces challenges in drawing comparisons between various methods used to simulate or generate blast overpressure. Overpressure threshold for lung injury has been widely studied[55, 105, 114-116] and is estimated to be between 30 and 40 kPa. Less clear are thresholds for bTBI; however, most studies use levels above 110 kPa,[57, 59, 117] or roughly one atmosphere above ambient. There is some evidence that bTBI can occur at much lower overpressures, possibly as low as 28 kPa.[57, 105, 117]

This wide variation in potential injury threshold reflects that peak overpressure is only one of several features that contribute to the overall energy carried by the waveform, and thus influence the potential damage done to tissue. Our own studies found no evidence of injury at 150 kPa,[59] well above injury levels reported by other work, and only minimal signs of dysfunction in cellular response and behavior at higher levels. The most obvious difference in our overpressure exposure is the extremely short positive phase duration and associated low-impulse. Longer blast wave duration has been associated with higher mortality in lung injury studies,[20, 55] and more recent work has begun to establish a link

between overpressure duration and increased brain injury.[51, 118, 119]

An obvious step forward would be to create blast injury with similar overpressure levels but widely different impulse levels, and then use identical assays to measure injury effects. Our group has the generous cooperation of Developmental Head Injury Biomechanics lab at the University of Utah, who possesses a much larger high-impulse blast tube capable of producing overpressures up to 250 kPa and positive phase duration of 8 milliseconds, and would function to produce bTBI in an entirely different overpressure regime. Blast testing was initiated, behavioral testing was performed, and cellular changes were measured immunohistologically to compare the effects of positive phase and impulse.

4.2 Materials and Methods

Blast exposure was produced using a 5.21 m long, 14 cm internal diameter shock tube (Agile Nano) with a 64 cm driver section and a 4.57 m driven section (Figure 4.1A). Compressed air was used to charge the driver section to 650-685 kPa, which was separated by a .254 mm Mylar membrane. Membrane rupture consistently produced a blast overpressure wave of 250 kPa and 8 ms positive phase duration (Figure 4.2). Flush mounted PCB pressure transducers (PCB 113B26) were positioned at 61 cm intervals along the length of the driven section of the tube to verify blast wave development. Pressure sensors are rated to 3447 kPa and 1 MHz response. Data were collected at 0.5 MHz through a 500 KS/s A/D sampling device (National Instruments 9222). Signals were passed through a custom hardware anti-aliasing filter with a critical frequency f_c = 180

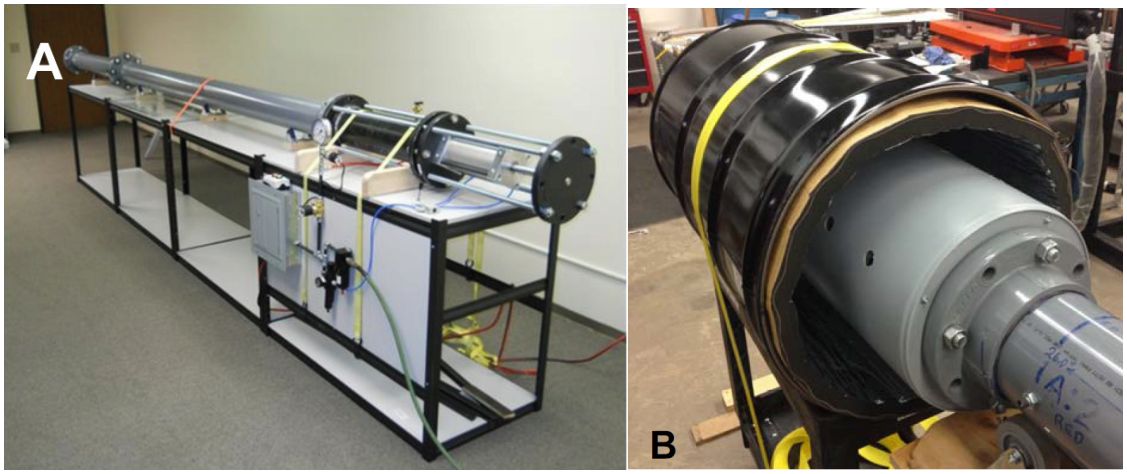

Figure 4.1: High-impulse blast tube setup showing (A) 5.2 m long, 14 cm diameter blast tube. (B) Silencer attachment for noise reduction.

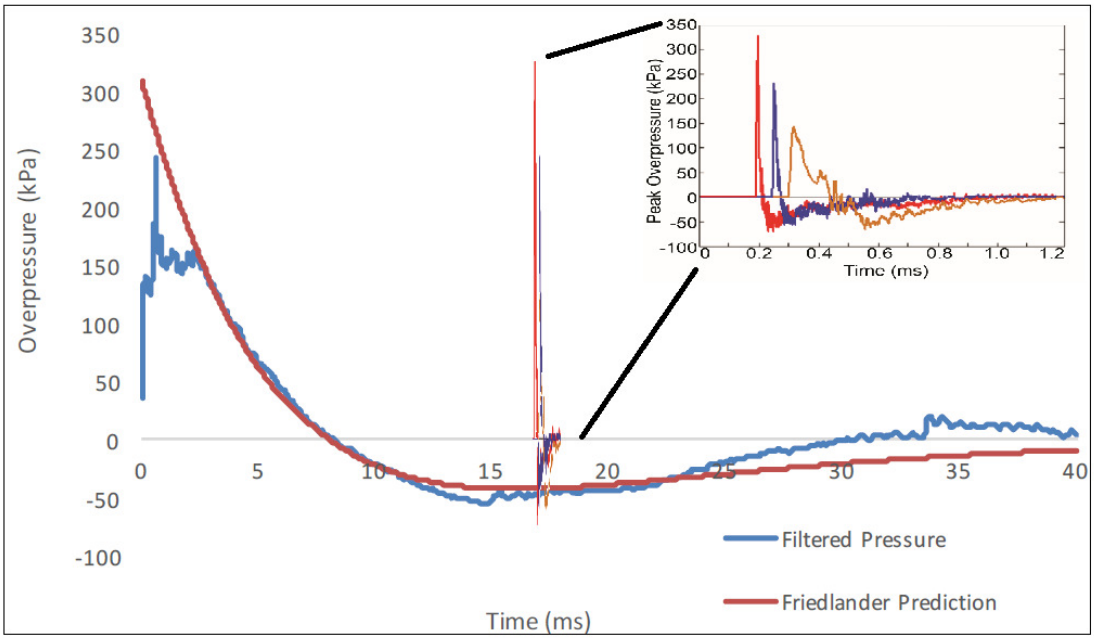

Figure 4.2: High-impulse blast overpressure trace, with scaled pressure traces from low-impulse rifle tube superimposed.

kHz, and post-filtered using a MATLAB fourth-order Butterworth filter. It was necessary to attach a muffling device to the muzzle of the tube built from concentric cylinders of foam and plastic and encased in a steel shell (Figure 4.1B). This introduced a reflected wave less than 10% of the magnitude of the primary wave, which was delayed until after the completion of the negative phase.

Male Sprague-Dawley rats (average weight 349 ± 36 g, n = 6 per group) were used according to protocols approved by University of Utah IACUC. Animals were allowed access to food and water ad libitum during testing. Prior to blast exposure, the animal was anesthetized with 5% inhalation isoflurane and immobilized in a Kevlar wrap to minimize injury to the lungs. The animal was positioned in a custom holder projecting perpendicularly from the shock tube barrel and projecting through a 7.62 cm hole that suspended the animal's head inside the tube. Blast overpressure was performed and animals were allowed to recover on a heated pad before being transferred back to their cages. Following blast exposure, animals were sacrificed at 2 days, 7 days, and 30 days for histology in order to ascertain long-term inflammatory consequences of blast injury. Animals performed behavioral testing before blast exposure, and then following at each time point for as long as they were scheduled to survive.

Euthanasia was performed by isoflurane overdose followed by transcardial perfusion with 150 ml of phosphate buffered saline (PBS) and 150 ml of 4% paraformaldehyde (PFA) at 42 $mL*min^{-1}$. Brains were removed and post-fixed in PFA for 24 hours. Control animals received isoflurane induction and suspension in the testing harness but no blast injury.

Brain tissue between the pineal gland and the olfactory lobes was serially sectioned into 100 µm coronal sections by vibratome. Sections were processed using indirect immunohistochemistry for rat IgG (0.5 mg/ml, Biotinylated GtxRt IgG1, Southern Biotech, Birmingham, AL). Briefly, antibodies were diluted in blocking solution consisting of 4% (v/v) goat serum, 0.1% (v/v) Triton-X, 0.5% (w/v) sodium azide in PBS. Free floating tissue sections were batch incubated in block for 1 hour at room temperature and then for 24 hours in primary antibody solution at room temperature. After three rinses in PBS (1 hour/rinse) to remove unadsorbed antibody, sections were incubated with fluorescently labeled secondary (0.5 mg/ml, Streptavidin-conjugated AlexaFluor-594 1:500, 2 Invitrogen, Carlsbad, CA) for 24 hours at room temperature and again rinsed three times with PBS (1 hour/rinse). Sections were counterstained with DAPI (10 mM) to image cell nuclei. Brain sections were mounted on glass microscope slides with Fluoromount-G (Southern Biotech) and then protected with glass cover slips.

Immunoglobulin G (IgG) extravasation was used to detect displaced plasma in brain tissue. Sections were imaged using a Coolsnap digital camera (1040x1392 image resolution) mounted to an upright epifluorescent microscope (Nikon; Eclipse E600) using a 4x (NA = 0.13) objective at 2.5 seconds exposure time and controlled mercury lamp and aperture settings. Images were light field corrected using no-primary controls. IgG lesions were quantified using color thresholding of images and particle filtering and analysis, described in detail previously.[59] GFAP (GFAP, 2.4 mg/ml, RbxRt anti-GFAP IgG1, Southern Biotech) and CD68 (ED-1, 0.5 mg/ml, AbD Serotec) were used as co-markers for

inflammatory activity in directly adjacent sections. Immunohistology procedure followed the process outlined in Chapter 2.

Open field and novel object recognition tests were performed in a circular arena 112 cm in diameter and enclosed in a confined space using black nylon curtains in a light- and temperature-controlled behavior room. A standard set of Von Frey fibers was used to elicit a pedal withdrawal response. Rat behavior was recorded using a video camera and analyzed using Ethovision v. 9.0 software.

Open field behavioral testing was used for evaluation of motor impairment and anxiety. Animals were acclimated to the behavior room for 1 hour before commencement of testing. At the beginning of testing, each rat was placed in a compartment (20x40 cm) in the open field arena for 1 minute acclimation, after which the compartment was lifted for the rat to freely explore the arena for 15 minutes. The arena was divided into four concentric zones and time spent in each zone was measured. Movement was recorded using a video capture system and metrics were analyzed with Ethnovision v9.0 tracking software to assess stressed or injured behavior. Each animal was then transported back to their cage after the session and the apparatus was cleaned with 70% ethanol to minimize scent cues between each tested animal.

Novel object recognition was used for evaluation of spatial memory. Animals were acclimatized to the arena for 15 minutes and then allowed to explore two identical objects for 5 minutes during the sample phase. The animal was then restrained in the 20x40 cm compartment and the objects were removed for a 5-minute inter-trial interval (ITI). Finally, one familiar sample object and a novel object were placed in the same positions as the original sample phase

objects and the animal's exploration was recorded for another 5 minutes. Each animal was then transported back to their cage after the session and the apparatus was cleaned. Testing occurred prior to blast, and then at 2, 7, and 30 days, depending on the survival group. Entirely new sets of novel and sample objects were used at each time point so that rats never saw the same novel or sample object in more than one test.

Animals were tested for nociception and reflex behavior using the Von Frey fiber test. Animals were again acclimated to the behavior room and placed in an array of six 15x30 cm mesh bottomed cages for 1 hour before commencement of testing. Von Frey hairs of ascending stiffness were applied to the bottom of the animal's paw until a pedal withdrawal reflex was observed using the up-down method, and pain thresholds were then calculated using Bruceton analysis. Following testing, animals were transported back to their cages after the session and the apparatus was cleaned.

4.3 Results

A significant increase ($p = 0.049$) in number of focal IgG depositions were seen following blast exposure, similar to what was seen with the low-impulse rifle blast tube (Figure 4.3). Interestingly, number of IgG lesions remained significantly different than control levels ($p = 0.044$) at 7 days post blast, a finding not seen using the low-impulse shock tube. GFAP expression showed a decrease in fluorescent intensity co-located with IgG lesion locations, which was common at 48 hours but rarely seen in 7 day animals and not seen at all in controls (Figure 4.4). Another finding not seen with the low-impulse tube was presence of

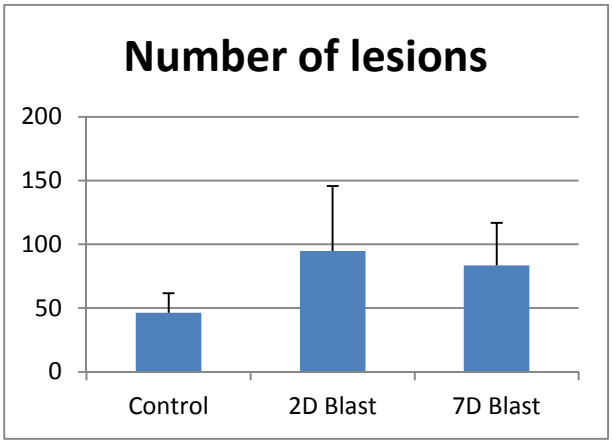

Figure 4.3: Number of focal IgG deposits seen in brain tissue per rat after blast exposure.

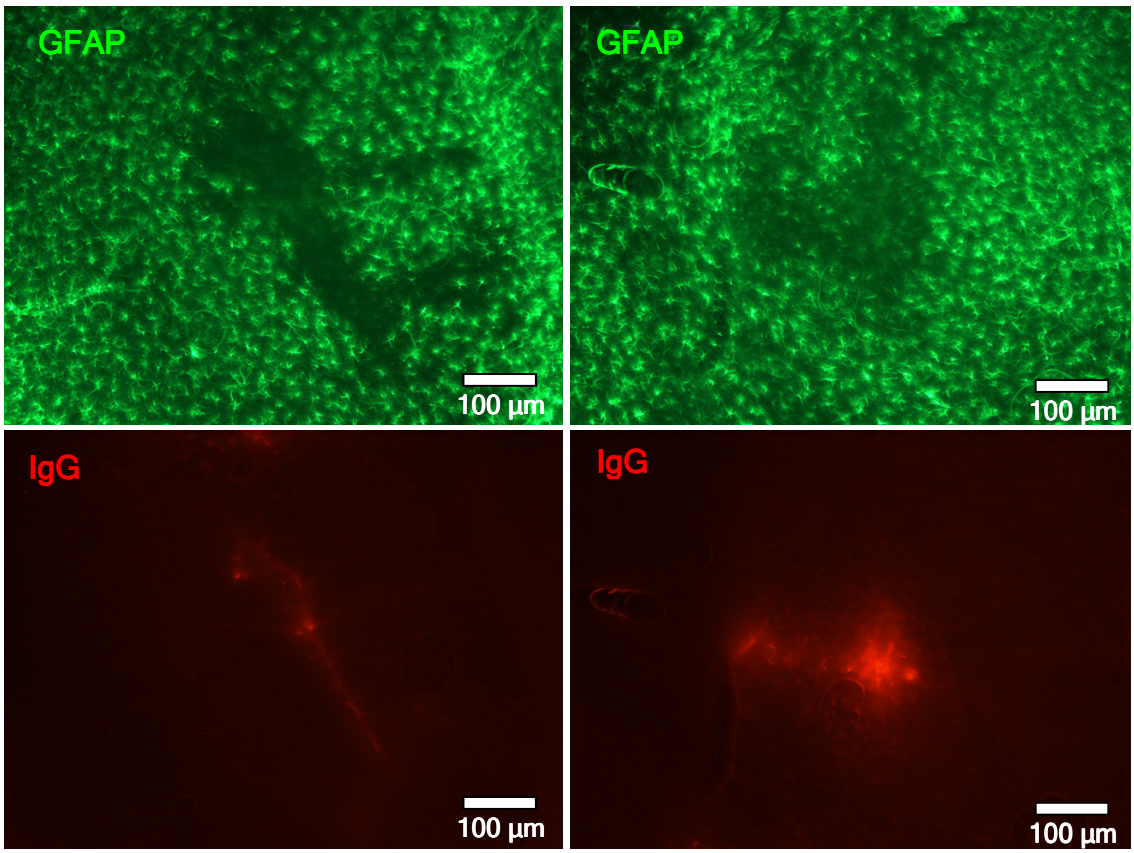

Figure 4.4: Two examples GFAP depletion (left pair in a 48-hour survival, right pair in a 7-day survival animal) at suspected lesion sites in 48-hour survival animals in a 10x image. This phenomenon not seen at IgG sites in controls.

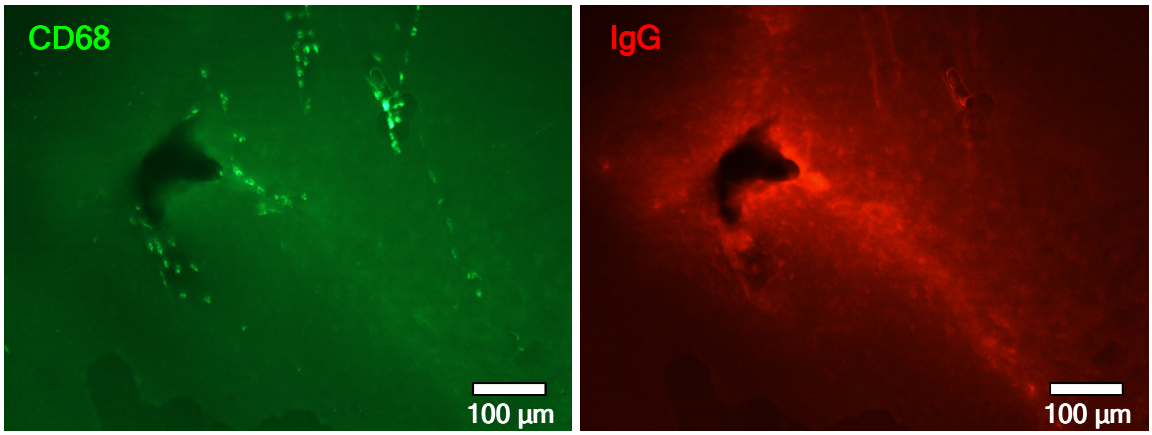

Figure 4.5: CD68 positive cells in vessels and tissue in 7-day survival animal, showing evidence of macrophage activity at suspected lesion area.

macrophage activity around blood vessels at suspected lesion locations (Figure 4.5).

Blast-exposed rats did not display a significant difference in behavior from controls during the open field test in measures of: locomotor activity (Figure 4.6) or anxiety (Figure 4.7). Novel object exploration was highly variable (Figure 4.8); however, a significant difference was measured between the control group at 48-hours and the blast-exposed groups ($p = 0.0002$ for the 2-day survivals and $p = 0.006$ for the 7-day group). Von Frey fiber testing again showed a significant ($p = 0.035$) decrease in sensitivity at 1-hour post blast (Figure 4.9), and also showed a nonsignificant ($p = 0.21$) increase in effect compared to low-impulse blast testing.

4.4 Discussion

The objective of this study was to compare the injury effects from a low-impulse blast tube device capable of BBB disruption with a much larger impulse device at a similar peak overpressure. In order to draw direct comparisons,

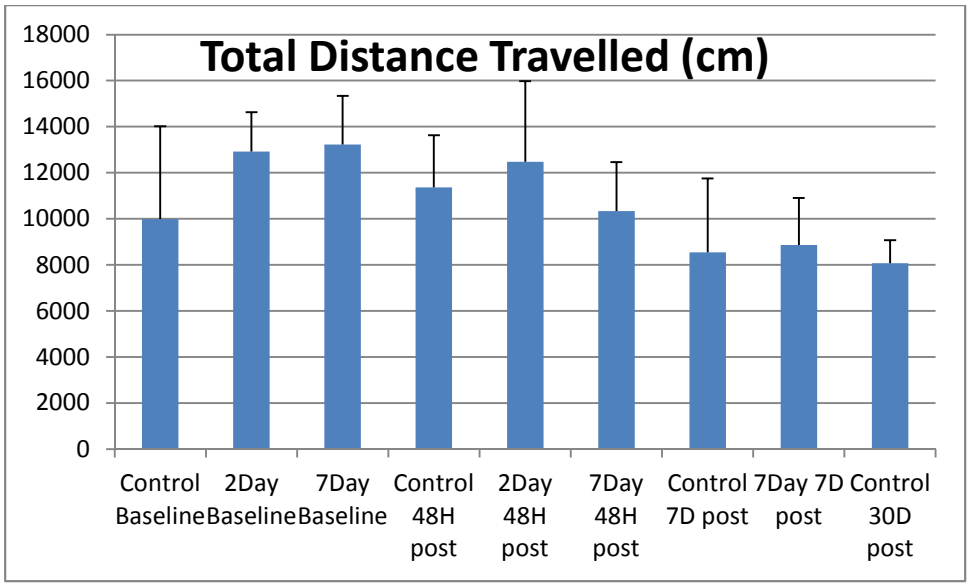

Figure 4.6: Distance travelled in free exploration over 15 minutes with no significant evidence of locomotor dysfunction in blast-exposed groups.

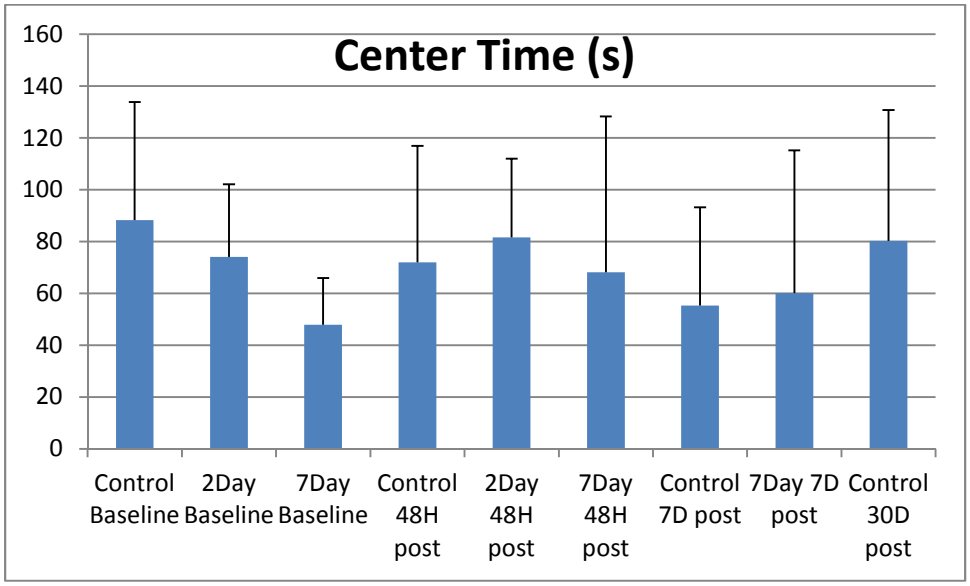

Figure 4.7: Center time fraction displaying anxiety measurement with no significant difference between control / baseline groups and blast-exposed animals.

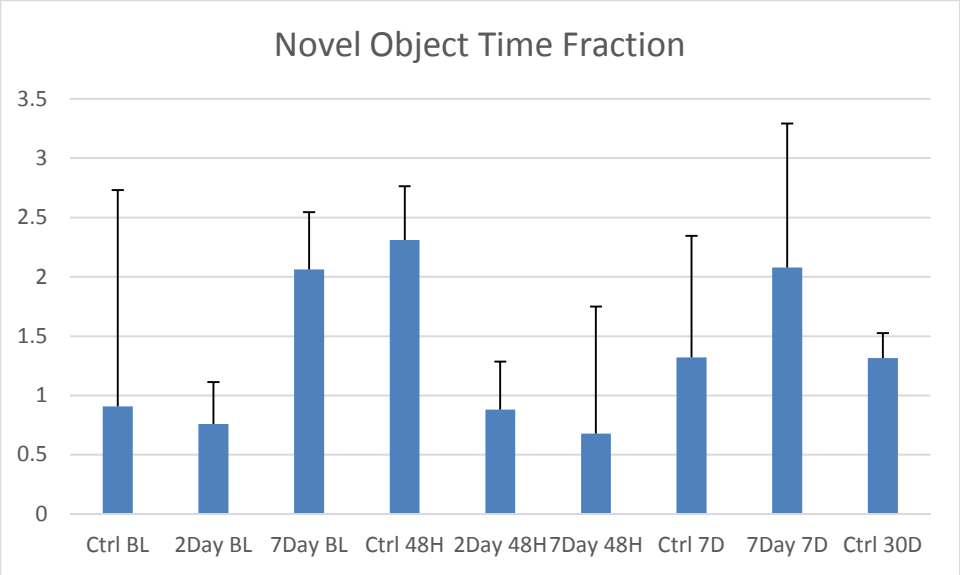

Figure 4.8 Novel object time fraction showing highly variable memory behavior for 3 groups n=6 at serial time points, comparing blast-exposed animals to controls.

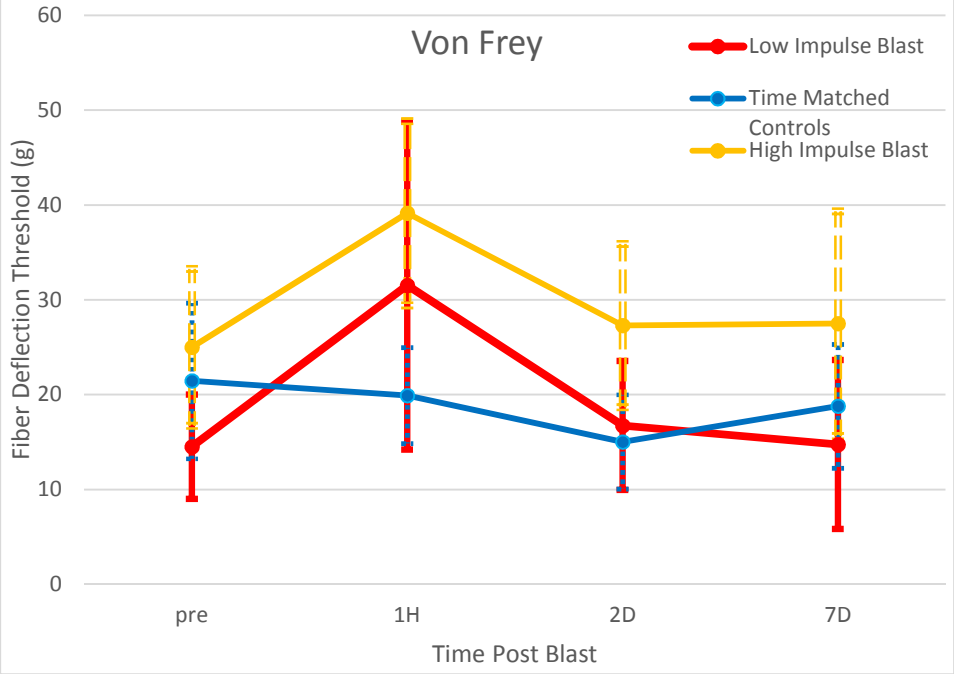

Figure 4.9: Von Frey fiber test showing significant increase in fiber stiffness needed to elicit response at 1-hour post-blast compared to controls. Averaged low-impulse blast response added for comparison.

identical methods were used as in Chapter 3 for immunohistological measurement of IgG extravasation, astrogliosis, and microglial response.

Functional changes were assayed using the open field, novel object recognition, and Von Frey pedal withdrawal paradigms. Although the maximum peak overpressure for the high-impulse device was slightly less than the low-impulse rifle blast tube (250 vs. 320 kPa), the vastly longer positive phase duration results in a greater than 300-fold increase in positive impulse, and thus energy carried by the wave form. Additionally, work from Chapter 2 shows that the difference in BBB disruption between 230 kPa and 320 kPa is non-significant for the low-impulse shock tube, giving us confidence that we may draw comparisons in injury severity between devices.

Histological measurements revealed increased persistence of IgG lesions in high-impulse bTBI animals up to 7 days post injury. Extravascular IgG in blast injury has been measured to taper off by 72 hours,[50] indicating that our blast exposure may have created a more severe injury, or increased vascular susceptibility to rupture at terminal perfusion. However, GFAP reduction at IgG locations provides evidence that at least some of the lesions seen existed in bTBI animals for some time before sacrifice.

Presence of CD68 positive macrophages at lesion locations is another indicator that long overpressure blast produces more serious injury. Macrophage activation has been recorded in blast injury[96, 120, 121]; however, whether activated cells are resident microglia, blood-borne macrophages, or both is unclear. In our histology, they appear to be densely clustered close to vessel walls, with fewer deep in tissue, which provides some evidence that they may be circulating

macrophages.

Behavioral testing results remained ambiguous, with the exception of the Von Frey test. Variability in distance travelled in the open field between sequential testing of the time matched control group had as wide of a spread as between controls and blast-exposed animals. Other studies using the open field test[16, 105, 122] have shown decreased spontaneous exploratory activity following blast. The open field test is relatively straightforward to administer, and no obvious issues with our methods or testing setup are apparent. Center time fraction, our anxiety measure, also displayed high variability within groups and no readily visible pattern, supporting the author's opinion that rats will do as they feel like on any given day.

Novel object testing did show a significant difference between blast animals and controls at 48 hours; however, the equally large difference between control animals on day 0 and the same group of control animals on day 2 (and therefore nonexistent difference between day 0 control measurements and blast-exposed animals) makes drawing any definitive conclusions from this testing unlikely. Another fact that creates doubt about these results is that four of nine testing groups, two being naive cases, had novel object exploration ratios less than one, which means they spent more time re-investigating the familiar object than the new one. Other groups that have used the novel object, Morris water maze, or other memory assays have reported a uniform decrease in memory performance following blast injury.[16, 85, 99, 100, 104] This bucks the expected paradigm of the test, and perhaps points to some problem in our methodology or testing setup. Objects used were similarly sized but variously shaped pieces of

solid aluminum, including cylinders, wedges, rectangular prisms, and irregularly cut shapes. Initial object bias was investigated during development of work in Chapter 3, but no noticeable preference was found for any of the selected pieces. In many cases, rats performed a cursory examination of an object and then ignored it for the rest of the trial, requiring novel object ratios to be set with only a few seconds of investigation. Uninteresting objects may have left our analysis vulnerable to low overall sampling times and few seconds either way of measurement variability.

The Von Frey fiber assay once again showed a significant ($p = 0.035$) decrease in nociception measured by pedal withdrawal reflex. The effect seen was nonsignificantly greater than the performance decrease in the low-impulse blast testing. This seems to confirm a decrease in tactile response and pain thresholds following blast injury, justifying further interest in peripheral nerve sensory dysfunction in blast injury. Natural endorphin release post-injury likely plays a role in this finding. As a practical matter, this supports the somewhat obvious recommendation that someone recently exposed to blast should avoid doing any critical tasks requiring fine motor skills, and also that the time period 1 hour after blast is the best window to perform potentially painful field medical techniques, such as moving the patient or setting a fracture.

A more serious issue affecting this study was the low number of animals available for blast injury and behavioral trials. Six animals per group is considered too low by many behaviorists, and more typical Ns for behavioral studies are 12-24 animals per group. We had hoped to at least see some new trends using resources available, but that was not seen with this round of

behavioral testing and we feel it would be more productive to explore other methods in the future for this research. It appears that more work is needed to elucidate the effects of impulse on blast injury severity.

CHAPTER 5

FURTHER IMMUNOHISTOLOGICAL EXAMINATION OF BLAST INJURY

5.1 Introduction

Inconclusive results in CD68 expression at IgG extravasation lesion locations following blast injury warranted further histological investigation. Macrophage and microglial involvement is classically seen when the blood-brain barrier is disrupted[123]; therefore, to either confirm or refute the lack of CD68 expression seen in Chapter 3, additional animals were exposed to blast using the tabletop rifle shock tube, and brains were sectioned at 30 μm and labeled for IgG, CD68, and IBA1. As some background and cross reactivity has been reported[124] using our previous NeuN marker, neuronal nuclear density was again measured using a non-mammalian antibody host species. Additionally, a single step anti-rat IgG secondary was used to visualize IgG in order to eliminate background fluorescence from endogenous biotin in the brain. Finally, quantification of volume of blood plasma leaked from blast-related BBB opening was estimated by measuring IgG fluorescence intensity.

5.2 Methods

Male Sprague-Dawley rats (n = 12, 352±26 g) were used according to protocols approved by University of Utah IACUC. Blast exposure was produced

in a fashion identical to Chapters 2 and 3. Briefly, animals were anesthetized with isoflurane and suspended in a Kevlar sling offset from the muzzle to produce a 323 kPa blast exposure. Following blast exposure, animals were sacrificed at 2 days and 7 days via isoflurane overdose and transcardial perfusion with 150 mL PBS followed by 150 mL 4% paraformaldehyde. Brains were post fixed in 4% PFA and then equilibrated in 30% sucrose for 5 days. Brains were cold mounted to blocks with OCT and tissue between the olfactory lobes and pineal gland was serially sectioned into 30 μm coronal sections by cryotome.

Our immunohistochemistry protocol for rat IgG was modified to use a single-step fluorescently conjugated antibody (IgG, 2 mg/mL, Gt anti-Rt IgG (H+L) AF-594, Invitrogen) in order to eliminate potential background fluorescence caused by streptavidin secondary binding to endogenous biotin in the brain. Antibody was diluted in blocking solution consisting of 4% (v/v) goat serum, 0.1% (v/v) Triton-X, 0.5% (w/v) sodium azide in PBS. Free floating tissue sections were batch incubated in block for 12 hours at room temperature and then for 12 hours in antibody solution at room temperature. After three rinses in PBS (4 hours/rinse) to remove unadsorbed antibody, sections were incubated with fluorescently labeled secondary (If applicable) for 12 hours at room temperature and again rinsed three times with PBS (4 hour/rinse). IgG sections were co-marked for GFAP (GFAP, 2.9 mg/ml, RbxRt anti-GFAP IgG1, Southern Biotech) using our standard primary-secondary indirect IHC protocol, while adjacent sections were examined for CD68 (ED-1, 0.5 mg/ml, MsxRt anti-CD68, AbD Serotec) and IBA1 (IBA1, 0.5 mg/mL, Rb anti-IBA1, Wako). On the opposing side of the IgG / GFAP section, tissue was taken and examined for NeuN using a low

background avian marker (NeuN, 0.2 mg/mL, Ck anti-NeuN, EMD Millipore) using the procedure outlined above. Sections were also stained with DAPI (10 mM) to image cell nuclei. Brain sections were mounted on glass microscope slides with Fluoromount-G (Southern Biotech) and then protected with glass cover slips.

Sections were imaged using a Coolsnap digital camera (1040x1392 image resolution) mounted to an upright epifluorescent microscope (Nikon; Eclipse E600) using 10x (NA = 0.45) and 20x (NA = 0.75) objectives with identical mercury lamp and aperture settings. Images were light field corrected using no-primary controls.

IgG quantification through fluorescence intensity was calibrated by taking serial dilutions of the AF-594 conjugated antibody used at 1:100, 1:1000, and 1:10000. Three wells were created by placing two glass cover slips 2 mm apart on a slide and then placing a drop of secondary dilution between the slips. A third cover slip was then placed over the droplet, creating a rectangular volume 145 ± 15 µm deep (Figure 5.1).

This well was then imaged at 4x (NA = 0.13) and 10x (NA = 0.45) at identical imaging exposure times and settings as IgG brain sections. Multiple images were taken, light field corrected, and then averaged to provide homogenous fluorescence fields. Average image pixel intensity was measured using ImageJ. Volume of a column created by each pixel was calculated from pixel area and well depth (Figure 5.2), and by using the molecular mass and concentration of the secondary antibody, an estimate of the number of IgG molecules per pixel volume was created.

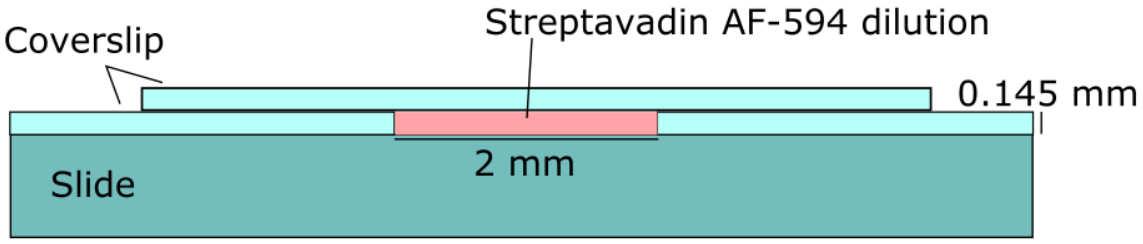

Figure 5.1: Immunofluorescence quantification calibration setup.

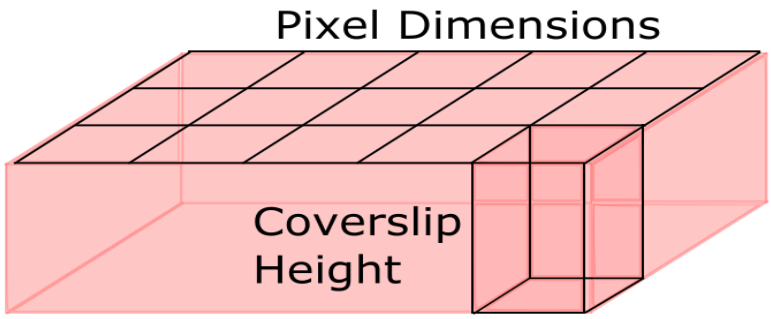

Figure 5.2: Pixel volume used for IgG quantification.

By comparing to literature values for IgG concentration in rat serum (1.67 g/L for 10-week-old SD rat[125]), we can draw an inference to the amount of blood plasma leaked for a given size and brightness of lesion. Due to unknown factors involving binding kinetics between substrate and fluorescent markers, a correction factor will be needed to make an accurate estimate.

5.3 Results

IgG was again seen in rats exposed to blast overpressure (Fig 5.3a), and the characteristic decrease in GFAP fluorescence at lesion locations was also observed (Figure 5.3b). When adjacent sections labeled with our NeuN marker were examined, we observed a decrease in NeuN marker expression in some of our larger lesions (>500 μm diameter, Figure 5.3c-d). However, in 88% of lesion

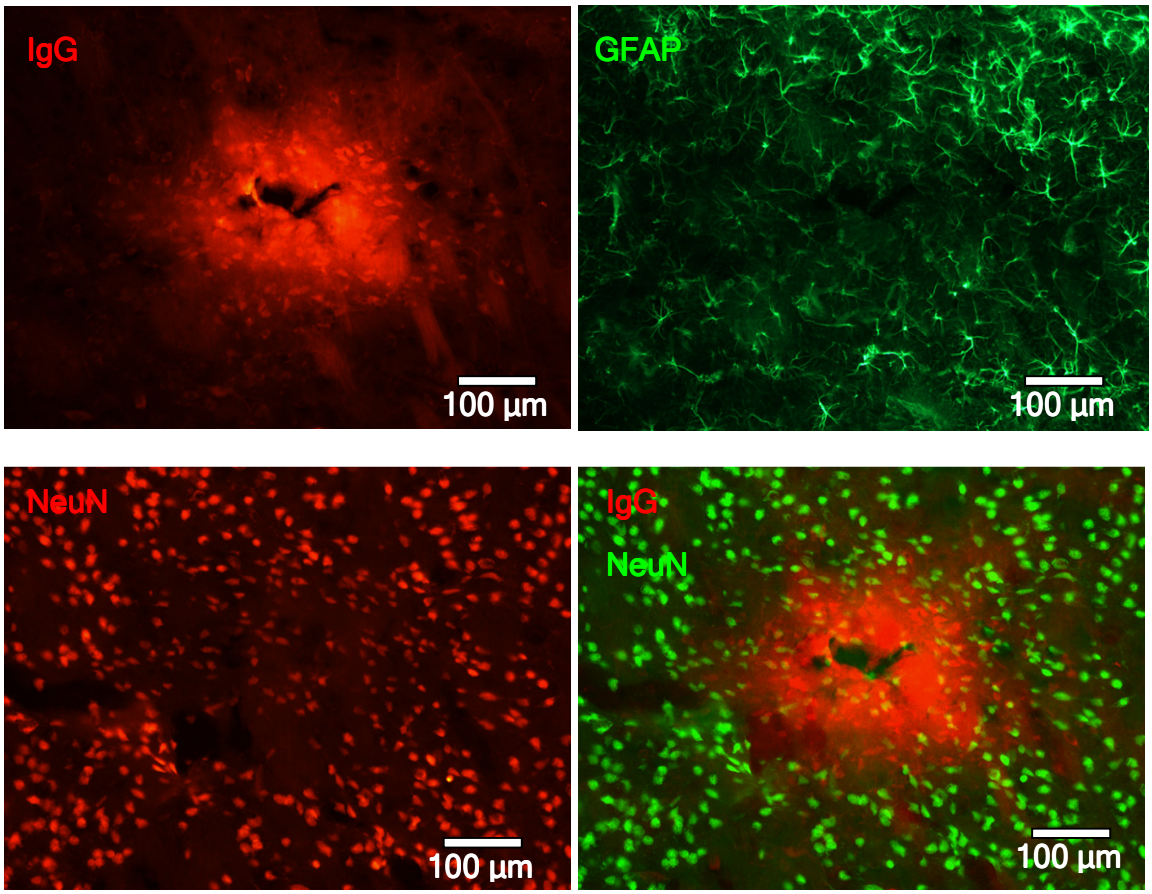

Figure 5.3: Lesion location in blast-exposed animal showing: (a) IgG lesion; (b) GFAP reduction at IgG lesion location in same section; (c) NeuN in adjacent section at registered location showing reduction in intensity of NeuN positive cells; (d) IgG and NeuN (pseudo-colored in green).

locations examined in this set of animals, we saw no discernible difference in neuronal density or brightness.

Separate adjacent sections labeled for CD68 and IBA1 were examined in proximity to IgG extravasation. Evidence of amoeboid IBA1-positive cells was found near IgG extravasation locations in 7-day survival animals and was often co-localized with CD68 positive cells (Figure 5.4). Amoeboid IBA and CD68 positive cells were almost always associated with a vascular structure, and appeared both within the lumen of the vessel and in close proximity in the

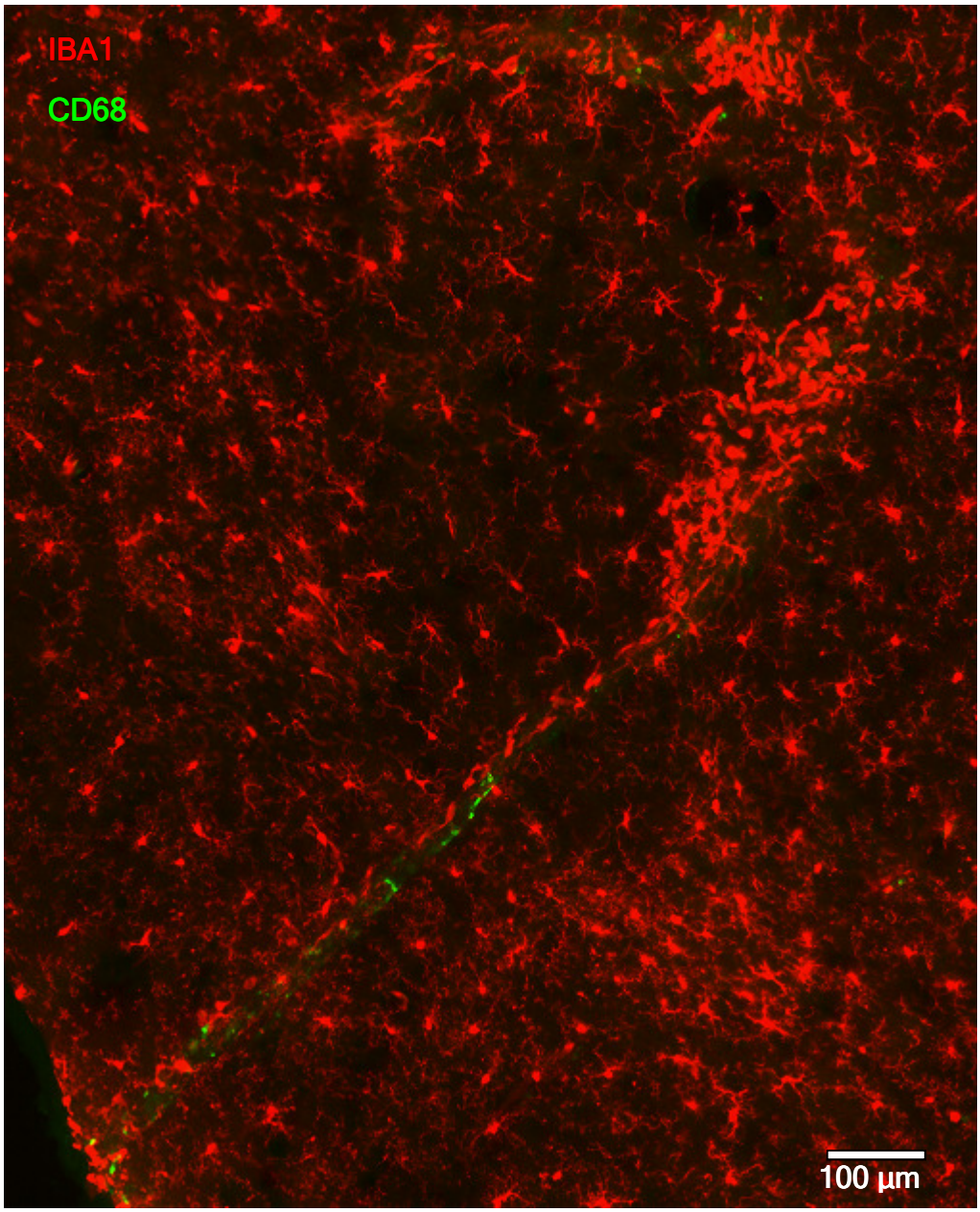

Figure 5.4: 10x image montage of IBA1 (red) and CD68 (green) positive cells in vascular or lymphatic channel in animal 7 days post injury, showing cluster of amoeboid IBA1 positive cells co-localized with CD68 expression.

parenchymal tissue. Isolated IBA1 and CD68 positive cells were also found in vascular structures up to 1 mm away from IgG locations. Our next investigation was to attempt to measure the amount of IgG, and thus leaked blood plasma, with a typical or specific lesion. First, fluorescent intensity was calibrated with respect to both camera exposure time (Figure 5.5) and antibody concentration (Figure 5.6). Good linearity was found except at the highest levels of antibody concentration (1:100) and longest exposure times.

Three representative lesions (bright, medium, faint) were selected to estimate the amount of plasma per section (Figure 5.7). Lesions were thresholded and pixel intensity within the threshold boundary was measured. IgG fluorescent intensity within the lesion volume corresponded to dilutions of between 1:700 and 1:3600 compared to original calibration concentrations. Assuming a 1:1 binding ratio for the fluorescent marker antibody to the endogenous substrate IgG gives an estimated blood plasma extravasation volume of ranging from 4 to 35 pL, which represents between 0.38% and 1.98% of the total volume of the lesion within the section (Table 5.1).

5.4 Discussion

Further immunohistological examination helped clarify inconclusive results regarding inflammation associated with BBB disruption found in Chapters 3 and 4. Both changes in neuronal nuclei and involvement of macrophage line cells was observed using more sensitive methods including: thinner section preparation, equalized rinse and block times, use of markers with reported greater specificity, and single marker panels to minimize the possibility of Ab cross reactivity.

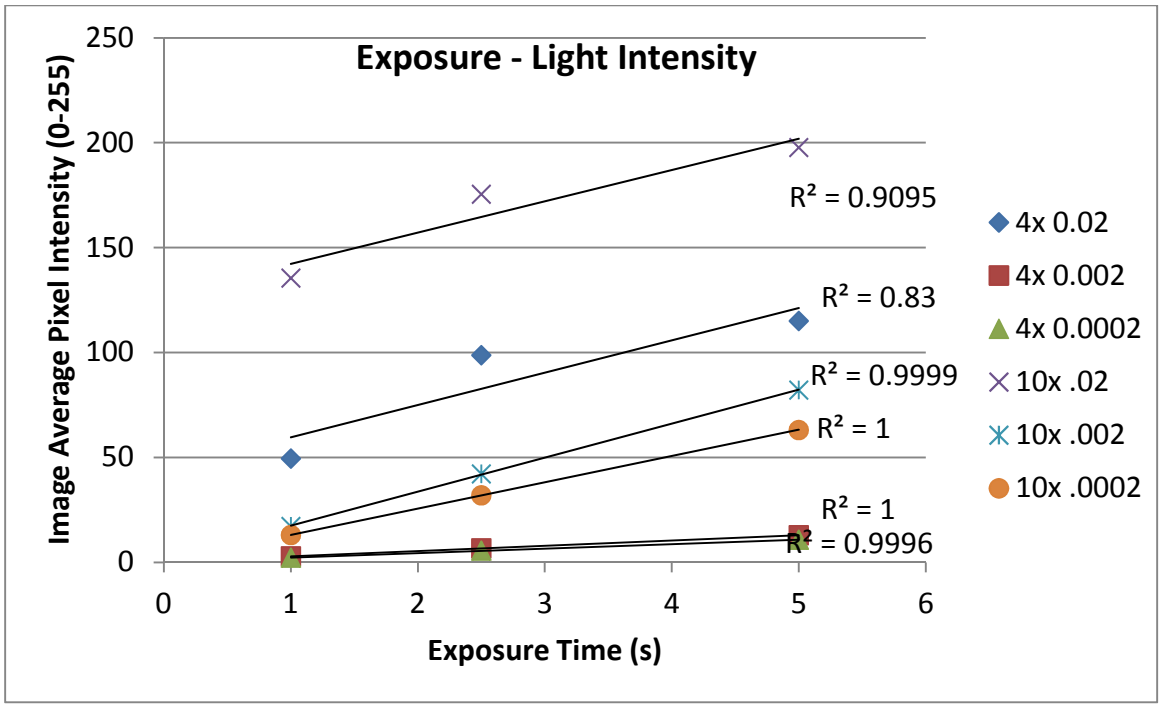

Figure 5.5: Exposure time shows a clear linear relationship until the highest antibody concentration (1:100, 0.02 mg/ml) and exposure time (5s) results in oversaturation of the image.

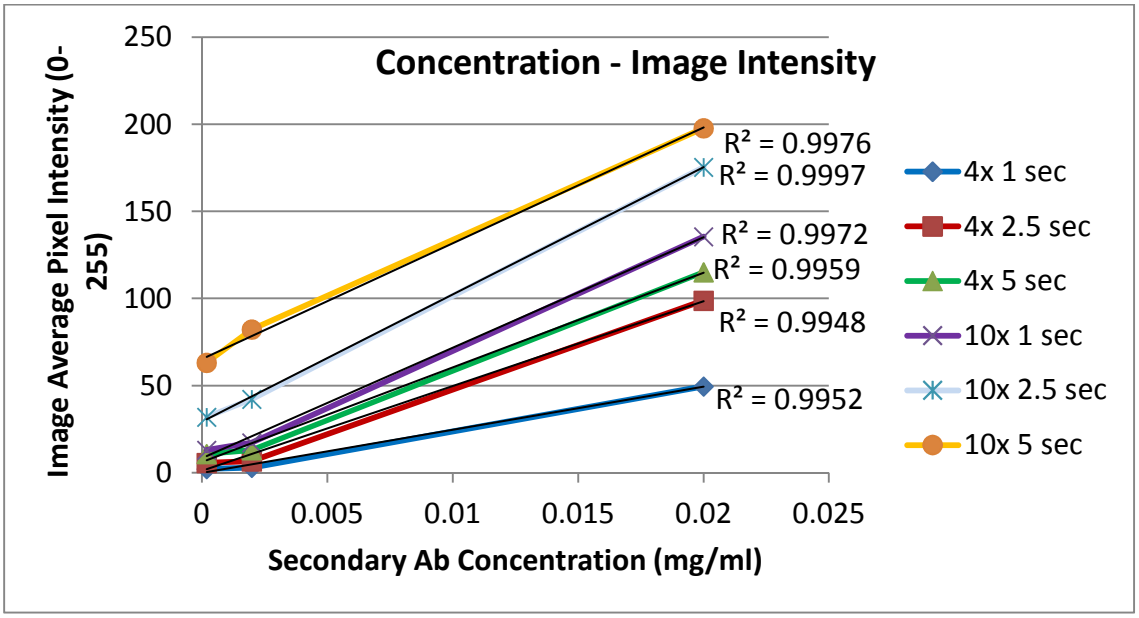

Figure 5.6: Various concentration / intensity curves for set exposure time and magnifications. Most commonly used in this dissertation are: (10x, 1 s = purple) and (4x, 2.5 s = red).

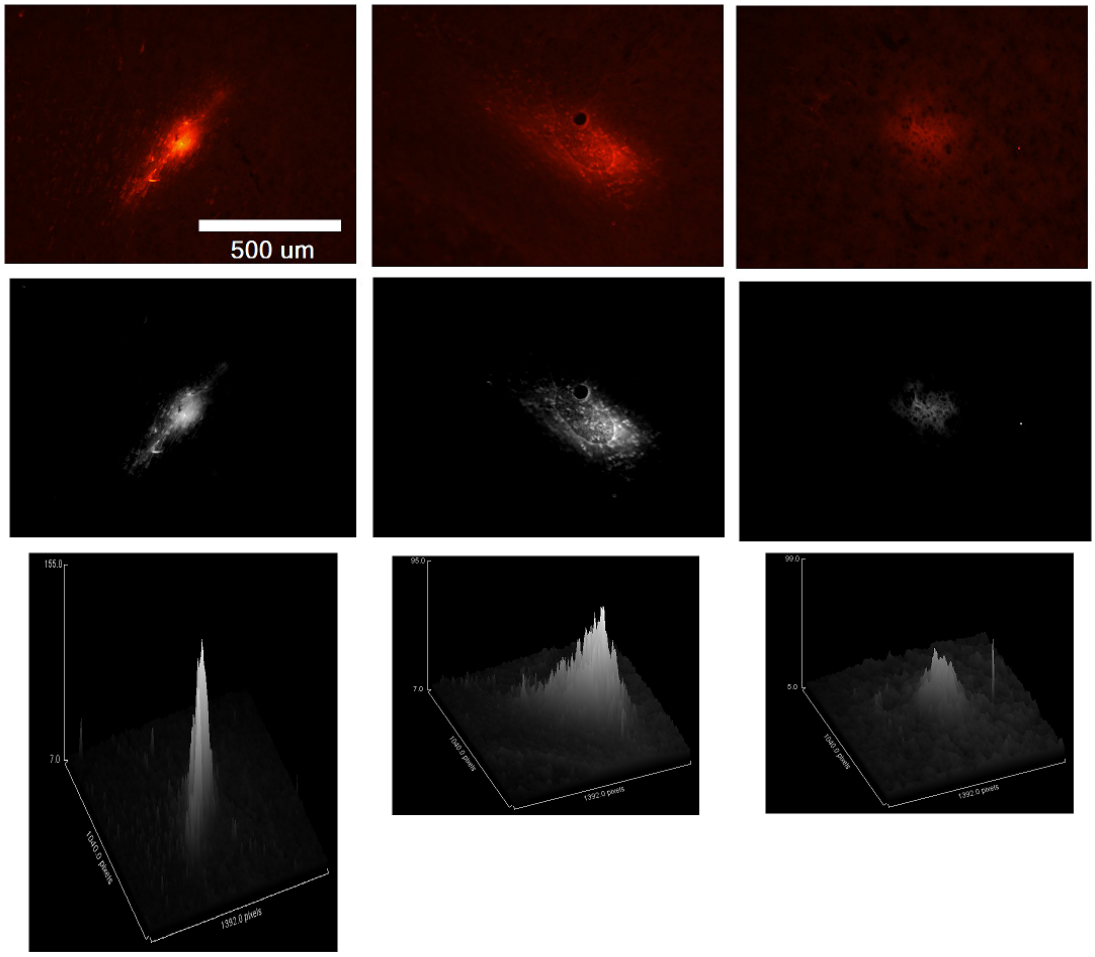

Figure 5.7: Representative bright, average, and faint IgG locations, with thresholded area and pixel intensity maps shown.

Table 5.1: Lesion area and estimated antibody concentrations for the representative lesions shown. Columns marked with (*) are estimated quantities of substrate IgG, plasma volume, and % of total lesion volume assuming a 1:1 binding ratio for the fluorescent marker to the substrate molecule, and may require a correction factor.

Lesion	Lesion Area (mm^2)	AF594 Conc (mg/ml)	Amount IgG (g)*	Plasma Vol (pL)*	% Lesion Vol*
Bright	0.058	0.00284	5.79E-11	34.7	1.98
Average	0.110	0.00123	4.75E-11	28.5	0.86
Faint	0.037	0.00055	7.16E-12	4.3	0.38

Changes in neuron density and marker fluorescence were seen in a small subset of lesions examined, typically in the largest or most intense instances of BBB disruption. This type of localized reduced NeuN intensity has been seen following traditional TBI models such as controlled cortical impact[126, 127] (CCI) at both early time points and up to 60 days following injury. The small changes in NeuN appearing in a limited number of injuries suggests that CCI is a more severe injury model than the low-impulse blast, and that assaying the health of neuronal nuclei and cell bodies may not be a sensitive enough metric to quantify injury from blast exposure. Examining myelin health following blast injury may give a more sensitive indicator for damage from bTBI. Demyelination is a common indicator of mild TBI,[128] and markers for MBP[113] have been used successfully in blast injury models.

Use of IBA1 antibody allowed for positive identification of the faint CD68 signal in low-impulse blast animals, where it had previously only been seen in high-impulse blast animals in Chapter 4. In addition, isolated amoeboid IBA1 and CD68 positive cells were often found in a radius of roughly 1 mm outside of the IgG lesion zone, indicating that focal injury may have wider effects on inflammation in brain tissue. Alternatively, this may be evidence of systemic inflammation following blast exposure, as detected activated macrophages near lesions may come from elsewhere upstream. For example, despite our best efforts at isolating bTBI through the use of positioning and protective gear, damage to lung or inner ear tissue could potentially cause inflammation and activated macrophage shedding to downstream locations. Future work may include examination of these tissues to validate or adjust our bTBI injury model.

There are a number of issues to address before an accurate estimate of extravasated blood plasma can be made from our IgG immunohistology. For work in Chapter 5, a single step fluorescent antibody was used, and therefore, the binding ratio of marker to substrate must be estimated. Unfortunately, the determinant epitope on the substrate IgG that the fluorescently conjugated marker binds to is unknown. Since our marker binds to all rat IgG, it is likely the determinant is on the Fc region, and therefore on a γ-C_H or γ-V_H chain. It may be possible to design an experiment using a known amount of substrate IgG and measuring the amount of fluorescent marker that will bind to it; however, it would be difficult to replicate the specific circumstances of steric hindrance and other contributions of the ECM and cells in the brain in our injury model.

These issues become magnified if an indirect IHC protocol is used. For example, in the IgG measurements made in Chapters 2-4, a streptavidin-biotin amplification step was used. Streptavidin is tetrameric and has 4 binding sites for biotin, making a 1:1 binding ratio unlikely. There are also an unknown number of biotin conjugates for each IgG primary, typically ranging from 3-6.[129]

There are also fluorescence issues to account for doing this type of quantification. Although modern fluorophores are resistant to photobleaching, bleaching still occurs at realistic imaging timescales. For AF-594, 92% of original intensity has been reported following 30 seconds of imaging with a typical fluorescent microscope setup, which drops to 87% after 90 seconds.[130] Quenching, where high spatial density of fluorophore interferes with photon emission, may also skew concentration estimates. Scattering, where each pixel column is not isolated, but instead is surrounded by tissue that is also emitting

light, may cause an overestimate of the amount of fluorescent material within the pixel column. In contrast, the limited depth of field and focus from the microscope aperture means that some photons originating outside of the plane of focus end up missing the objective, leading to an underestimate of fluorophore quantity. Finally, areas with high concentrations of IgG, such as thrombus trapped in blood vessels, may saturate the camera and not accurately represent the amount of IgG present.

A method used to quantify BBB disruption is radiographic labeling of a blood-borne marker such as sucrose,[131] albumin and other endogenous proteins such as TNF-α,[132] or drug delivery vehicles such as PEGylated liposomes.[133] Radiographic labeling has the advantage of accurate quantification of extravasated marker in brain tissue by use of photographic plate, γ-counter, or scintillation spectrometer. The main limitation of this method is imaging resolution, which is lower than what is available with fluorescent microscopy,[92] and may not be sufficient to capture details about our lesions which average a diameter of a few hundred microns. Additionally, uncertain transfer constants for intact blood-brain barriers, marker renal clearance, and tissue binding are all factors that may skew result accuracy and need to be carefully considered before experimental design.[134]

Confirmation of CD68 expression and changes in neuronal nuclei at areas of IgG extravasation helps verify that focal blood-brain barrier disruption following blast is in fact an injury event, and not a perfusion artifact or other phenomenon. With the groundwork laid for tools to estimate the volume of blood leaked into the brain, we can continue to further quantify damage to cerebral vessels from blast.

CHAPTER 6

ADDITIONAL METHODS USED TO QUANTIFY BLAST INJURY

6.1 Introduction

Several additional methods were explored to probe cerebrovascular injury from primary blast. Prior to adoption of IgG extravasation as our standard BBB permeability assay we performed molecular weight matched FITC-dextran perfusion post injury. Susceptibility weighted imaging (SWI) MRI was examined as a method to visualize hemorrhage, hematoma, or edema in the intact brain following blast. Finally, fluorescent microsphere injection, the gold standard for cerebral blood flow measurement,[135] was examined in conjunction with our injury model.

6.2 FITC Dextran Perfusion

Fluorescently labeled dextran perfusion is a well-established assay for blood vessel permeability.[92] Dextran polysaccharides are selected that match the molecular weight and hydrodynamic radius of the diffusate or plasma protein of interest, and are covalently bonded to a fluorescent marker, fluorescein isothiocyanate. We selected 70 kDa dextran, which closely matches serum protein albumin at 65 kDa, and thus allows us to examine the lower threshold of vascular permeability to blood plasma proteins which are typically restricted from

the tissue of the brain by the blood-brain barrier.

Male Sprague-Dawley rats (n = 8) were used according to protocols approved by University of Utah IACUC. 1.0 mL of 25 mg/mL FITC-dextran (70 kDa, Invitrogen) was administered to animals 5 minutes prior to blast exposure via femoral vein injection. Rats were then exposed to 220 kPa lateral blast, and sacrificed after either 5 or 30 minutes by isoflurane overdose and transcardial perfusion of 250 ml PBS followed by 100 ml 4% PFA. Brains were then either sectioned 50 μm thick and every 10^{th} section was examined microscopically. The remaining sections were homogenized in 0.5 mL 80% trichloroacetic acid, centrifuged at 10000 RPM for 20 minutes, and supernatant measured using a fluorescent microplate reader.

During microscopic examination, some FITC was seen in the vascular space of one animal suspected of having a less than ideal perfusion process (Figure 6.1). Other animals rarely exhibited the same phenomena, but overall fluorescent signal for the fluorescein channel was low. No examples of FITC diffusing from vascular space into tissue were seen. Microplate reader results also showed very low fluorescent signal in homogenized brains (Table 6.1). Serial dilution of stock concentration FITC solution gave us an estimated 100-500 ng/mL concentration, which was nearing the limit of detection for the reader and did not appear to be a viable way to determine differences in fluorescent intensity. This method was abandoned in favor of using IgG as an endogenous contrast agent.

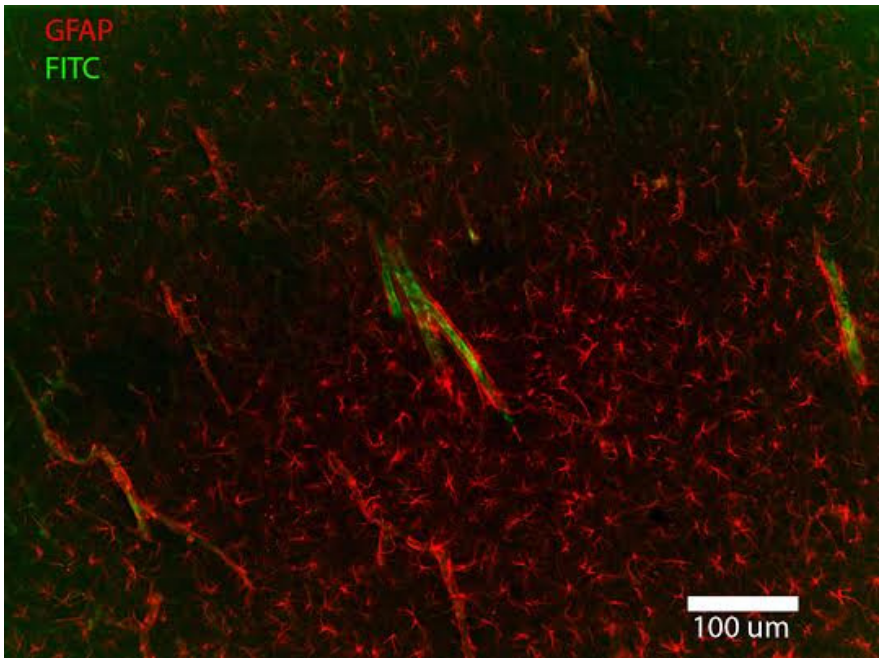

Figure 6.1: Traces of FITC found in blood vessels following FITC dextran perfusion and blast in one animal, with GFAP co-marker to help locate blood vessels.

Table 6.1: Microplate reader results from rats injected with 70 kDa FITC-dextran prior to blast exposure, compared with calibration concentration curve, where each well is 50% concentration of the previous, starting at 0.1 mg/mL (501) and ending with 50 ng/mL.

Rats 5-9	2	2	2	1
Rats 10-14	1	1	0	1
Calibration 1	501 (100 µg/mL)	243 (50 µg/mL)	128 (25 µg/mL)	57 (12.5 µg/mL)
Calibration 2	29 (6.25 µg/mL)	13 (3.13 µg/mL)	7 (1.56 µg/mL)	3 (0.78 µg/mL)
Calibration 3	2 (0.39 µg/mL)	1 (0.20 µg/mL)	1 (0.10 µg/mL)	1 (0.05 µg/mL)

6.3 MRI Imaging for Vascular Leakage

Susceptibility-weighted imaging (SWI) is an MRI technique used to image cerebral microhemorrhage and strain-induced white matter injury in TBI.[136] This imaging modality depends on sensitive measurement of differences in magnetic susceptibility in different materials, i.e., how materials interact with the field. Either they create an induced magnetic field in the direction of the external field and are attracted by it, which is called paramagnetic, or create an oppositely aligned magnetic field and are repelled, called dimagnetic. SWI is extremely sensitive to blood oxygen levels, hemorrhage, and iron storage.[137] Deoxygenated hemoglobin in extravasated red blood cells shows strongly and allows for noninvasive detection of hemorrhage down to sub-cubic millimeter volumes.[137] Both the magnitude image and high-pass filtered phase image are combined to create an enhanced contrast magnitude image.[136]

Imaging was performed in cooperation with the Small Animal Imaging Core Facility at the University of Utah. Male Sprague-Dawley rats (n = 2) were used according to protocols approved by University of Utah IACUC. Animals were anesthetized, immobilized in a Kevlar sling, and exposed to 320 kPa blast overpressure from the low-impulse rifle shock tube device described previously.[59]

1 hour and also 24 hours post-injury animals were anaesthetized (Isoflurane, 5% induction, 2% maintenance) and imaged using a Bruker Biospec 7T MRI scanner with a 30 cm diameter cylindrical bore. Signal was acquired using a flow-compensated long gradient recalled echo using a combination of a volume transmit RF coil (72 mm inner diameter, Bruker Biospec) and a quadrature receive-only surface coil for signal reception. Animals were sacrificed

after 24-hour imaging by isoflurane overdose and transcardial perfusion of 250 ml PBS followed by 100 ml 4% PFA. Brains serially were sectioned at 100 μm, examined for IgG (Biotinylated GtxRt IgG1 and Streptavidin-conjugated AlexaFluor-594) and for vascular location using labeled lectin (Dylight 488 tomato lectin), which binds to the glycocaylx of blood vessels. Sections were imaged with an upright epifluorescent microscope (Nikon; Eclipse E600) and compared to SWI scans.

Examination of SWI images failed to show any unusual features that would indicate hemorrhage had occurred in blast-exposed animals. When compared to histological measurement of extravasated IgG, several IgG depositions were seen that failed to correspond to any change in contrast in the MRI image (Figure 6.2). This may indicate that our IgG lesions generally lack gross hemorrhage and extravasated red blood cells, and are typically more of a leaky BBB, but not fully ruptured vessel phenomena. Examination for work done in Chapter 2 using light microscopy saw red blood cells (RBCs) at a small fraction of lesion locations, but the majority of lesions had few or no associated RBCs. With so few RBCs at lesions, paramagnetic hemoglobin detection using SWI was unlikely. Due to these issues, as well as greater resolution available with histological analysis, we chose to stay with IgG extravasation as our primary measure of BBB disruption.

6.4 Cerebral Blood Flow Measurement Using Microsphere Deposition

A well-established method for cerebral blood flow (CBF) measurement[135, 138] is fluorescent or radiolabeled microsphere perfusion. A bolus of polystyrene microspheres 15 μm in diameter (suspended in saline and treated to increase

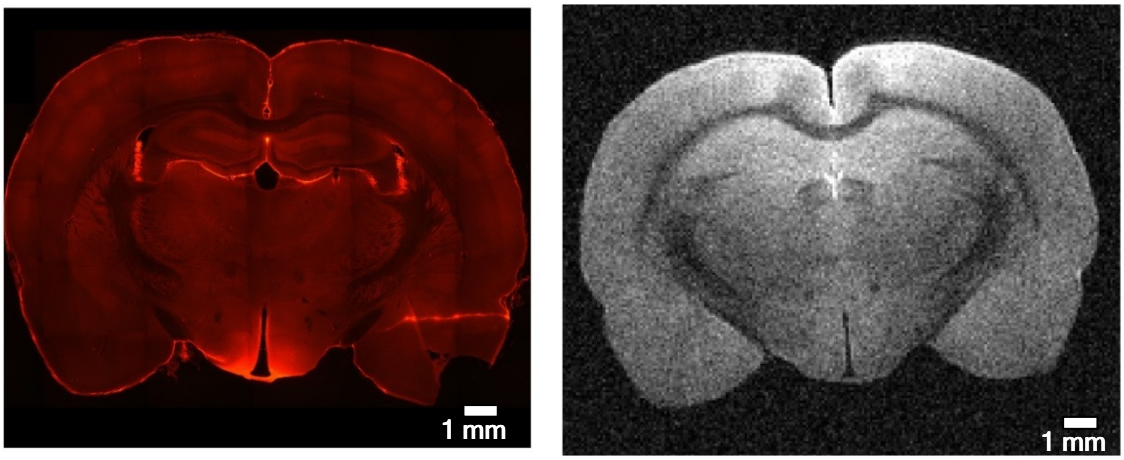

Figure 6.2: Comparison of IgG extravasation with SWI MRI image showing scanning resolution limits, and lack of any indication the IgG deposition seen in lower right of IgG image.

hydrophilicity) is injected into the left ventricle of the heart, and allowed to mix well and circulate freely. Microspheres cannot fit through terminal capillaries, which are 5-10 μm in diameter, and deposit proportionally based on the amount of blood flow to various tissues.

Tissue is then extracted, and either fixed and sectioned or homogenized. Microsphere counts are made using fluorescent microscopy or automated flow-based fluorescent counting equipment.

Male Sprague-Dawley rats (n = 8) were used according to protocols approved by University of Utah IACUC. Animals were first implanted with left femoral artery and left common carotid artery catheters prior to blast exposure. Animals were anesthetized with 5% inhalation isoflurane, incision sites were shaved and washed with betadine, and incisions were made in the ventral femoral region and neck. Arteries were exposed by blunt dissection and 0.5 mm ID diameter silane tubing (Braintree Scientific, Boston, MA) was inserted into the

femoral artery and carotid artery towards the heart. The femoral artery catheter, used for reference blood draws to determine the number of microspheres per mL blood in systemic circulation, was advanced 10-12 mm and secured with three sets of 5-0 suture. Catheters were filled with 250 μg/ml heparinized saline lock solution, and patency was ensured by blood flash.

Carotid catheter lines, used for microsphere injection directly into the heart, were advanced 25-30 mm into the left ventricle. We attempted to use a custom in-line pressure gauge to verify pressure drop and ensure ventricular placement, but small catheter diameter made measurements unreliable, so placement was based on catheter advance distance and tactile aortic valve threshold passage. Catheter lines were secured at vessel site by one distal and two proximal sutures and threaded subcutaneously to an incision on the upper back in the region of T2-T3 and secured to the skin. Animals were administered carprofen and allowed to recover for 48 hours prior to blast exposure.

A reference bolus of 1 mL of 0.1 mg/mL (~1.35 million particles / mL) 554 nm emission (red) microspheres were injected into the carotid catheter at 1 mL/min 1 hour pre-blast to establish baseline regional cerebral blood flow. An equivalent volume of blood was drawn concurrently from the femoral artery catheter line. For blast exposure, animals were anesthetized and immobilized in a Kevlar wrap. Rats experienced 320 kPa blast overpressure from our short-duration rifle shock tube. After 5 minutes, an equivalent second bolus of 486 nm emission (green) microspheres were injected, and a second reference blood draw was taken. Microspheres were allowed to circulate for 30 minutes and then euthanasia was performed by isoflurane overdose followed by transcardial

perfusion with 150 ml of phosphate buffered saline (PBS) and 150 ml of 4% paraformaldehyde (PFA) at 42 $mL*min^{-1}$. Brains were removed and post-fixed in PFA for 24 hours. Control animals (n=4) received identical catheter implantation and isoflurane induction cycles, but no blast injury. Reference blood samples were centrifuged, supernatant extracted, and pellet sonicated and diluted in PBS. 100 µL of diluted solution was extracted, dropped onto glass slides x 3, and allowed to dry for microsphere counting. Brain slices were section serially 100 µm thick and mounted on glass slides, where microsphere counts (Figure 6.3) were made using an upright epifluorescent microscope (Nikon; Eclipse E600).

Complications arose at nearly every step of this process. Out of twelve initial implanted animals, four were able to dislodge their subcutaneous catheters internally during the recovery period and either hemorrhaged out or required euthanasia. Another four had issues with catheter patency and it was not possible to inject microspheres at 48 hours. Four remaining animals had the procedure completed successfully (2 control, 2 blast); however, when microsphere counts were made, high levels of variability were found between first and second injections (Figure 6.4).

Total perfusion counts ranged from 44 total microspheres to 541 per injection bolus, and no discernible pattern was seen for ratio of microsphere deposition from first injection to second injection. In blast animals, we saw one indication of higher blood flow post blast, and one for lower blood flow, and the same case for controls. Additionally, for control animals we expected to see fairly close counts between identical concentration and injection volume; however, this was not the case, with as much as 290% difference between animals. We

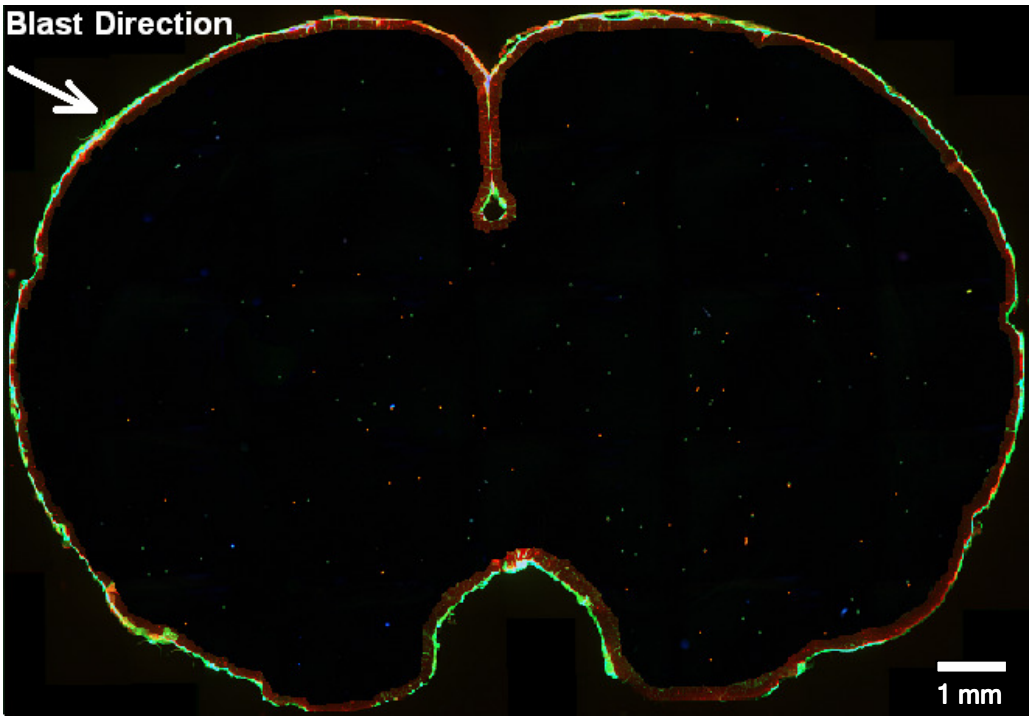

Figure 6.3: Representative microsphere distribution following blast injury.

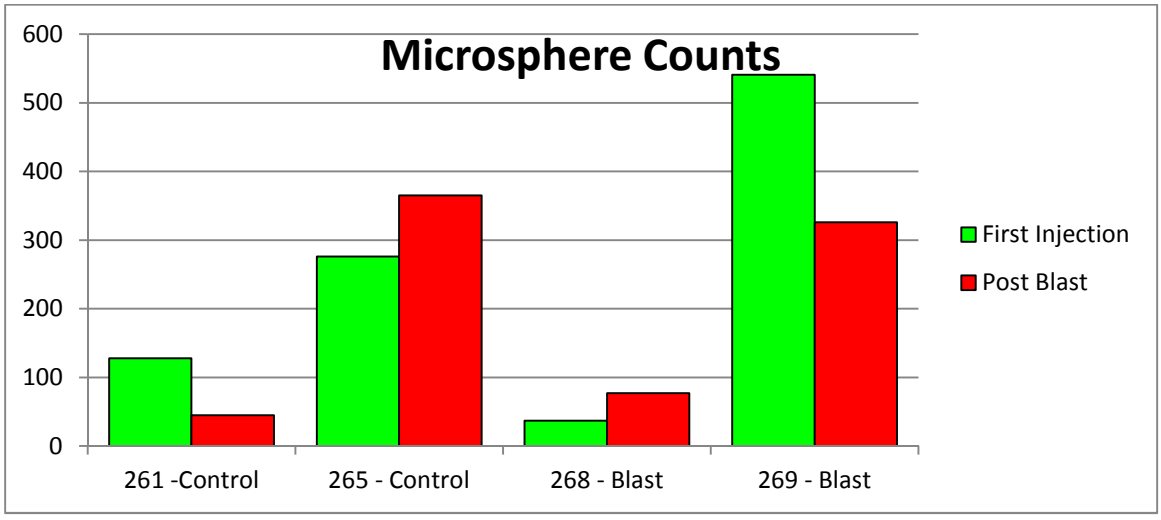

Figure 6.4: Microsphere perfusion for sequential injections in four preliminary study animals. Considerable variability was found between animal cases and between injection bolus in the same animal.

suspected that the high variability of this test was due to incorrect ventricular placement of the carotid catheter tip, leading to non-uniform mixing of microspheres in the circulatory system. We also questioned the effects of the significant injury created by catheter placement had on the systemic vasculature, as well as what consequences occlusion of the carotid artery would have on cerebral blood flow, despite redundant perfusion around the Circle of Willis. Due to our first impressions of high variability using this method, as well as poor success rates in viable surgical procedure and testing protocol, further investigation into cerebral blood flow following blast was halted.

CHAPTER 7

SUMMARY AND CONCLUSION

The aim of research done for this thesis was to characterize vascular dysfunction in the brain following primary blast injury in order to further define injury mechanisms. Although challenges were encountered in determining vascular injury thresholds from both low- and high-impulse blast wave exposure, insights were developed about patterns of blood-brain barrier disruption in bTBI, as well as further evidence of vascular-related inflammatory response. Appropriateness of several behavioral techniques was investigated with mixed success, and imaging and cerebral blood flow measurements were explored to broaden the scope of this work and define blast injury mechanisms.

Blood-brain barrier integrity played a central role in this thesis, with valid reason. Barrier function plays a critical role in brain homeostasis, and disruption of any of its components such as endothelial cells, tight junction (TJ) molecules, basement membrane, pericytes, or astrocyte end feet, whether through mechanical stretching and shearing or through secondary inflammatory insult, can lead to neuronal injury and neurological deficits. Mild blast overpressure exposure is thought to disrupt TJ proteins, alter basement membrane function, detach pericytes, and cause swelling of astrocyte end feet that creates leakiness that sets up inflammatory conditions, including chronic upregulation of reactive

oxygen species (ROS), MMP activation, and proinflammatory cytokines.[52, 89] An in-vitro blast model of the BBB[139] saw decreased trans-endothelial electrical resistance and compromised ZO-1 immunoreactivity, a TJ-cellular membrane binding protein. Secondary oxidative damage involving NOX1, iNOS, 4-HNE, and 3-NT has been reported in the first 24 hours following low-intensity blast exposure.[54] More severe blast injury adds physical rupture of capillaries and larger vessels and direct extravasation of whole blood into the parenchymal brain tissue.[52] A high-intensity blast exposure study[26] showed infiltration of PMN leukocyte and lymphocyte infiltration, as well as COX-2, IL1- β, TNF-α, and 4-HNE which appeared after 1 hour and persisted for three weeks. Clearly, BBB disruption in bTBI not only involves initial mechanical damage, but ongoing and evolving processes. Any study of bTBI should include chronic time points to record these changes in function.

Blood-brain barrier disruption in our study was found to create a diffuse array of focal deposits of IgG in tissue following blast injury. Despite lateral blast exposure, lesions were found to be evenly distributed between hemispheres, a distinct difference from conventional TBI where hemorrhage is most likely on the surface of the brain at the site of impact, on the opposite side where contrecoup injury occurs, and near internally projecting parts of the skull, such as the sphenoid ridge and tentorium cerebelli.[140] These lesions are most often sub-millimeter in diameter and are unlikely to show up in imaging scans, as most represent transient leakiness of the blood-brain barrier rather than complete rupture.

Although lesions were evenly split between hemispheres, they were not

equally distributed among various brain structures. Some areas, such as the caudate putamen, corpus callosum, septal nuclei, and basal ganglia, appeared particularly vulnerable to blast, having a higher proportionally number of lesions and volume lesioned tissue than average. Other areas, such as the hippocampus and thalamus, seemed more resistant to blast and had a lower number of lesions. Reasons for this were suggested in Chapter 2 and include macroscopic explanations such as positive and negative blast wave interference from the skull and internal structures such as ventricles, and microscopic explanations dealing with blood vessel orientation, white matter tracts, and local anisotropy of the brain. There may be a correlation between regional blast injury and specific complaints commonly reported following bTBI, such as depression or memory loss, and better understanding of the intricacies of injury patterns may lead to improved helmet design.

The most immediate and tangible benefit of defining vascular role in bTBI will be development of more accurate and complete constituent models for blast injury computer simulation. Many groups have begun development of bTBI models with promising results,[30, 141-145] and are typically focused on blast wave propagation through the human skull and brain and the effects of current generation Kevlar helmets. However, no studies as of yet explicitly model the cerebral vasculature and the role it plays in bTBI. The elastic moduli of gray matter and white matter average 0.29 kPa and 0.45 kPa,[146] while veins have been measured at 300 kPa,[147] and arteries up to 2.9 MPa.[148] Therefore, since blood vessels are four to five orders of magnitude stiffer than neural tissue, the brain may be considered a relatively soft matrix permeated by a stiff and complex

anisotropic fiber network. As most simulations have only represented the brain as an isotropic viscoelastic material, they are missing the contributions from specific major and minor blood vessel orientation.

Prevention and protection is one side of reducing the health impact of bTBI, and the other major problem to be solved lies in treatment of those impacted. Early treatment involves diagnosis, surgical intervention, and drug therapies to prevent neuronal death and subsequent loss of function. Administration of minocycline post injury has been shown to improve outcomes in neurodegenerative diseases such as Parkinson's,[149] as well as in rodent models of bTBI[104]; however, successful translation to treatment in humans has not yet occurred.

Understanding of inflammatory consequences of vascular disruption in bTBI will be critical to development of pharmaceutical therapies. Our studies highlight the role of astrocytes in this process with the unusual pattern of GFAP expression developed around blast lesion locations. Astrocytes are important mediators of metabolism, inflammation, and wound healing in the brain, and are an integral part of the blood-brain barrier, so it is not surprising that they exhibit a dramatic change following blast injury. Other blast studies using GFAP are detailed in the Chapter 3 discussion, but seem to provide a mixed picture of astrocyte role in blast injury, with some reporting an increase[22, 32-34], others a decrease[98], and many no change[49, 99-102]. One possible explanation for the controversy may lie in quantification methods, as any group who is simply measuring a net difference in fluorescent intensity will see the decrease in brightness in the center of lesioned area partially or totally cancelled out by the

increase at the lesion periphery.

Another significant finding is the presence of CD68 positive cells, indicative of macrophage activation, at lesion locations in both our high- and low-impulse blast testing. Macrophages arrive to the scene of an injury after 48 hours and play a key role in inflammation and phagocytosis. Cytotoxic effects of macrophage activation may cause secondary injury to neurons, so anti-inflammatory medication is a likely component of bTBI therapy, although it is not clear what the most effective drug pathway will be. Subtle changes in NeuN expression hint at damage to neurons. The decrease seen in NeuN expression at lesion sites may be indicative of apoptosis, and could be confirmed by TUNEL or examining caspase-3. Alternatively, a more sensitive marker that looks at neural processes or myelination may give further insight into blast injury.

Further insight into the role of vasculature in bTBI will help inform development of a serum biomarker for blast traumatic brain injury, one of the holy grails for early detection and treatment of bTBI. No clinical marker yet exists; however, many potential markers have been investigated including, but not limited to: axonal injury (NF-H, Tau),[98, 150] neuronal damage (NSE),[39, 150, 151] glial response (GFAP, S-100B, MPB),[26, 39, 98, 150, 151] inflammation (fibrinogen, MIP-1a, MCP-1, interleukins, TNF-α, MDA),[26, 150, 151] vascular function (Aquaporin, VEGF, vWF),[152] cellular adhesion and extracellular matrix (integrins, connexins),[152] metabolism (4HNE, HIF-1α),[150, 151] prion protein,[153] and small nucleolar RNA and DNA fragments[154] have all been explored without successful clinical translation. Development of a field assay for bTBI will inform triage and treatment efforts, and cerebral vasculature's central role in bTBI will undoubtedly be involved in any

successful assay panel.

The behavioral studies performed highlight some of the challenges of using functional assays to measure injury severity in bTBI, but also provide some tantalizing leads for paths forward in blast research and treatment. Open field testing did not reveal any significant changes in animal locomotor ability post blast from either level of impulse severity, so a more rigorous test such as a rotarod might be able to reveal differences in motor function. Using open field thigmotaxis to investigate anxiety also failed to reveal any clear results, so another system such as an elevated plus maze may be able to tease out information on animal's anxious state, although the elevated plus maze works on the same principles of open space avoidance and may have the same result.

Novel object testing was likewise ambiguous for both low-impulse and high-impulse blast testing, and no clear deficits in memory performance were seen. The classic spatial memory alternative is the Morris water maze; however, it is considered a more stressful test for rats and there were concerns it would influence the anxiety assay. An alternative is the cheese board or dry land water maze, where animals navigate a platform with many holes and find a food reward based on visual navigation clues.[155] It is important to note that all of these tests have been used to assay memory in blast injury and shown significant results (except the cheese board): Open field,[16, 100, 101, 103-105, 156] rotarod,[16, 99, 105] elevated plus maze,[100, 104, 156] novel object,[85, 99, 107] Morris water maze,[100] and others.

The clearest behavioral finding came from the Von Frey fiber assay, in which both low- and high-impulse blast animals experienced a significant

decrease in sensitivity after bTBI. This may have implications for treatment or safety guidelines as discussed at the end of Chapter 4, and more broadly may have implications on the consequences of blast exposure on the peripheral nervous system. As the nociceptive withdrawal reflex is a spinal mediated polysynaptic reflex that acts independently of guidance from the brain,[157] changes in response sensitivity may indicate damage to the spinal cord or peripheral nerves from blast, and warrants further investigation.

Careful selection and refinement of immunohistological techniques in any study of TBI is important to obtain accurate and meaningful results. Markers and methods used in Chapter 3 against CD68 and NeuN lacked the sensitivity to show macrophage activation or changes in neuronal health, which is in disagreement with the bulk of the literature on TBI that finds macrophage recruitment and neuronal degeneration with any leakage of IgG into the brain tissue. This disagreement led to further development of methods in Chapter 5, which did show subtle changes in both CD68 and NeuN using the low-impulse blast device. In fact, studies have shown that the occlusion of a single descending arteriole results in CD68 expression, depletion of NeuN, and even negative cognitive consequences.[158] This study used a sensitive macrovibrissa behavioral test and precisely targeted occlusion to a single cortical column, resulting in detection of behavioral changes that would be difficult to see in the random injury distribution in our blast model, and the more generalized behavioral tests used. Another example of differences in testing sensitivity was that the use of a single step secondary antibody for detection of IgG in Chapter 5 showed some qualitative differences from the biotin-streptavidin amplification

protocol used in Chapters 2-4. The amplification protocol was potentially more sensitive to small lesions and low concentration of IgG in the lesion periphery; however, possible binding of fluorescent secondary to endogenous biotin in the brain makes clear determination of the superior method difficult.

Trauma from explosive blast is an unfortunate consequence of warfare and terrorism in our modern world. As nations feel the strain of climate change, soil degradation and desertification of arable land, ecosystem collapse, and dwindling natural resources, unrest will continue to spread throughout unstable and formerly stable areas of our world, making it imperative that we not only attempt to mitigate the root causes of conflict but also develop superior treatment and protective measures for when explosive violence strikes. Explosive detonation deals with forces that are almost unimaginable in our everyday experience – objects flying thousands of meters per second, air compressed to denser than steel, temperatures thousands of degrees Kelvin. Blast injuries are some of the most traumatic and damaging that a person could experience and survive, but there is a limit to what medicine can be expected to accomplish given the initial injury. Harm reduction from explosive blast will need to rely on political and economic solutions to minimize the number of soldiers and civilians who ever have to experience such awful trauma just as much as it leans on medicine to develop improved treatment methods, or engineering to develop better protective measures.

Sadly, blast trauma is unlikely to ever disappear in our lifetimes, and as bioengineers we need to address the consequences of blast injury to help those afflicted and protect those at risk. The consequences of primary blast

overpressure exposure and subsequent traumatic brain injury has become all too evident in the United States' military involvement in Iraq and Afghanistan over the last two decades, with thousands of veterans arriving home with evidence of bTBI during their deployment. We need to do all we can to understand blast injury mechanisms to help these individuals.

The work in this dissertation has been guided by our desire to improve understanding of bTBI and hopefully help reduce the suffering of its victims. We have highlighted disruption of the blood-brain barrier as a primary injury mechanism, and a target for further investigation and therapy. Inflammatory and behavioral consequences of vascular disruption in bTBI have been described in order to synthesize knowledge of BBB dysfunction into the bigger picture of blast injury mechanics. It is our sincere hope that the information gained in this body of work informs the ongoing worldwide effort to understand blast traumatic brain injury, and to promote protection, preventative therapy, and peace.

REFERENCES

[1] Coupland RM, Meddings DR. Mortality associated with use of weapons in armed conflicts, wartime atrocities, and civilian mass shootings: literature review. *BMJ* 1999; 319: 407-10.

[2] Belmont PJ, Jr., McCriskin BJ, Sieg RN, Burks R, Schoenfeld AJ. Combat wounds in Iraq and Afghanistan from 2005 to 2009. *J Trauma Acute Care Surg* 2012; 73: 3-12.

[3] Bogen KT, Jones ED. Risks of mortality and morbidity from worldwide terrorism: 1968-2004. *Risk Anal* 2006; 26: 45-59.

[4] Kapur GB, Hutson HR, Davis MA, Rice PL. The United States twenty-year experience with bombing incidents: implications for terrorism preparedness and medical response. *J Trauma* 2005; 59: 1436-44.

[5] Cullis IG. Blast waves and how they interact with structures. *J R Army Med Corps* 2001; 147: 16-26.

[6] Fox RW, McDonald AT. *Introduction to fluid mechanics*, 4th edition. New York: J. Wiley, 1992.

[7] Rigby SE. Blast wave clearing effects on finite-sized targets subjected to explosive loads 2014: 1 online resource.

[8] Cernak I, Noble-Haeusslein LJ. Traumatic brain injury: an overview of pathobiology with emphasis on military populations. *J Cereb Blood Flow Metab* 2010; 30: 255-66.

[9] Chavko M, Prusaczyk WK, McCarron RM. Lung injury and recovery after exposure to blast overpressure. *J Trauma* 2006; 61: 933-42.

[10] Cooper GJ. Protection of the lung from blast overpressure by thoracic stress wave decouplers. *J Trauma* 1996; 40: S105-10.

[11] Guy RJ, Kirkman E, Watkins PE, Cooper GJ. Physiologic responses to primary blast. *J Trauma* 1998; 45: 983-7.

[12] Avidan V, Hersch M, Armon Y, Spira R, Aharoni D, Reissman P*, et al.* Blast lung injury: clinical manifestations, treatment, and outcome. *Am J Surg* 2005; 190: 927-31.

[13] Sasser SM, Sattin RW, Hunt RC, Krohmer J. Blast lung injury. *Prehosp Emerg Care* 2006; 10: 165-72.

[14] Taylor PA, Ludwigsen JS, Ford CC. Investigation of blast-induced traumatic brain injury. *Brain Inj* 2014; 28: 879-95.

[15] H. Hosseini SM-N, H. Akiyama, and V. Menezes. *Shock wave interaction with interfaces between materials having different acoustic*

impedances. Applied Physics Letters, 2012.

[16] Cernak I, Merkle AC, Koliatsos VE, Bilik JM, Luong QT, Mahota TM*, et al.* The pathobiology of blast injuries and blast-induced neurotrauma as identified using a new experimental model of injury in mice. *Neurobiol Dis* 2011; 41: 538-51.

[17] Champion HR, Holcomb JB, Young LA. Injuries from explosions: physics, biophysics, pathology, and required research focus. *J Trauma* 2009; 66: 1468-77; discussion 1477.

[18] Champion HR. Abdominal trauma in primary blast injury (Br J Surg DOI: 10.1002/bjs.7268). *Br J Surg* 2011; 98: 179-80.

[19] Ritenour AE, Blackbourne LH, Kelly JF, McLaughlin DF, Pearse LA, Holcomb JB*, et al.* Incidence of primary blast injury in US military overseas contingency operations: a retrospective study. *Ann Surg* 2010; 251: 1140-4.

[20] White CS. The scope of blast and shock biology and problem areas in relating physical and biological parameters. *Ann N Y Acad Sci* 1968; 152: 89-102.

[21] Richmond DR, Damon EG, Fletcher ER, Bowen IG, White CS. The relationship between selected blast-wave parameters and the response of mammals exposed to air blast. *Ann N Y Acad Sci* 1968; 152: 103-21.

[22] Cernak I, Savic J, Ignjatovic D, Jevtic M. Blast injury from explosive munitions. *J Trauma* 1999; 47: 96-103; discussion 103-4.

[23] Trudeau DL, Anderson J, Hansen LM, Shagalov DN, Schmoller J, Nugent S*, et al.* Findings of mild traumatic brain injury in combat veterans with PTSD and a history of blast concussion. *J Neuropsychiatry Clin Neurosci* 1998; 10: 308-13.

[24] Hicks RR, Fertig SJ, Desrocher RE, Koroshetz WJ, Pancrazio JJ. Neurological effects of blast injury. *J Trauma* 2010; 68: 1257-63.

[25] Rosenfeld JV, Ford NL. Bomb blast, mild traumatic brain injury and psychiatric morbidity: a review. *Injury* 2010; 41: 437-43.

[26] Tompkins P, Tesiram Y, Lerner M, Gonzalez LP, Lightfoot S, Rabb CH*, et al.* Brain injury: neuro-inflammation, cognitive deficit, and magnetic resonance imaging in a model of blast induced traumatic brain injury. *J Neurotrauma* 2013; 30: 1888-97.

[27] Hoge CW, Castro CA. Blast-related traumatic brain injury in U.S. military personnel. *N Engl J Med* 2011; 365: 860; author reply 860-1.

[28] Dal Cengio Leonardi A, Keane NJ, Bir CA, Ryan AG, Xu L, Vandevord PJ. Head orientation affects the intracranial pressure response resulting from shock wave loading in the rat. *J Biomech* 2012; 45: 2595-602.

[29] Bolander R, Mathie B, Bir C, Ritzel D, VandeVord P. Skull flexure as a contributing factor in the mechanism of injury in the rat when exposed to a shock wave. *Ann Biomed Eng* 2011; 39: 2550-9.

[30] Moss WC, King MJ, Blackman EG. Skull flexure from blast waves: a mechanism for brain injury with implications for helmet design. *Phys Rev Lett* 2009; 103: 108702.

[31] Mott FW. Lecture Paper, "The Effects of High Explosives upon the Central Nervous System," 1916.

[32] Chen Y, Huang W, Constantini S. The Differences between blast-induced and sports-related brain injuries. *Front Neurol* 2013; 4: 119.

[33] Long JB, Bentley TL, Wessner KA, Cerone C, Sweeney S, Bauman RA. Blast overpressure in rats: recreating a battlefield injury in the laboratory. *J Neurotrauma* 2009; 26: 827-40.

[34] Chavko M, Watanabe T, Adeeb S, Lankasky J, Ahlers ST, McCarron RM. Relationship between orientation to a blast and pressure wave propagation inside the rat brain. *J Neurosci Methods* 2011; 195: 61-6.

[35] Cernak I, Savic J, Malicevic Z, Zunic G, Radosevic P, Ivanovic I*, et al.* Involvement of the central nervous system in the general response to pulmonary blast injury. *J Trauma* 1996; 40: S100-4.

[36] Elsayed NM. Toxicology of blast overpressure. *Toxicology* 1997; 121: 1-15.

[37] Agoston DV, Elsayed M. Serum-based protein biomarkers in blast-induced traumatic brain injury spectrum disorder. *Front Neurol* 2012; 3: 107.

[38] Agoston DV, Kamnaksh A. Modeling the Neurobehavioral Consequences of Blast-Induced Traumatic Brain Injury Spectrum Disorder and Identifying Related Biomarkers. In: Kobeissy FH. *Brain Neurotrauma: Molecular, Neuropsychological, and Rehabilitation Aspects*. Boca Raton (FL), 2015.

[39] Svetlov SI, Prima V, Kirk DR, Gutierrez H, Curley KC, Hayes RL*, et al.* Morphologic and biochemical characterization of brain injury in a model of controlled blast overpressure exposure. *J Trauma* 2010; 69: 795-804.

[40] Newsome MR, Durgerian S, Mourany L, Scheibel RS, Lowe MJ, Beall EB*, et al.* Disruption of caudate working memory activation in chronic blast-related traumatic brain injury. *Neuroimage Clin* 2015; 8: 543-53.

[41] Huang M, Risling M, Baker DG. The role of biomarkers and MEG-based imaging markers in the diagnosis of post-traumatic stress disorder and blast-induced mild traumatic brain injury. *Psychoneuroendocrinology* 2016; 63: 398-409.

[42] Stemper BD, Shah AS, Budde MD, Olsen CM, Glavaski-Joksimovic A, Kurpad SN*, et al.* Behavioral Outcomes Differ between Rotational Acceleration and Blast Mechanisms of Mild Traumatic Brain Injury. *Front Neurol* 2016; 7: 31.

[43] Bauman RA, Ling G, Tong L, Januszkiewicz A, Agoston D, Delanerolle N*, et al.* An introductory characterization of a combat-casualty-care relevant swine model of closed head injury resulting from exposure to explosive blast. *J Neurotrauma* 2009; 26: 841-60.

[44] Armonda RA, Bell RS, Vo AH, Ling G, DeGraba TJ, Crandall B*, et al.* Wartime traumatic cerebral vasospasm: recent review of combat casualties. *Neurosurgery* 2006; 59: 1215-25; discussion 1225.

[45] Cernak I, Wang Z, Jiang J, Bian X, Savic J. Ultrastructural and functional characteristics of blast injury-induced neurotrauma. *J Trauma* 2001; 50: 695-706.

[46] Axelsson H, Hjelmqvist H, Medin A, Persson JK, Suneson A. Physiological changes in pigs exposed to a blast wave from a detonating high-explosive charge. *Mil Med* 2000; 165: 119-26.

[47] Säljö A, Arrhén F, Bolouri H, Mayorga M, Hamberger A. Neuropathology and pressure in the pig brain resulting from low-impulse noise exposure. *J Neurotrauma* 2008; 25: 1397-406.

[48] DeWitt DS, Prough DS. Blast-induced brain injury and posttraumatic hypotension and hypoxemia. *J Neurotrauma* 2009; 26: 877-87.

[49] Garman RH, Jenkins LW, Switzer RC, Bauman RA, Tong LC, Swauger PV*, et al.* Blast exposure in rats with body shielding is characterized primarily by diffuse axonal injury. *J Neurotrauma* 2011; 28: 947-59.

[50] Readnower RD, Chavko M, Adeeb S, Conroy MD, Pauly JR, McCarron RM*, et al.* Increase in blood-brain barrier permeability, oxidative stress, and activated microglia in a rat model of blast-induced traumatic brain injury. *J Neurosci Res* 2010; 88: 3530-9.

[51] Reneer DV. Blast-induced brain injury influence of shockwave components 2012.

[52] Shetty AK, Mishra V, Kodali M, Hattiangady B. Blood-brain barrier dysfunction and delayed neurological deficits in mild traumatic brain injury induced by blast shock waves. *Front Cell Neurosci* 2014; 8: 232.

[53] Hue CD, Cao S, Dale Bass CR, Meaney DF, Morrison B, 3rd. Repeated primary blast injury causes delayed recovery, but not additive disruption, in an in

vitro blood-brain barrier model. *J Neurotrauma* 2014; 31: 951-60.

[54] Abdul-Muneer PM, Schuetz H, Wang F, Skotak M, Jones J, Gorantla S*, et al.* Induction of oxidative and nitrosative damage leads to cerebrovascular inflammation in an animal model of mild traumatic brain injury induced by primary blast. *Free Radic Biol Med* 2013; 60: 282-91.

[55] Bowen IG, Fletcher ER, Richmond DR, Hirsch FG, White CS. Biophysical mechanisms and scaling procedures applicable in assessing responses of the thorax energized by air-blast overpressures or by nonpenetrating missiles. *Ann N Y Acad Sci* 1968; 152: 122-46.

[56] Zou YY, Kan EM, Lu J, Ng KC, Tan MH, Yao L*, et al.* Primary blast injury-induced lesions in the retina of adult rats. *J Neuroinflammation* 2013; 10: 79.

[57] Pun PB, Kan EM, Salim A, Li Z, Ng KC, Moochhala SM*, et al.* Low level primary blast injury in rodent brain. *Front Neurol* 2011; 2: 19.

[58] Courtney MW, Courtney AC. Note: A table-top blast driven shock tube. *Rev Sci Instrum* 2010; 81: 126103.

[59] Yeoh S, Bell ED, Monson KL. Distribution of blood-brain barrier disruption in primary blast injury. *Ann Biomed Eng* 2013; 41: 2206-14.

[60] Hayda R, Harris RM, Bass CD. Blast injury research: modeling injury effects of landmines, bullets, and bombs. *Clin Orthop Relat Res* 2004: 97-108.

[61] Reneer DV, Hisel RD, Hoffman JM, Kryscio RJ, Lusk BT, Geddes JW. A multi-mode shock tube for investigation of blast-induced traumatic brain injury. *J Neurotrauma* 2011; 28: 95-104.

[62] Vandevord PJ, Bolander R, Sajja VS, Hay K, Bir CA. Mild neurotrauma indicates a range-specific pressure response to low level shock wave exposure. *Ann Biomed Eng* 2012; 40: 227-36.

[63] Courtney AC, Andrusiv LP, Courtney MW. Oxy-acetylene driven laboratory scale shock tubes for studying blast wave effects. *Rev Sci Instrum* 2012; 83: 045111.

[64] Needham CE, Ritzel D, Rule GT, Wiri S, Young L. Blast testing issues and TBI: experimental models that lead to wrong conclusions. *Front Neurol* 2015; 6: 72.

[65] Bass CR, Panzer MB, Rafaels KA, Wood G, Shridharani J, Capehart B. Brain injuries from blast. *Ann Biomed Eng* 2012; 40: 185-202.

[66] Bass CR, Rafaels KA, Salzar RS. Pulmonary injury risk assessment for short-duration blasts. *J Trauma* 2008; 65: 604-15.

[67] Risling M, Davidsson J. Experimental animal models for studies on the mechanisms of blast-induced neurotrauma. *Front Neurol* 2012; 3: 30.

[68] Sonden A, Svensson B, Roman N, Ostmark H, Brismar B, Palmblad J*, et al.* Laser-induced shock wave endothelial cell injury. *Lasers Surg Med* 2000; 26: 364-75.

[69] Satoh Y, Sato S, Saitoh D, Tokuno S, Hatano B, Shimokawaji T*, et al.* Pulmonary blast injury in mice: a novel model for studying blast injury in the laboratory using laser-induced stress waves. *Lasers Surg Med* 2010; 42: 313-8.

[70] McCabe JT, Moratz C, Liu Y, Burton E, Morgan A, Budinich C*, et al.* Application of high-intensity focused ultrasound to the study of mild traumatic brain injury. *Ultrasound Med Biol* 2014; 40: 965-78.

[71] Divani AA, Murphy AJ, Meints J, Sadeghi-Bazargani H, Nordberg J, Monga M*, et al.* A novel preclinical model of moderate primary blast-induced traumatic brain injury. *J Neurotrauma* 2015; 32: 1109-16.

[72] Svetlov SI, Prima V, Glushakova O, Svetlov A, Kirk DR, Gutierrez H*, et al.* Neuro-glial and systemic mechanisms of pathological responses in rat models of primary blast overpressure compared to "composite" blast. *Front Neurol* 2012; 3: 15.

[73] Croll SD, Ransohoff RM, Cai N, Zhang Q, Martin FJ, Wei T*, et al.* VEGF-mediated inflammation precedes angiogenesis in adult brain. *Exp Neurol* 2004; 187: 388-402.

[74] Lossinsky AS, Shivers RR. Structural pathways for macromolecular and cellular transport across the blood-brain barrier during inflammatory conditions. Review. *Histol Histopathol* 2004; 19: 535-64.

[75] Paxinos G, Watson C. *The rat brain in stereotaxic coordinates*, 4th edition. San Diego: Academic Press, 1998.

[76] Graham DI. Neuropathology of head injury. In: Nrayan RK, Wilberger JE, Povlishock JT. *Neurotrauma*. New York: McGraw-Hill, 1996:43-59.

[77] Dal Cengio Leonardi A, Keane NJ, Bir CA, Ryan AG, Xu L, VandeVord PJ. Head orientation affects the intracranial pressure response resulting from shock wave loading in the rat. *Journal of Biomechanics* 2012; 45: 2595-2602.

[78] Mao HJ, Wagner C, Guan FJ, Yeni YN, Yang KH. Material properties of adult rat skull. *Journal of Mechanics in Medicine and Biology* 2011; 11: 1199-1212.

[79] Cavaglia M, Dombrowski SM, Drazba J, Vasanji A, Bokesch PM, Janigro D. Regional variation in brain capillary density and vascular response to ischemia. *Brain Res* 2001; 910: 81-93.

[80] Ohtake M, Morino S, Kaidoh T, Inoue T. Three-dimensional structural changes in cerebral microvessels after transient focal cerebral ischemia in rats: scanning electron microscopic study of corrosion casts. *Neuropathology* 2004; 24: 219-27.

[81] Goldstein LE, Fisher AM, Tagge CA, Zhang XL, Velisek L, Sullivan JA*, et al.* Chronic traumatic encephalopathy in blast-exposed military veterans and a blast neurotrauma mouse model. *Sci Transl Med* 2012; 4: 134ra60.

[82] Klatzo I. Blood-brain barrier and ischaemic brain oedema. *Z Kardiol* 1987; 76 Suppl 4: 67-9.

[83] Rafaels KA, Bass CR, Panzer MB, Salzar RS, Woods WA, Feldman SH*, et al.* Brain injury risk from primary blast. *J Trauma Acute Care Surg* 2012; 73: 895-901.

[84] Mouritz AP. The effect of underwater explosion shock loading on the fatigue behaviour of grp laminates. *Composites* 1995; 26: 3-9.

[85] Sajja VS, Perrine SA, Ghoddoussi F, Hall CS, Galloway MP, VandeVord PJ. Blast neurotrauma impairs working memory and disrupts prefrontal myo-inositol levels in rats. *Mol Cell Neurosci* 2014; 59: 119-26.

[86] Wang H, Zhang YP, Cai J, Shields LB, Tuchek CA, Shi R*, et al.* A compact blast-induced traumatic brain injury model in mice. *J Neuropathol Exp Neurol* 2016.

[87] Abbott NJ, Patabendige AA, Dolman DE, Yusof SR, Begley DJ. Structure and function of the blood-brain barrier. *Neurobiol Dis* 2010; 37: 13-25.

[88] Hamm S, Dehouck B, Kraus J, Wolburg-Buchholz K, Wolburg H, Risau W*, et al.* Astrocyte mediated modulation of blood-brain barrier permeability does not correlate with a loss of tight junction proteins from the cellular contacts. *Cell Tissue Res* 2004; 315: 157-66.

[89] Obermeier B, Daneman R, Ransohoff RM. Development, maintenance and disruption of the blood-brain barrier. *Nat Med* 2013; 19: 1584-96.

[90] Zhao J, Pati S, Redell JB, Zhang M, Moore AN, Dash PK. Caffeic Acid phenethyl ester protects blood-brain barrier integrity and reduces contusion volume in rodent models of traumatic brain injury. *J Neurotrauma* 2012; 29: 1209-18.

[91] Saunders NR, Dreifuss JJ, Dziegielewska KM, Johansson PA, Habgood MD, Mollgard K*, et al.* The rights and wrongs of blood-brain barrier permeability studies: a walk through 100 years of history. *Front Neurosci* 2014; 8: 404.

[92] Saunders NR, Dziegielewska KM, Mollgard K, Habgood MD. Markers for blood-brain barrier integrity: how appropriate is Evans blue in the twenty-first century and what are the alternatives? *Front Neurosci* 2015; 9: 385.

[93] Poduslo JF, Curran GL, Berg CT. Macromolecular permeability across the blood-nerve and blood-brain barriers. *Proc Natl Acad Sci U S A* 1994; 91: 5705-9.

[94] Zhang CJ, Li HZ, Zhou SX, Yang J, Huang QY. Expression of vascular endothelial growth factor during the early stage of maxillofacial blast injury. *Chin*

J Dent Res 2000; 3: 40-3.

[95] Sawyer AJ, Kyriakides TR. Nanoparticle-based evaluation of blood-brain barrier leakage during the foreign body response. *J Neural Eng* 2013; 10: 016013.

[96] Turner RC, Naser ZJ, Logsdon AF, DiPasquale KH, Jackson GJ, Robson MJ*, et al.* Modeling clinically relevant blast parameters based on scaling principles produces functional & histological deficits in rats. *Exp Neurol* 2013; 248: 520-9.

[97] Kamnaksh A, Kwon SK, Kovesdi E, Ahmed F, Barry ES, Grunberg NE*, et al.* Neurobehavioral, cellular, and molecular consequences of single and multiple mild blast exposure. *Electrophoresis* 2012; 33: 3680-92.

[98] Arun P, Abu-Taleb R, Oguntayo S, Tanaka M, Wang Y, Valiyaveettil M*, et al.* Distinct patterns of expression of traumatic brain injury biomarkers after blast exposure: role of compromised cell membrane integrity. *Neurosci Lett* 2013; 552: 87-91.

[99] Baalman KL, Cotton RJ, Rasband SN, Rasband MN. Blast wave exposure impairs memory and decreases axon initial segment length. *J Neurotrauma* 2013; 30: 741-51.

[100] Budde MD, Shah A, McCrea M, Cullinan WE, Pintar FA, Stemper BD. Primary blast traumatic brain injury in the rat: relating diffusion tensor imaging and behavior. *Front Neurol* 2013; 4: 154.

[101] Heldt SA, Elberger AJ, Deng Y, Guley NH, Del Mar N, Rogers J*, et al.* A novel closed-head model of mild traumatic brain injury caused by primary overpressure blast to the cranium produces sustained emotional deficits in mice. *Front Neurol* 2014; 5: 2.

[102] Sajja VS, Galloway MP, Ghoddoussi F, Thiruthalinathan D, Kepsel A, Hay K*, et al.* Blast-induced neurotrauma leads to neurochemical changes and neuronal degeneration in the rat hippocampus. *NMR Biomed* 2012; 25: 1331-9.

[103] Huang E, Ngo M, Yee S, Held L, Norman K, Scremin AM*, et al.* Repeated blast exposure alters open field behavior recorded under low illumination. *Brain Res* 2013; 1529: 125-33.

[104] Kovesdi E, Kamnaksh A, Wingo D, Ahmed F, Grunberg NE, Long JB*, et al.* Acute minocycline treatment mitigates the symptoms of mild blast-induced traumatic brain injury. *Front Neurol* 2012; 3: 111.

[105] Park E, Eisen R, Kinio A, Baker AJ. Electrophysiological white matter dysfunction and association with neurobehavioral deficits following low-level primary blast trauma. *Neurobiol Dis* 2013; 52: 150-9.

[106] Xie K, Kuang H, Tsien JZ. Mild blast events alter anxiety, memory, and

neural activity patterns in the anterior cingulate cortex. *PLoS One* 2013; 8: e64907.

[107] Cho HJ, Sajja VS, Vandevord PJ, Lee YW. Blast induces oxidative stress, inflammation, neuronal loss and subsequent short-term memory impairment in rats. *Neuroscience* 2013; 253: 9-20.

[108] Genovese RF, Simmons LP, Ahlers ST, Maudlin-Jeronimo E, Dave JR, Boutte AM. Effects of mild TBI from repeated blast overpressure on the expression and extinction of conditioned fear in rats. *Neuroscience* 2013; 254: 120-9.

[109] Park E, Gottlieb JJ, Cheung B, Shek PN, Baker AJ. A model of low-level primary blast brain trauma results in cytoskeletal proteolysis and chronic functional impairment in the absence of lung barotrauma. *J Neurotrauma* 2011; 28: 343-57.

[110] Harrison FE, Hosseini AH, McDonald MP. Endogenous anxiety and stress responses in water maze and Barnes maze spatial memory tasks. *Behav Brain Res* 2009; 198: 247-51.

[111] Kuehn R, Simard PF, Driscoll I, Keledjian K, Ivanova S, Tosun C*, et al.* Rodent model of direct cranial blast injury. *J Neurotrauma* 2011; 28: 2155-69.

[112] Huber BR, Meabon JS, Martin TJ, Mourad PD, Bennett R, Kraemer BC*, et al.* Blast exposure causes early and persistent aberrant phospho- and cleaved-tau expression in a murine model of mild blast-induced traumatic brain injury. *J Alzheimers Dis* 2013; 37: 309-23.

[113] Gyorgy A, Ling G, Wingo D, Walker J, Tong L, Parks S*, et al.* Time-dependent changes in serum biomarker levels after blast traumatic brain injury. *J Neurotrauma* 2011; 28: 1121-6.

[114] Yang Z, Wang Z, Tang C, Ying Y. Biological effects of weak blast waves and safety limits for internal organ injury in the human body. *J Trauma* 1996; 40: S81-4.

[115] Rafaels K, Bass CR, Salzar RS, Panzer MB, Woods W, Feldman S*, et al.* Survival risk assessment for primary blast exposures to the head. *J Neurotrauma* 2011; 28: 2319-28.

[116] Kirkman E, Watts S. Characterization of the response to primary blast injury. *Philos Trans R Soc Lond B Biol Sci* 2011; 366: 286-90.

[117] Ahlers ST, Vasserman-Stokes E, Shaughness MC, Hall AA, Shear DA, Chavko M*, et al.* Assessment of the effects of acute and repeated exposure to blast overpressure in rodents: toward a greater understanding of blast and the potential ramifications for injury in humans exposed to blast. *Front Neurol* 2012; 3: 32.

[118] Panzer MB, Bass CR, Rafaels KA, Shridharani J, Capehart BP. Primary blast survival and injury risk assessment for repeated blast exposures. *J Trauma Acute Care Surg* 2012; 72: 454-66.

[119] Kane MJ, Angoa-Perez M, Francescutti DM, Sykes CE, Briggs DI, Leung LY*, et al.* Altered gene expression in cultured microglia in response to simulated blast overpressure: possible role of pulse duration. *Neurosci Lett* 2012; 522: 47-51.

[120] Sajja VS, Hubbard WB, VandeVord PJ. Subacute oxidative stress and glial reactivity in the amygdala are associated with increased anxiety following blast neurotrauma. *Shock* 2015; 44 Suppl 1: 71-8.

[121] Choi JH, Greene WA, Johnson AJ, Chavko M, Cleland JM, McCarron RM*, et al.* Pathophysiology of blast-induced ocular trauma in rats after repeated exposure to low-level blast overpressure. *Clin Experiment Ophthalmol* 2015; 43: 239-46.

[122] Koliatsos VE, Cernak I, Xu L, Song Y, Savonenko A, Crain BJ*, et al.* A mouse model of blast injury to brain: initial pathological, neuropathological, and behavioral characterization. *J Neuropathol Exp Neurol* 2011; 70: 399-416.

[123] Muldoon LL, Alvarez JI, Begley DJ, Boado RJ, Del Zoppo GJ, Doolittle ND*, et al.* Immunologic privilege in the central nervous system and the blood-brain barrier. *J Cereb Blood Flow Metab* 2013; 33: 13-21.

[124] Mao S, Xiong G, Zhang L, Dong H, Liu B, Cohen NA*, et al.* Verification of the cross immunoreactivity of A60, a mouse monoclonal mntibody against neuronal nuclear protein. *Front Neuroanat* 2016; 10: 54.

[125] Salauze D, Serre V, Perrin C. Quantification of total IgM and IgG levels in rat sera by a sandwich elisa technique. *Comparative Haematology International* 1994; 4: 30-33.

[126] Ajao DO, Pop V, Kamper JE, Adami A, Rudobeck E, Huang L*, et al.* Traumatic brain injury in young rats leads to progressive behavioral deficits coincident with altered tissue properties in adulthood. *J Neurotrauma* 2012; 29: 2060-74.

[127] Atkins CM, Cepero ML, Kang Y, Liebl DJ, Dietrich WD. Effects of early rolipram treatment on histopathological outcome after controlled cortical impact injury in mice. *Neurosci Lett* 2013; 532: 1-6.

[128] Fehily B, Fitzgerald M. Repeated mild traumatic brain injury: potential mechanisms of damage. *Cell Transplant* 2016.

[129] Website TS. Goat-anti-Rat biotinylated IgG Product Page. *https://www.thermofisher.com/antibody/product/Goat-anti-Rat-IgG-H-L-Secondary-Antibody-Polyclonal/31830* 2016.

[130] Website TS. AF-594 Product Page. *https://www.thermofisher.com/us/en/home/life-science/cell-analysis/fluorophores/alexa-fluor-594.html* 2016.

[131] Evans CA, Reynolds JM, Reynolds ML, Saunders NR, Segal MB. The development of a blood-brain barrier mechanism in foetal sheep. *J Physiol* 1974; 238: 371-86.

[132] Pan W, Zhang L, Liao J, Csernus B, Kastin AJ. Selective increase in TNF alpha permeation across the blood-spinal cord barrier after SCI. *J Neuroimmunol* 2003; 134: 111-7.

[133] Boyd BJ, Galle A, Daglas M, Rosenfeld JV, Medcalf R. Traumatic brain injury opens blood-brain barrier to stealth liposomes via an enhanced permeability and retention (EPR)-like effect. *J Drug Target* 2015; 23: 847-53.

[134] Preston E, Foster DO, Mills PA. Effects of radiochemical impurities on measurements of transfer constants for [14C]sucrose permeation of normal and injured blood-brain barrier of rats. *Brain Res Bull* 1998; 45: 111-6.

[135] Bernard SL, Ewen JR, Barlow CH, Kelly JJ, McKinney S, Frazer DA*, et al.* High spatial resolution measurements of organ blood flow in small laboratory animals. *Am J Physiol Heart Circ Physiol* 2000; 279: H2043-52.

[136] Kou Z, Ye Y, Haacke EM. Evaluating the role of reduced oxygen saturation and vascular damage in traumatic brain injury using magnetic resonance perfusion-weighted imaging and susceptibility-weighted imaging and mapping. *Top Magn Reson Imaging* 2015; 24: 253-65.

[137] Haacke EM, Xu Y, Cheng YC, Reichenbach JR. Susceptibility weighted imaging (SWI). *Magn Reson Med* 2004; 52: 612-8.

[138] Montandon G, Kinkead R, Lomenech AM, Bairam A, Guenard H. Heterogeneity of brainstem blood flow response to hypoxia in the anesthetized rat. *Respir Physiol Neurobiol* 2006; 150: 301-6.

[139] Hue CD, Cao S, Haider SF, Vo KV, Effgen GB, Vogel E, 3rd*, et al.* Blood-brain barrier dysfunction after primary blast injury in vitro. *J Neurotrauma* 2013; 30: 1652-63.

[140] Bigler ED. Anterior and middle cranial fossa in traumatic brain injury: relevant neuroanatomy and neuropathology in the study of neuropsychological outcome. *Neuropsychology* 2007; 21: 515-31.

[141] Nyein MK, Jason AM, Yu L, Pita CM, Joannopoulos JD, Moore DF*, et al.* In silico investigation of intracranial blast mitigation with relevance to military traumatic brain injury. *Proc Natl Acad Sci U S A* 2010; 107: 20703-8.

[142] Sundaramurthy A, Alai A, Ganpule S, Holmberg A, Plougonven E, Chandra N. Blast-induced biomechanical loading of the rat: an experimental and

anatomically accurate computational blast injury model. *J Neurotrauma* 2012; 29: 2352-64.

[143] Panzer MB, Myers BS, Bass CR. Mesh considerations for finite element blast modelling in biomechanics. *Comput Methods Biomech Biomed Engin* 2013; 16: 612-21.

[144] Wang C, Pahk JB, Balaban CD, Miller MC, Wood AR, Vipperman JS. Computational study of human head response to primary blast waves of five levels from three directions. *PLoS One* 2014; 9: e113264.

[145] Sarvghad-Moghaddam H, Jazi MS, Rezaei A, Karami G, Ziejewski M. Examination of the protective roles of helmet/faceshield and directionality for human head under blast waves. *Comput Methods Biomech Biomed Engin* 2015; 18: 1846-55.

[146] Christ AF, Franze K, Gautier H, Moshayedi P, Fawcett J, Franklin RJ*, et al.* Mechanical difference between white and gray matter in the rat cerebellum measured by scanning force microscopy. *J Biomech* 2010; 43: 2986-92.

[147] Lee MC, Haut RC. Insensitivity of tensile failure properties of human bridging veins to strain rate: implications in biomechanics of subdural hematoma. *J Biomech* 1989; 22: 537-42.

[148] Bell ED, Kunjir RS, Monson KL. Biaxial and failure properties of passive rat middle cerebral arteries. *J Biomech* 2013; 46: 91-6.

[149] Parashos SA, Luo S, Biglan KM, Bodis-Wollner I, He B, Liang GS*, et al.* Measuring disease progression in early Parkinson disease: the National Institutes of Health Exploratory Trials in Parkinson Disease (NET-PD) experience. *JAMA Neurol* 2014; 71: 710-6.

[150] Ahmed F, Plantman S, Cernak I, Agoston DV. The temporal pattern of changes in serum biomarker levels reveals complex and dynamically changing pathologies after exposure to a single low-intensity blast in mice. *Front Neurol* 2015; 6: 114.

[151] Liu MD, Luo P, Wang ZJ, Fei Z. Changes of serum Tau, GFAP, TNF-alpha and malonaldehyde after blast-related traumatic brain injury. *Chin J Traumatol* 2014; 17: 317-22.

[152] Ahmed F, Gyorgy A, Kamnaksh A, Ling G, Tong L, Parks S*, et al.* Time-dependent changes of protein biomarker levels in the cerebrospinal fluid after blast traumatic brain injury. *Electrophoresis* 2012; 33: 3705-11.

[153] Pham N, Sawyer TW, Wang Y, Jazii FR, Vair C, Taghibiglou C. Primary blast-induced traumatic brain injury in rats leads to increased prion protein in plasma: a potential biomarker for blast-induced traumatic brain injury. *J Neurotrauma* 2015; 32: 58-65.

[154] Ho L, Lange G, Zhao W, Wang J, Rooney R, Patel DH*, et al.* Select small nucleolar RNAs in blood components as novel biomarkers for improved identification of comorbid traumatic brain injury and post-traumatic stress disorder in veterans of the conflicts in Afghanistan and Iraq. *Am J Neurodegener Dis* 2014; 3: 170-81.

[155] Llano Lopez L, Hauser J, Feldon J, Gargiulo PA, Yee BK. Evaluating spatial memory function in mice: a within-subjects comparison between the water maze test and its adaptation to dry land. *Behav Brain Res* 2010; 209: 85-92.

[156] Kamnaksh A, Kovesdi E, Kwon SK, Wingo D, Ahmed F, Grunberg NE*, et al.* Factors affecting blast traumatic brain injury. *J Neurotrauma* 2011; 28: 2145-53.

[157] Sandrini G, Serrao M, Rossi P, Romaniello A, Cruccu G, Willer JC. The lower limb flexion reflex in humans. *Prog Neurobiol* 2005; 77: 353-95.

[158] Shih AY, Blinder P, Tsai PS, Friedman B, Stanley G, Lyden PD*, et al.* The smallest stroke: occlusion of one penetrating vessel leads to infarction and a cognitive deficit. *Nat Neurosci* 2013; 16: 55-63.